Kart Tire Data Collection Rig

A Baccalaureate thesis submitted to the
Department of Mechanical and Materials Engineering
College of Engineering and Applied Science
University of Cincinnati

in partial fulfillment of the
requirements for the degree of

Bachelor of Science

in Mechanical Engineering Technology

by

James Barth, Aaron Christner, Michael Parks

April 2017

Thesis Advisor:
Professor Amir Salehpour

TABLE OF CONTENTS

LIST OF FIGURES

LIST OF TABLES

ABSTRACT

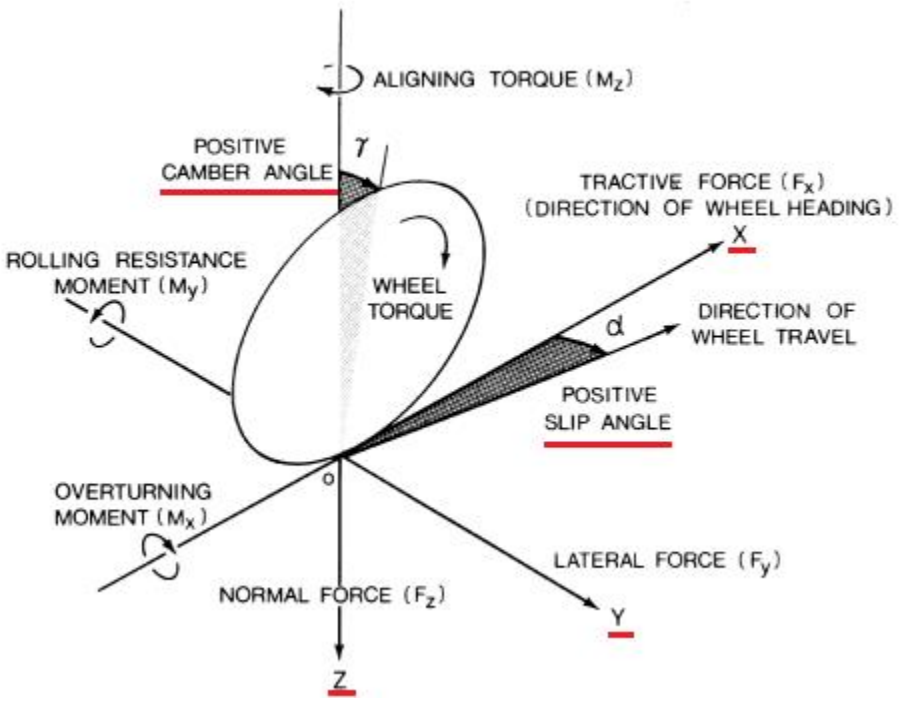

Figure 1: SAE Tire Axis System (7)

Dirt oval kart racing is a popular form of grassroots racing in the United States. With few limitations on tire selection and no objective way to measure one tire against another, budgets skyrocket as teams attempt to find a slight advantage from a slightly different rubber compound, wheel width, mechanical modification, or chemical application. In order to properly evaluate one tire compared to another, a testing method is needed that is capable of using an actual dirt track surface while holding a kart tire at a set normal force (z-axis), camber angle, and slip angle while measuring the resulting lateral (y-axis) and longitudinal (x-axis) forces as well as tire surface temperatures. The test rig is able to reliably collect this data while simulating the loading conditions a tire would see during normal operation.

PROBLEM DEFINITION AND RESEARCH

PROBLEM DEFINITION AND BACKGROUND

Tires are one of the biggest costs to racing. Quite a bit of knowledge is required in order to make good decisions when choosing tires during a race. Devoting massive amounts of time and money to collecting data on tires is not as much of a problem for professional teams that have budgets to account for an engineering staff and track or lab testing. For the local racer this time and money commitment is not possible. The primary way to learn about tires is to bolt a set on and see how they react. This can be costly, especially in classes where there are multiple tire options or tire modifications are allowed. One set of mounted, cut, and chemically prepped dirt kart tires can cost anywhere between $350-450 and could be rendered useless in just a few laps if too soft for the track conditions. With most racers learning the tire game through trial and error, it becomes an expensive proposition.

Our goal was to devise a method of tire testing that is within reach of the local racer. This means not only designing a method of testing but also doing it at a price point that can be justified by a local team. We wanted to be able to capture usable data that teams can apply to see results on the track- primarily lateral and longitudinal forces generated at various tire loads, slip angles, camber angles, and temperatures. It is also important that the testing is portable and use an actual track surface, especially for dirt tracks where racers will encounter the widest variety of track surface conditions. Our plan was to design, build, and test a rig that will be able to be towed behind a pickup truck and can control the slip angle, camber angle, and normal load of a single go kart tire while logging the generated lateral force, longitudinal force, and surface temperatures.

Speed costs money- how fast do you want to go?

RESEARCH, TECHNOLOGY, AND EXISTING PRODUCTS

The inspiration for this project came from current tire testing methods used by the Formula SAE Tire Testing Consortium.

Current go kart tire testing outside of the tire manufacturers themselves is conducted on track with a stopwatch in a trial-and-error method. There are only a couple of published examples of this strategy (2, 9). This data does not account for any changes in the track surface, weather, or driver inconsistencies. The only quantitative data are the lap times themselves. This form of testing is something that any racer can do on any weekend with little additional

cost but it introduces many variables that can skew their results. By eliminating the driver and changing track conditions the tire testing rig will give customers more concrete data that can be used to evaluate their tire and tire treatment options.

After speaking with tire specialists and racers at several local dirt tracks, it became apparent that the type of data we were interested in capturing for dirt tires likely only exists at the top speed shop and manufacturer level, if it exists at all, and they are not interested in sharing.

CUSTOMER NEEDS

Potential customers for the tire data collection rig were any kart racers looking to be able to quantify the performance characteristics of different kart tires. The general demographic for kart racers is primarily male, age 10-65. This rig will be able to be used by all skill levels but will focus on someone who is able to interpret the data collected to make the best decision when using a set of tires for a race. Someone who spends a lot of money on tires would be a more likely candidate to invest in this new technology. They would likely have experience with modifying tires and chassis tuning too. With good data and the right decision, they can save money by not using a set of tires that will not perform to their expectations.

The most viable market for the tire data rig (and therefore our target market) was local and regional level speed shops. These shops provide tires to local and regional level kart racers. Many racers also hire out at-the-track tire services from these shops for larger events, where the speed shop provides tires and chemicals for that event as well as at the track support. The speed shops have an advantage in this case over a single racer in that they have multiple karts to draw information from. By trying several different things on several different karts they can hone in on what the track needs faster and all of the racers they supply can benefit from the knowledge. Quantitative data on different tire compounds and chemicals would allow them to figure out the track faster and more accurately while lowering the risk of destroying an entire set of tires “just trying something.” These speed shops are usually run by males in their mid-twenties to mid-fifties. Some have an engineering background. Nearly all have some kind of technical background and are experienced racers. Most have experience in using simple data acquisition. Their budget would be dependent on what they perceive as the benefit to their business. For context, one of the popular go kart tire cutting machines retails for $4,700 (5).

PRODUCT/ENGINEERING FEATURES AND IMPORTANCE WEIGHTS

The main and most important customer feature for this rig is that it is easy to use by a speed shop owner to collect reliable data. The data they collect is able to help them prep/set up tires in a way that provides a better track experience come race time. The rig is also easy to use and set up, along with being portable so that it can be driven to dirt tracks to take accurate data. The rig is also relatively cheap so more speed shops could afford using one.

An initial ranking of the customer requirements is:

- 25%- Collects all required data
- 20%- Adjustable slip angle, camber angle, and normal load
- 15%- Provides easy way to interpret captured data
- 15%- Portable
- 10%- Works with most truck hitch heights
- 10%- Fits in the speed shop budget range
- 5%- Easy to use

PRODUCT OBJECTIVES

The main product objective was to collect consistent and reliable data on tires that can be analyzed for better prepped conditions. Some of the main parts that were measured include normal loading, slip angle, and camber angle on the tire. The rig also allowed logging tire, surface and ambient temperatures, tire speed, effective radius, ground speed, true heading, and lateral, longitudinal, and normal force. The product has a transport position, storage stand, and ability to change height to compensate for different trucks. The data output objective was to provide excel data analysis.

HOUSE OF QUALITY

			Engineering Requirements (units)													
		Importance wt.	Weight (lbs)	Length (in)	Width (in)	Height (in)	Hitch Height (in)	Hub Size (in)	Incremental CA Adjustment	Infinite CA Adjustment	Manual SA Adjustment	Automatic SA Adjustment	Normal Load Range (lbf)	Data Anaylsis Templates		
	Customer Requirements		1	2	3	4	5	6	7	8	9	10	11	12	13	14
1	Collects Required Data	0.25							1	3	1	3	3			
2	Adjustable SA, CA, F_N	0.20							3	9	3	9	9			
3	Intuitive Data Interpretation	0.15										-3		9		
4	Portable	0.15	9	9	9	9										
5	Works with most Truck Hitch Heights	0.10					9									
6	Fits in Speed Shop Budget	0.10									9	-1				
7	Ease of Use	0.05	3				3	3	3	-1	1	9		3		
8																
9																
10																
	Total Importance	1.00	1.5	1.4	1.4	1.4	1.1	0.2	1	2.5	1.8	2.5	2.6	1.5		

Figure 2: House of Quality

DESIGN PROCESS

LOAD CELL CONFIGURATION

Our goal was to devise a method of tire testing that is within reach of the local racer. This means not only designing a method of testing but also doing it at a price point that can be justified by a local team. We wanted to be able to capture usable data that teams can apply to see results on the track- primarily lateral and longitudinal forces generated at various tire loads, slip angles, camber angles, and temperatures.

The primary objective of the rig is to hold a kart tire at a set loading, camber, and slip condition while logging the resulting forces and temperatures generated. The biggest challenge, and therefore the first one tackled, was to configure the load cell(s) in a cost-effective manner that would allow isolation of the normal, lateral, and longitudinal forces acting on the tire

S-Beam Between Parallel Plates Concept:

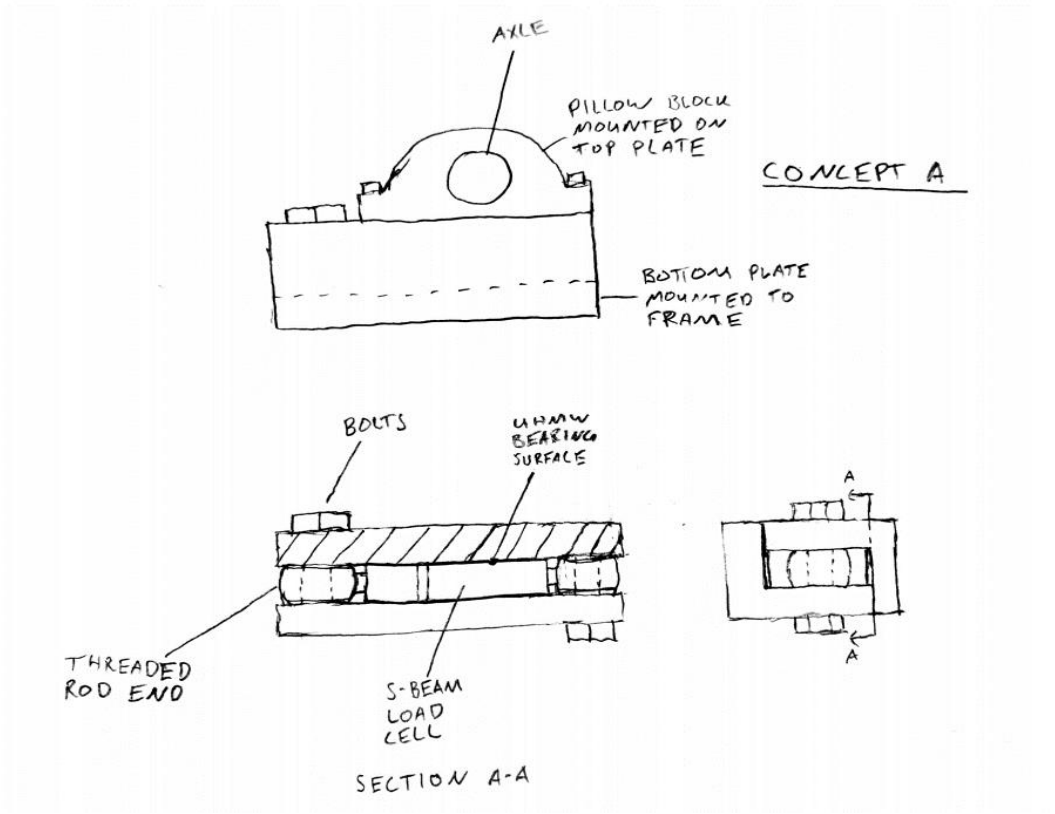

Figure 3: S-Beam Between Parallel Plates Load Cell Concept

This concept consisted of two parallel plates. The S-beam load cell was mounted between the plates with each end of the load cell attached to one of the plates. The mounting points were offset so that the load cell is put into tension or compression based on the direction of the load. A low friction (UHMW or similar) bearing surface allowed the plates to slide on the surface of the load cell in independent directions. The bearing block which supports the axle was mounted on the top plate and the bottom plate was mounted to the frame. This way, if a load is applied to the tire in the direction of the load cell, the force would cause the plates to move independently of each other and put the cell into tension or compression. Three of these load cell modules needed to be interfaced together to capture forces in the x, y, and z direction.

Compression Button Type Load Cells Concept:

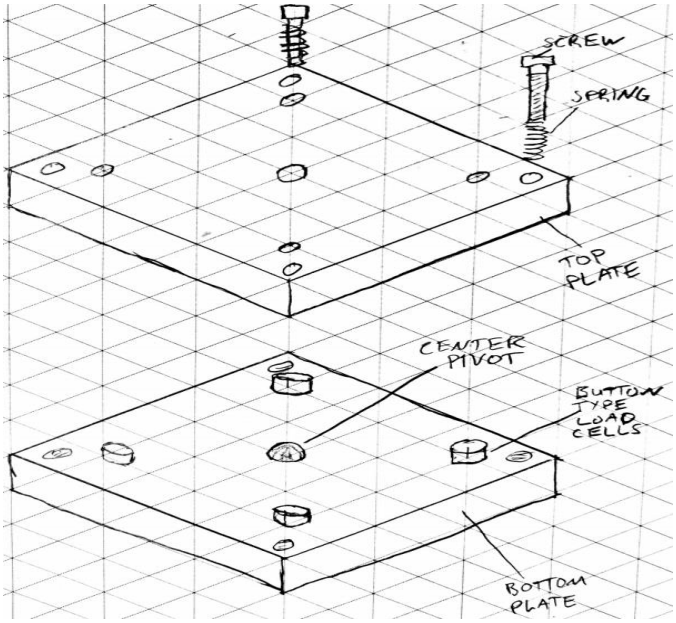

Figure 4: Compression Button Type Load Cells Concept

`

This concept design consisted of two parallel plates with four compression button type load cells oriented in a square. There was a pivot point in the center to allow the top plate to pivot in any direction relative to the bottom plate. Four spring-preloaded, screws held the plates together. The springs held the plates together but allowed the plates to pivot relative to each other a small amount. The bearing block (which supports the axle) was mounted on the top plate. As loads are applied to the tire, they are transmitted through the bearing into the top plate which is allowed to pivot relative to the bottom plate. This pivoting transmits the loads to the load cells in the configurations shown below.

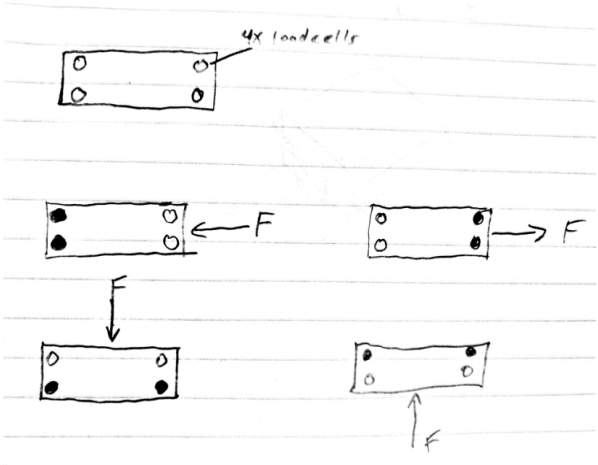

Figure 5: Compression Button Type Load Cells Concept Cont.

Bearing Carrier Constrained to Frame Concept:

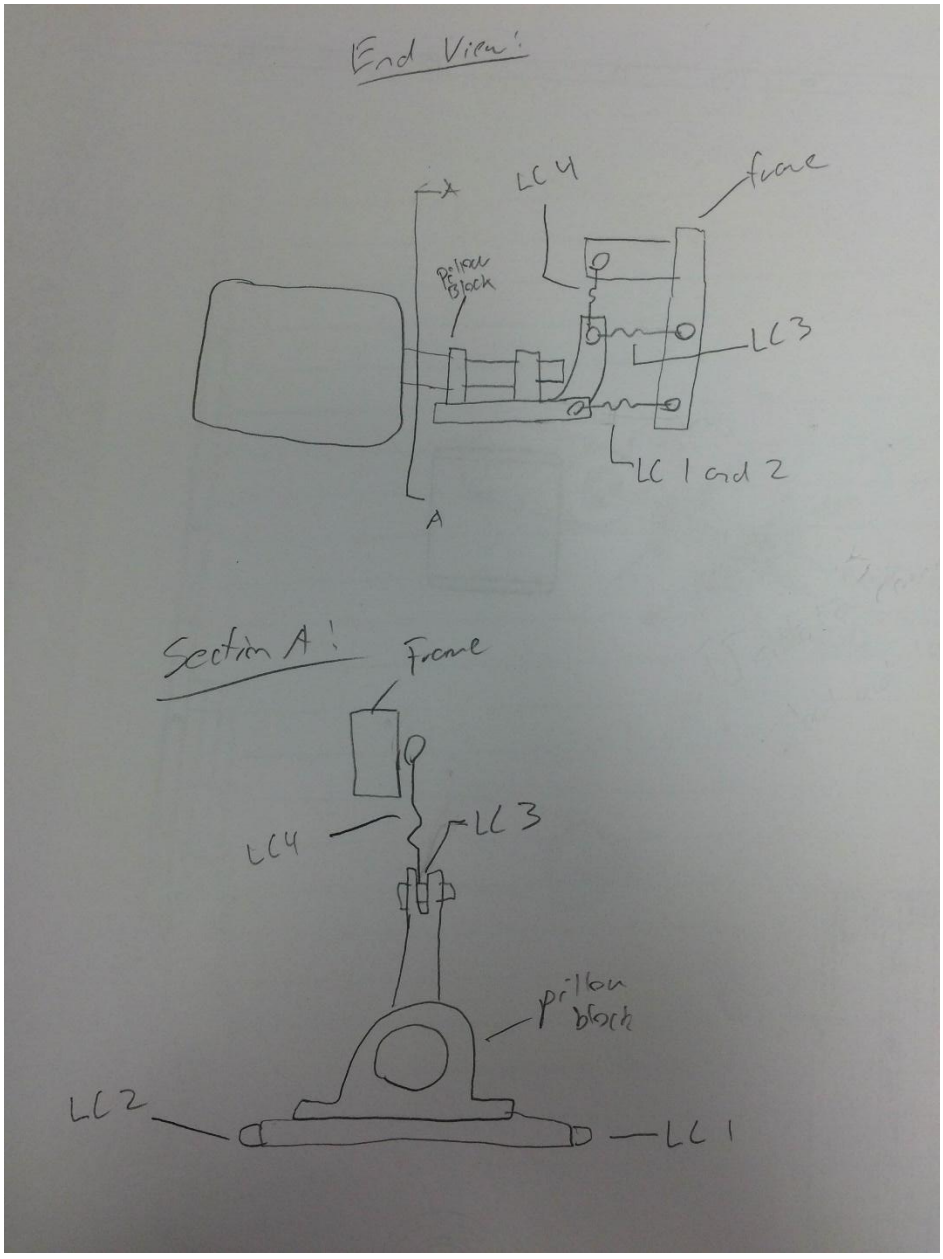

Figure 6: Bearing Carrier Constrained to Frame Concept

This load cell concept involved a bearing carrier constrained by load cells to the rigid frame of the rig. The intent was for load cell 4 to capture the normal loading on the tire. Load cells 1, 2, and 3 all captured lateral loading from the tire. Load cells 1 and 2 were used to determine the longitudinal load from the tire. The primary drawback to this concept was that the principal loads from the tire are not isolated to one load cell. Normal loading on the tire would affect all four load cells. This concept also required at least four load cells to measure forces in three axes, not particularly efficient.

Fixed and Floating Bearing on Axle Concept:

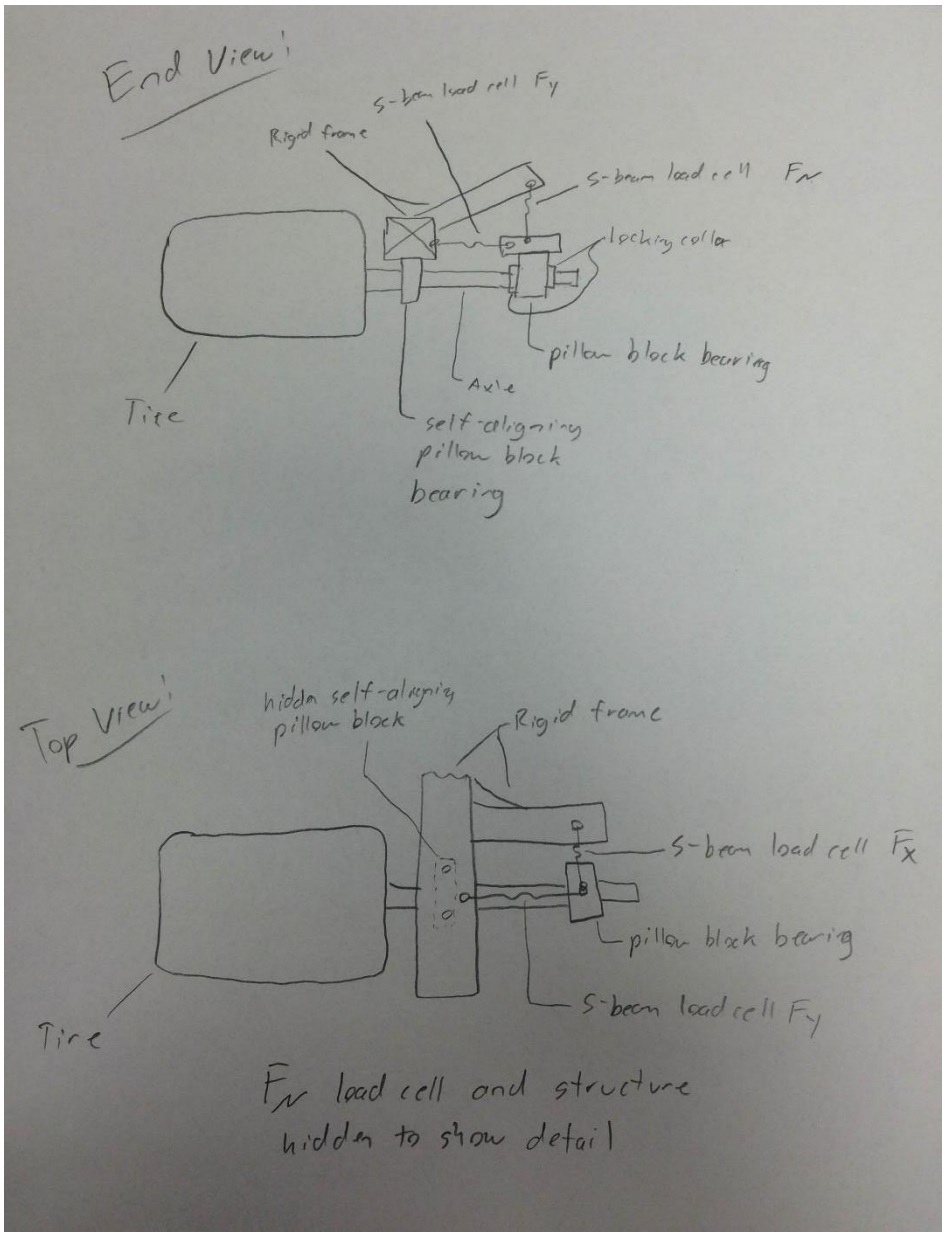

Figure 7: Fixed and Floating Bearing on Axle Concept

This concept used a fixed and floating bearing on the axle to capture normal loading (F_N), generated lateral force (F_Y), and generated longitudinal force (F_X) each with a dedicated load cell. A self-aligning pillow block bearing was hard mounted to the rigid tire rig frame in the center of the axle. The shaft is allowed to move axially within the bearing. On one end of the axle is the tire and hub assembly. The other end has an additional bearing with the three load cells mounted between it and the rigid tire rig frame. Lock collars prevent the shaft from moving axially within this bearing. Because the self-aligning pillow block in the middle of

the axle acts like a spherical joint, loading at the tire contact patch creates a moment about the center bearing. This moment is reacted by the three load cells mounted to the bearing on the other end of the shaft.

3-Axis Load Cell Concept:

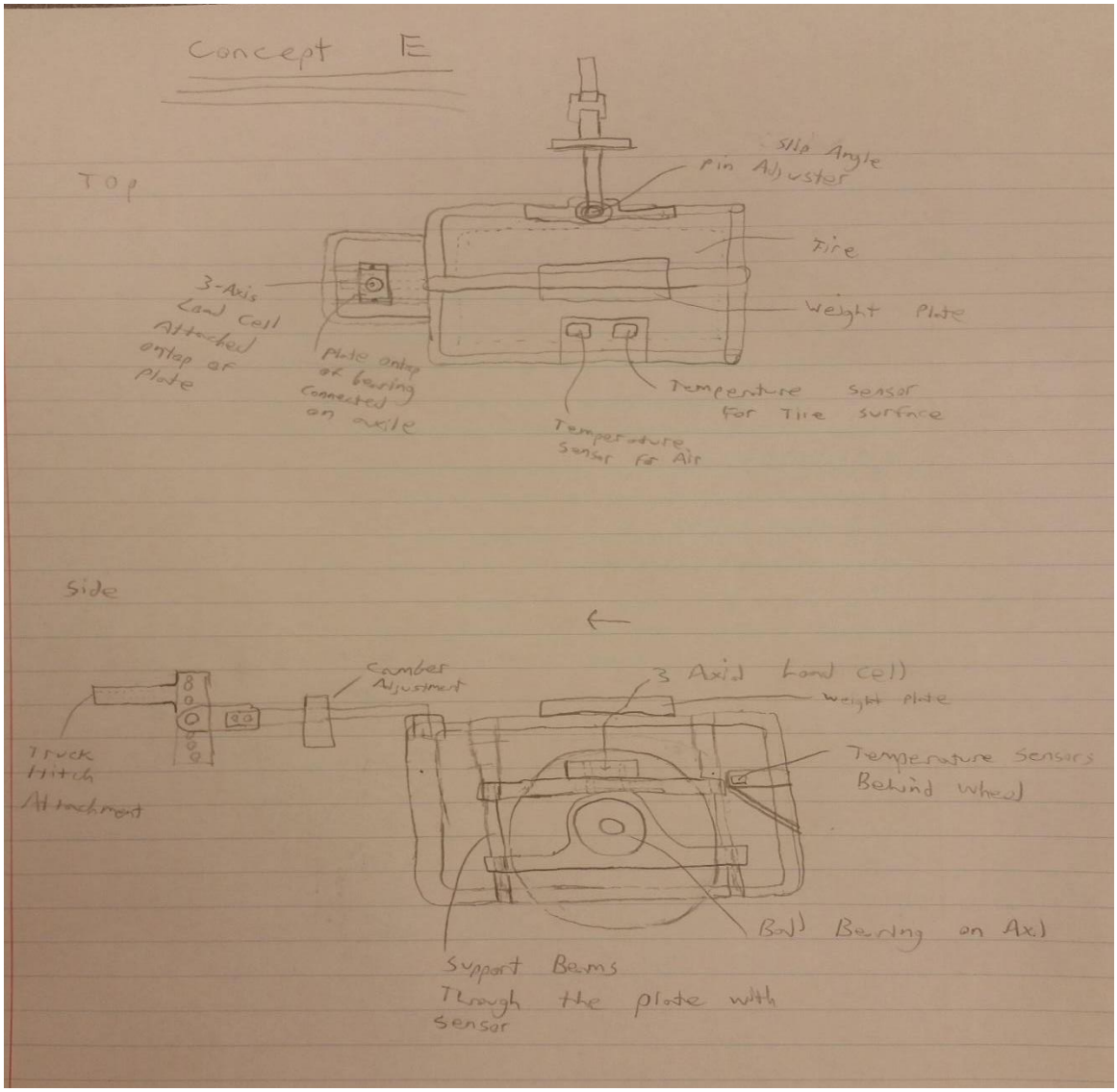

Figure 8: 3-Axis Load Cell Concept

This concept had a three axis load cell attached to the rigid frame of the rig on the side of the wheel hub. This cell was attached to a plate that attaches to a pillow block bearing. The axle that holds the wheel also holds the bearing, while there would also be support beams through the bearing attaching to the frame of the rig.

Concept Evaluation:

Weighted Rating Load Cell Configuration Concept Alternatives											
		S-Beam Between Parallel Plates		Compression Button Type		Bearing Carrier Constrained		Fixed and Floating Bearing on Axle		3-Axis Load Cell	
Criteria	Importance Weight	Rating	Weighted Rating	Rating	Weighted Rating	Rating	Weighted Rating	Rating	Weighted Rating	Rating	Weighted Rating
cost	0.25	1	0.25	2	0.5	2	0.5	3	0.75	0	0
ease of use	0.15	3	0.45	4	0.6	3	0.45	3	0.45	4	0.6
manufacturability	0.15	2	0.3	3	0.45	2	0.3	4	0.6	4	0.6
ease of repair	0.1	1	0.1	1	0.1	3	0.3	4	0.4	1	0.1
robustness	0.15	3	0.45	2	0.3	2	0.3	2	0.3	2	0.3
data capture complexity	0.15	4	0.6	1	0.15	0	0	4	0.6	4	0.6
Safety	0.05	2	0.1	3	0.15	2	0.1	1	0.05	3	0.15
Total	**1**	**n/a**	**2.25**	**n/a**	**2.25**	**n/a**	**1.95**	**n/a**	**3.15**	**n/a**	**2.35**

Rating	Value
Unsatisfactory	0
Just Tolerable	1
Adequate	2
Good	3
Very Good	4

Figure 9: Load Cell Configuration Weighted Rating

After listing out the criteria the rig needed to follow, the best concept design in terms of the load cell layout was chosen. The concept for “Fixed and Floating Bearing on Axle” had the highest rating and was the concept used.

CAMBER ADJUSTMENT METHOD

The tire rig must be able to match any camber angle a tire may see on a kart. This includes both positive and negative camber angles. The camber angle is the angle between the vertical axis of the tire and the vertical axis of the vehicle the tire is on. When this angle is adjusted, the whole tire rig behind the camber plate will be set to that angle.

“Camber Cat” Concept:

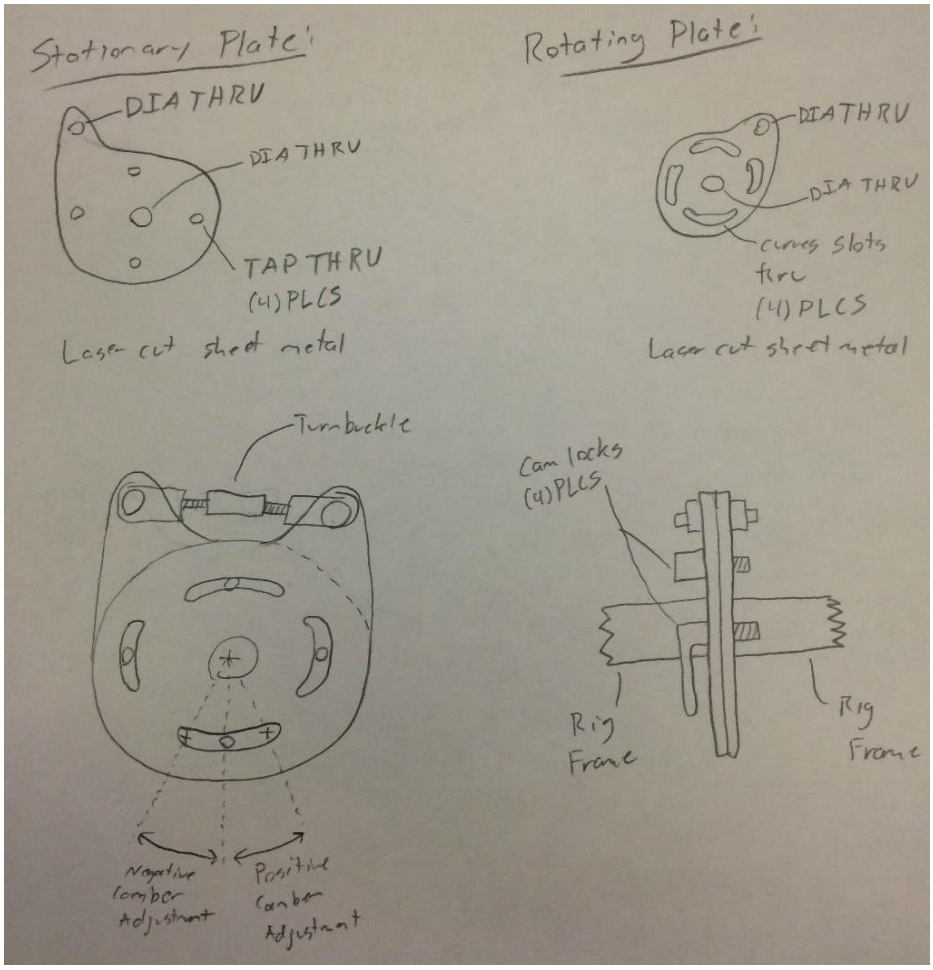

Figure 10: "Camber Cat" Concept

The “Camber Cat” concept involved two sheet metal plates rotating about the same axis with a turnbuckle to control the camber adjustment. The stationary plate had four tapped holes at 90 degree intervals centered around the center hole. The rotating plate had four slots at 90 degree intervals that were concentric with its center hole and at the same radius as the four tapped holes in the stationary plate. During testing, cam locks would sandwich the plates together creating a solid link between the front and rear parts of the testing rig. For camber adjustment, the cam locks would be released allowing the plates to rotate about a pin or bolt through their center axis. The turnbuckle would then allow control of the angle between the front and rear parts of the rig, setting the camber angle. The camber angle itself would be measured by using a standard camber gage on the test rig’s axle. Once the desired angle was reached, the cam locks would be engaged again locking the rig to that angle.

Camber Angle “Crock-Pot” Concept:

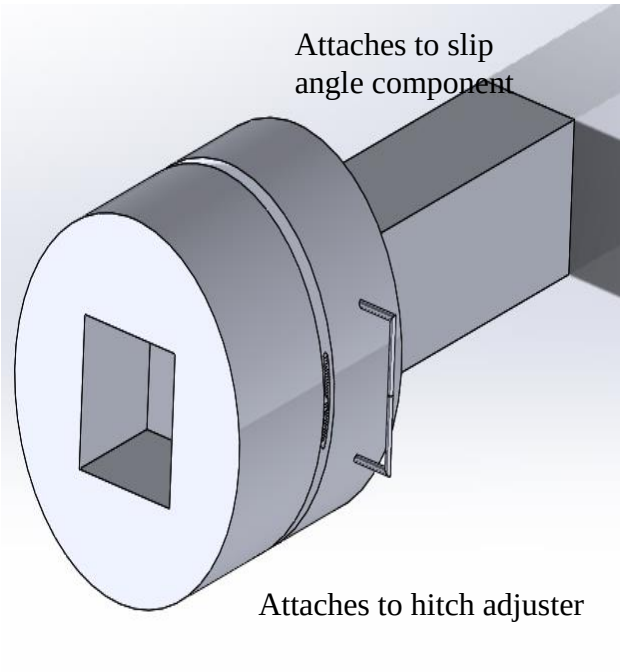

Figure 11: "Crock-Pot" Concept

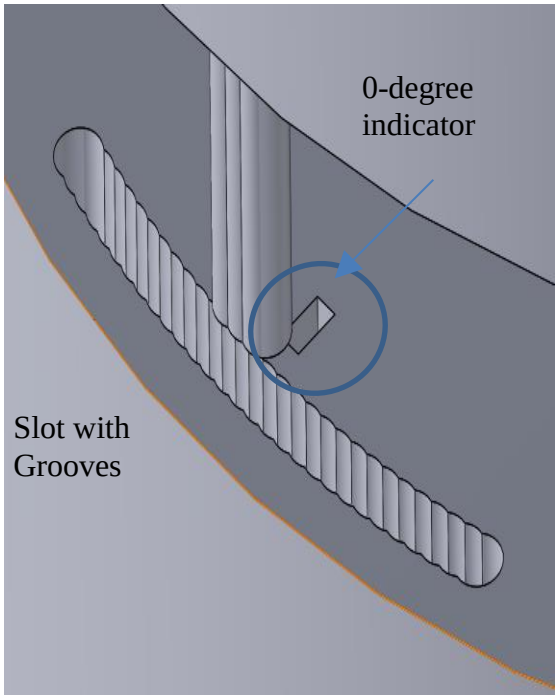

Figure 12: Pin Location on "Crock-Pot"

This design had the top section connect to the hitch adjuster portion of the tire rig. The bottom section has the piece that can rotate, allowing for different camber angles to be tested. The bottom of this component attached to the part of the rig that adjusts the slip angle. This piece has a slot on two sides with cylinder-shaped grooves at 1 degree intervals. The top section has a 3-piece cylindrical peg that fits into this groove to lock at the desired angle. There are also handles on both sides to allow for easier adjustment.

“Swiss-Cheese” Concept:

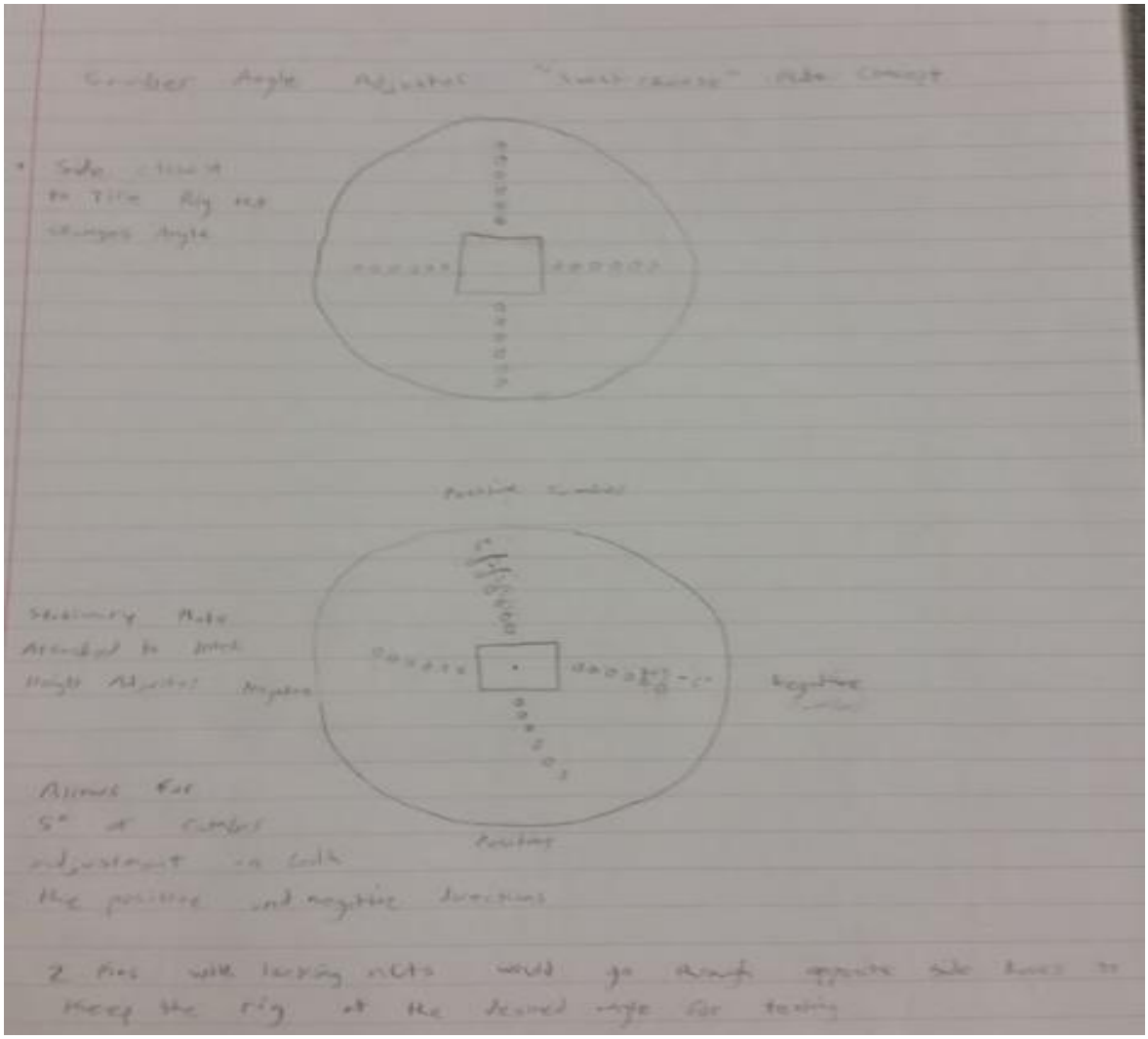

Figure 13: "Swiss-Cheese" Concept

This concept had two plates with .25” holes in each. The plate closest to the frame of the rig and the slip angle component has 6 holes evenly space apart on 4 sides of the plate. The holes closest to the center set the rig at a camber angle of 0 degrees. This plate rotates the rig to adjust to 5 degrees in both the positive and negative direction. The other plate has 6 holes on 4 sides, but these holes slightly change distances apart and are placed between 0 and 5 degrees from the center of the plate. Locking pins go through the holes of the two plates, 2 total which are placed on the opposite side of each other. The top and bottom holes put the rig in positive camber while the holes on the left and right lock the rig at negative camber.

Concept Evaluation:

Weighted Rating Camber Angle Adjustment Concept Alternatives							
		"Swiss Cheese" Plates		"Crock Pot" Concept		"Camber Cat" Concept	
Criteria	Importance Weight	Rating	Weighted Rating	Rating	Weighted Rating	Rating	Weighted Rating
cost	0.25	3	0.75	0	0	2	0.5
ease of use	0.15	3	0.45	3	0.45	4	0.6
manufacturability	0.15	4	0.6	1	0.15	4	0.6
ease of repair	0.1	2	0.2	2	0.2	2	0.2
robustness	0.15	2	0.3	2	0.3	3	0.45
data capture complexity	0.15	2	0.3	2	0.3	3	0.45
Safety	0.05	3	0.15	2	0.1	3	0.15
Total	**1**	**n/a**	**2.75**	**n/a**	**1.5**	**n/a**	**2.95**

Rating	Value
Unsatisfactory	0
Just Tolerable	1
Adequate	2
Good	3
Very Good	4

Figure 14: Camber Angle Weighted Rating

After evaluating each option based on the rig criteria the “Camber Cat” concept had the highest rating and was the concept chosen.

SLIP ANGLE ADJUSTMENT METHOD

Slip Angle “Crock-Pot” Concept:

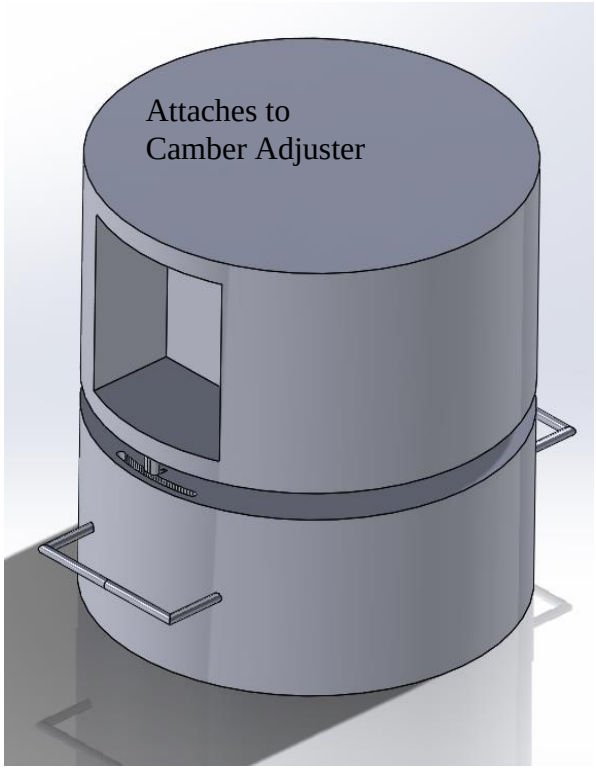

Figure 15: "Crock-Pot" Slip Angle Concept

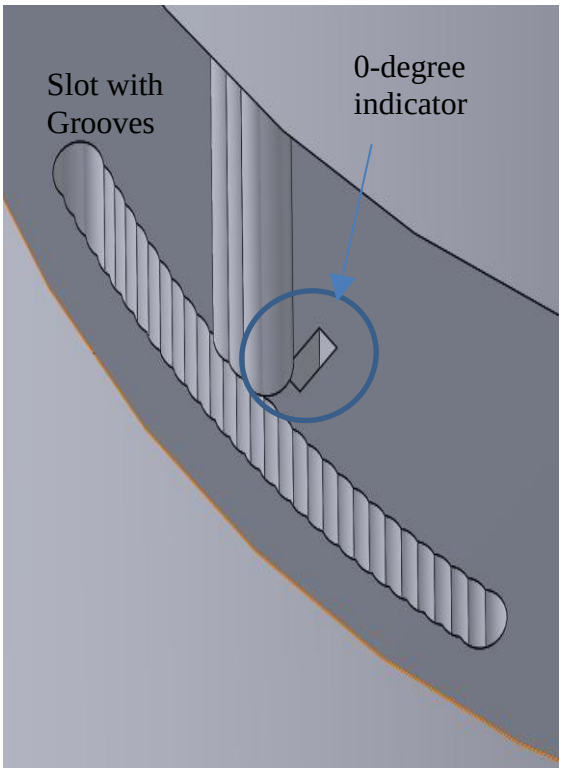

Figure 16: "Crock-Pot" Pin Location

This design had the top section connect to the camber angle portion of the tire rig. The bottom section is the piece that can rotate, allowing for different slip angles to be tested. This piece has a slot on two sides with cylinder-shaped grooves at 1 degree intervals. The top section has a 3-piece cylindrical peg that fits into this groove to lock at the desired angle. There are also handles on both sides to allow for easier adjustment.

Motor and Pulley System Concept:

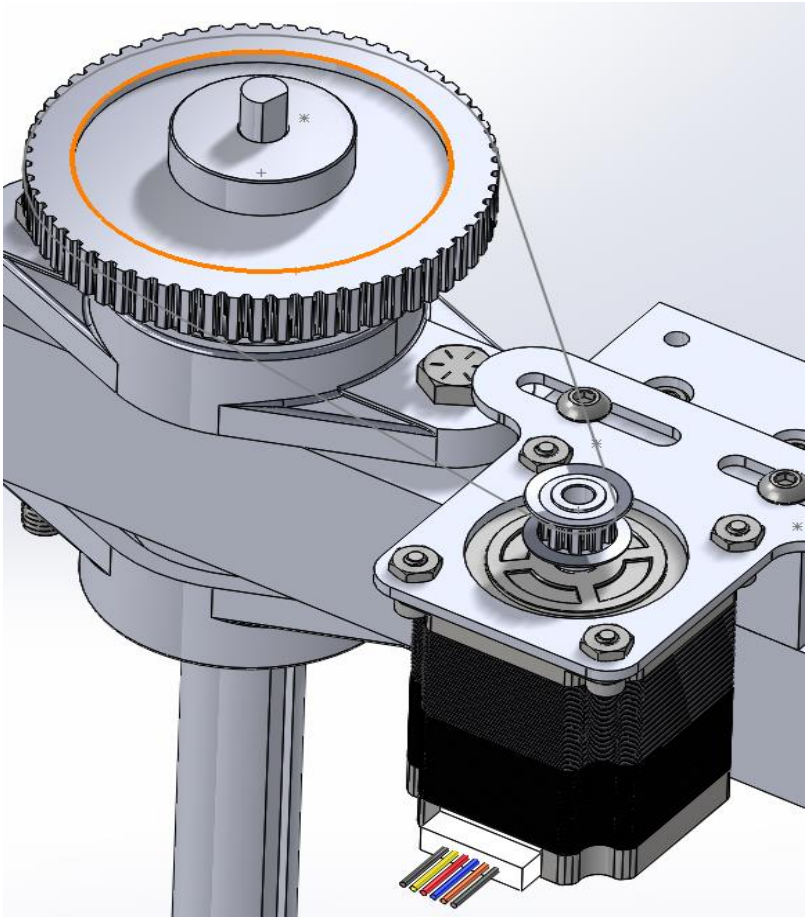

Figure 17: Motor/Pulley Concept

This concept had a motor with a small driver pulley drive a larger timing pulley. The large pulley sits directly above the tire cage and is connected to a keyed shaft which is connected to the top of the tire cage. The driver pulley is run by a CNC stepper motor Nema 23. This would allow a more precise change of slip angle and allow the angle to be automatically changed while a test is being conducted to save time. This concept would also allow a bigger size motor or another motor parallel to the one shown by bolting to the other side of the mounting block.

Weighted Rating Slip Angle Adjustment Concept Alternatives					
		"Crock Pot" Concept		Motor/Driver and Pulley	
Criteria	Importance Weight	Rating	Weighted Rating	Rating	Weighted Rating
cost	0.25	0	0	2	0.5
ease of use	0.15	3	0.45	4	0.6
manufacturability	0.15	1	0.15	3	0.45
ease of repair	0.1	2	0.2	2	0.2
robustness	0.15	2	0.3	2	0.3
data capture complexity	0.15	2	0.3	3	0.45
Safety	0.05	2	0.1	2	0.1
Total	**1**	**n/a**	**1.5**	**n/a**	**2.6**

Rating	Value
Unsatisfactory	0
Just Tolerable	1
Adequate	2
Good	3
Very Good	4

Figure 18: Slip Angle Weighted Rating

After evaluating each option based on the rig criteria the “Motor/Driver and Pulley” concept had the highest rating and was the concept chosen.

LOAD CELL INTERFACE

The load cell mounting concept that was chosen has all of the load cells interface to the axle at one point. The design required that all load cells lines of action be centered with the axle in order to eliminate any large moments that could interfere with the load measurement.

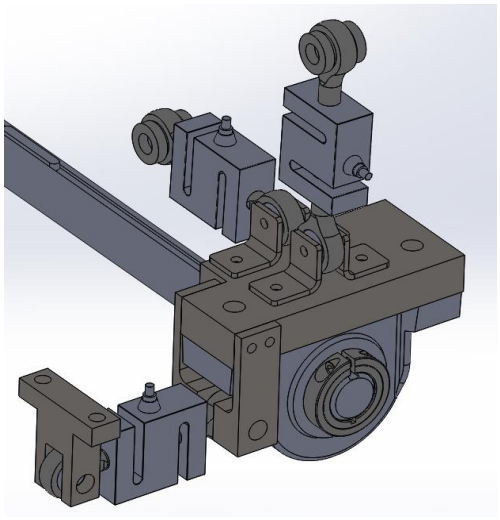

Figure 19: Original Load Cell Interface view a

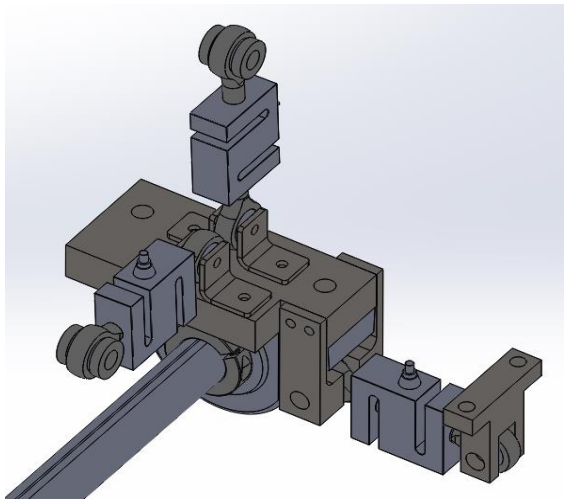

Figure 20: Original Load Cell Interface view b

An initial concept used the same pillow block bearing that is used to support the axle. The bearing would be fixed to the end of the axle and an adapter plate would interface the y-axis and z-axis load cells to the bearing. The y-axis load cell would be mounted to the frame and the z-axis load cell would be mounted to the vertical support gusset. Since the design required that all load cells lines of action be centered with the axle in order to eliminate any large moments, the x-axis load cell had to be spaced off of the load cell mounting surface. This required two spacing support block to be machined. The load cell would then be mounted to the frame with a machined clevis block.

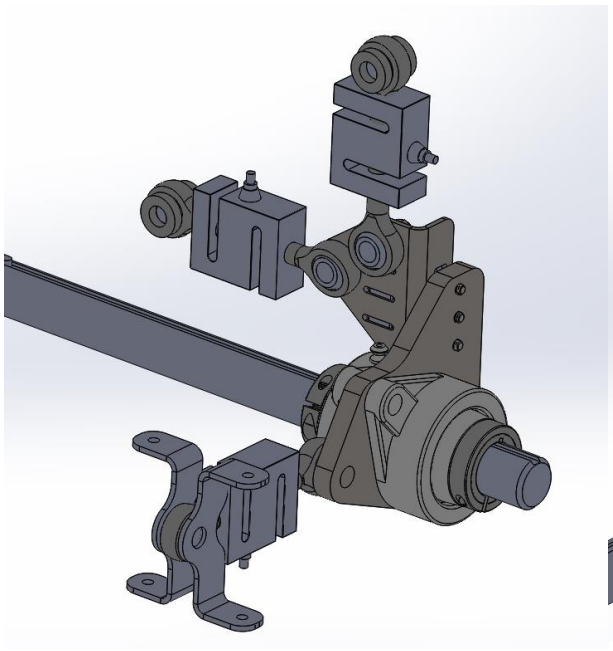

Figure 21: Current Load Cell Interface view a

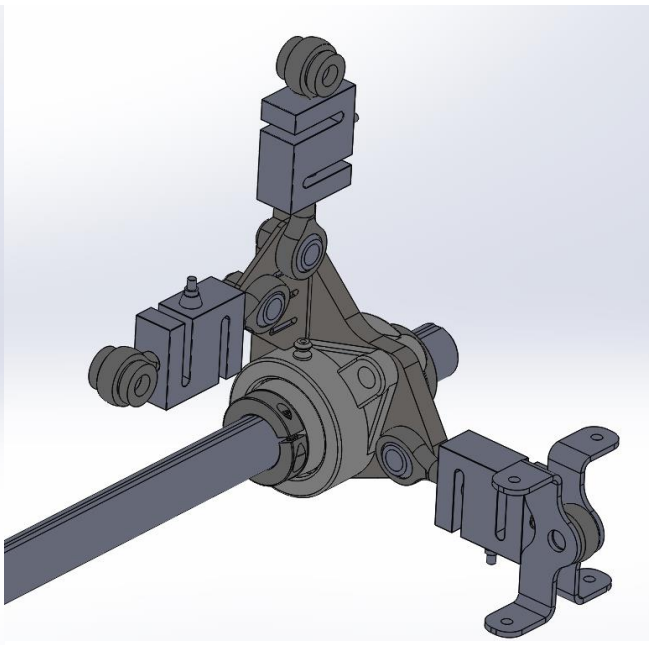

Figure 22: Current Load Cell Interface view b

This design was updated to use two flange bearings fixed to the end of the axle. The flange bearings are mounted to a plate which acts as the mounting surface for the load cells. The y-axis and z-axis load cells are mounted to a separate bracket which is bolted to the bearing plate. The x-axis load cell mounts directly to the bearing plate and is mounted to the frame with two sheet metal brackets.

This design made it easier to position the load cells. The use of sheet metal, rather than machined parts, also reduced cost and fabrication time.

ELECTRONICS

The rig took its power from the seven-way trailer plug on the back of the tow vehicle. The parking light circuit was used to allow the operator an easy way of cycling the rig power on and off and because it would not be affected by turning the vehicle on and off. This power is at the vehicle system voltage, ranging from 11 to 14.5 volts DC. On the rig this voltage is stepped down to five volts DC to power the computer and data logging electronics. Another circuit steps the voltage up to 24 volts DC to drive the stepper motor. During testing current draw from the entire rig never exceeded 1.0 amps at 12 volts DC.

The load cells chosen were Optima Scale OP-312 500 pound s-type load cells. Advantages of this load cell included the ability to be loaded in both tension and compression, a safe

overload of 750 pounds, a relatively compact size, and the availability of higher capacity models in the same physical housing. The manufacturer's specifications are given below:

Rated Capacity:	25/50/75/100/150/200/250/300/500/750/1K/1.5K/2K/2.5K/3K/5K/10K/15K/20K/30K/40K lb.
Rated Output:	3.0mV/V.
Non-linearity:	±0.03% F.S .
Hysteresis:	±0.02% F.S .
Non-Repeatability:	0.01% F.S .
Creep(30min):	±0.03% F.S .
Tempertature effect span:	15PPM/℃ of Applied Load .
Tempertature effect zero:	26PPM/℃ of Applied Load .
Operation Temperature:	-40℃-65℃.
Input Impedance:	385±20Ω.
Output Impedance:	350±3Ω.
Safe overload:	150%F.S .
Destructive Load:	300%F.S .
Excitation Recommended:	10~15V AC/DC.
Construction:	Alloy Steel/Stainless Steel .

Table 1: Load Cell Specifications

The computer selected was the Raspberry Pi B Model 3. With a 1.2GHz processor it was the fastest Raspberry Pi available at the time and offered the most digital input/output pins at 40. It also was the easiest to interface with for development with four USB ports, an HDMI port, and integrated wireless LAN.

The load cell amplifiers used were the Avia Electronics HX711 chip. They convert the signal from the strain gages inside the load cells to 24 bit logic level digital signals for the Raspberry Pi to process.

The infrared temperature sensors were the Texas Instruments TMP007 on Adafruit breakout boards. They provided 14 bit object surface temperatures and ambient temperatures measured at the sensor with a stated accuracy of +/- 3F. The sensors communicated to the Raspberry Pi over an I2C communication bus. The ambient temperatures from each individual sensor were averaged and used to determine the ambient temperature inside of the test rig.

ADDITIONAL DESIGN CONSIDERATIONS

Loading Conditions

Dirt oval karts only turn left. Their chassis and tires are asymmetric. Due to their center of gravity heights, typical oval kart setups carry 85-95 percent of their weight on the right side tires at peak lateral acceleration. (3) For determining the design loads, the worst case scenario was taken to be a 400 pound kart at a lateral acceleration of 1.5G. (1,4) It was assumed that all of the kart's weight would be evenly distributed between the right side tires, with no weight on the left side tires. At this condition, each right side tire would experience a normal load of 200 pounds and generate a lateral load of 300 pounds. It was decided that a design factor of 2.5 should be applied to the normal load, to account for bumps in the track surface, boosting the design load to 500 pounds in the normal direction (z-axis). Because of the nature of pneumatic tires lateral force generation does not increase linearly with an increased normal load, such as a bump. Tires loose efficiency as normal load is increased resulting in diminishing returns of lateral force. (6) Due to this phenomena, the design load in the lateral direction (y-axis) was set at 500 pounds. The design load for the longitudinal direction (x-axis) was also set at 500 pounds for consistency, though the anticipated longitudinal loads generated by the tires were expected to be far less than the lateral loads.

Deflection and Axle Misalignment

Due to the way the “Fixed and Floating Bearing on Axle” load cell mounting concept constrained the axle of the test rig, deflection in the load cells would lead to misalignment of the axle. Deflection of the y-axis load cell would alter the tire’s actual slip angle and deflection of the z-axis load cell would alter the tire’s actual camber angle. According to the load cell manufacturer, the maximum deflection would be .005 inches in tension and compression for the model chosen.

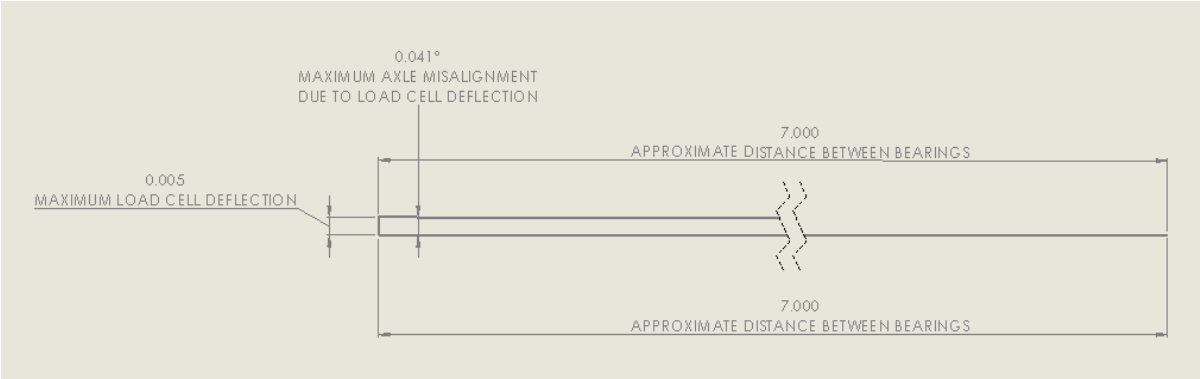

Figure 23: Impact Load Cell Deflection

Figure 23 illustrates the impact load cell deflection had on axle misalignment. The maximum change to slip angle or camber angle due to load cell deflection was .04 degrees which was deemed to be acceptable.

It was decided that slip angle and camber angle changes due to compliance in the rig should be kept below .2 degrees. This meant that, factoring in load cell deflection, the load cell mounting points needed to deflect less than .02 inches at the worst case loading condition. However, the rig also needed to be portable and able to test tires at lighter loads. This meant stiffness and weight had to be optimized together.

FINAL DESIGN

Coordinate System

For the remainder of the report the following axes definitions will be used:

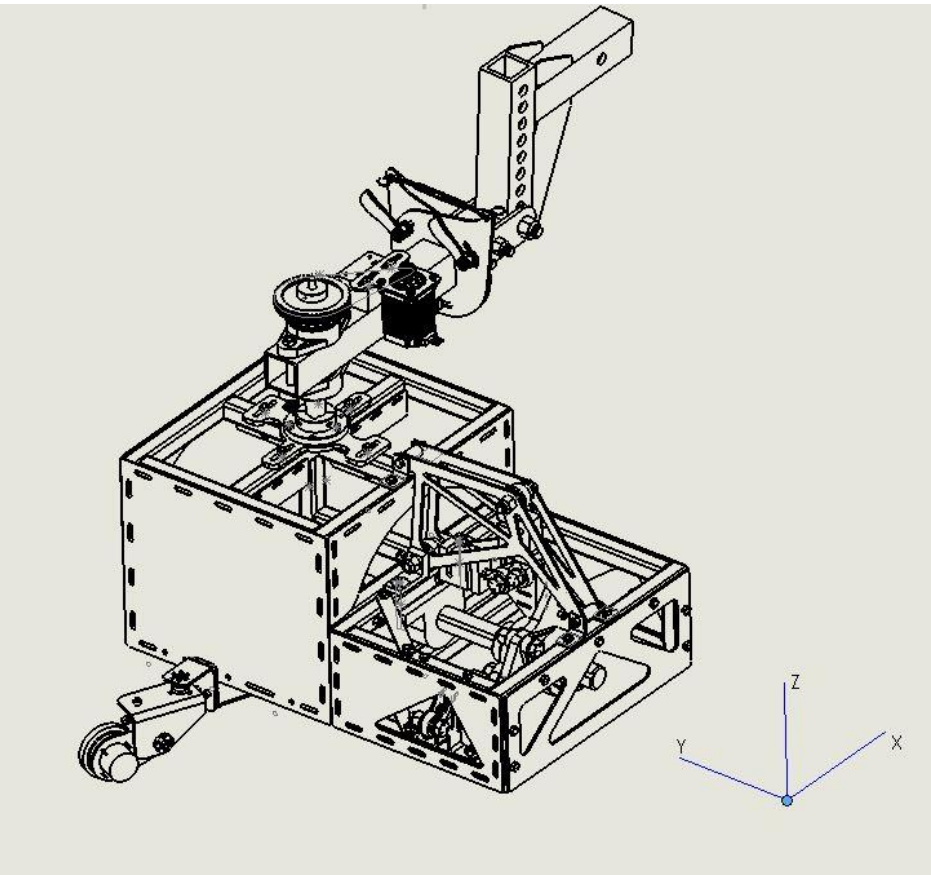

Figure 24: Coordinate System Full Assembly view a

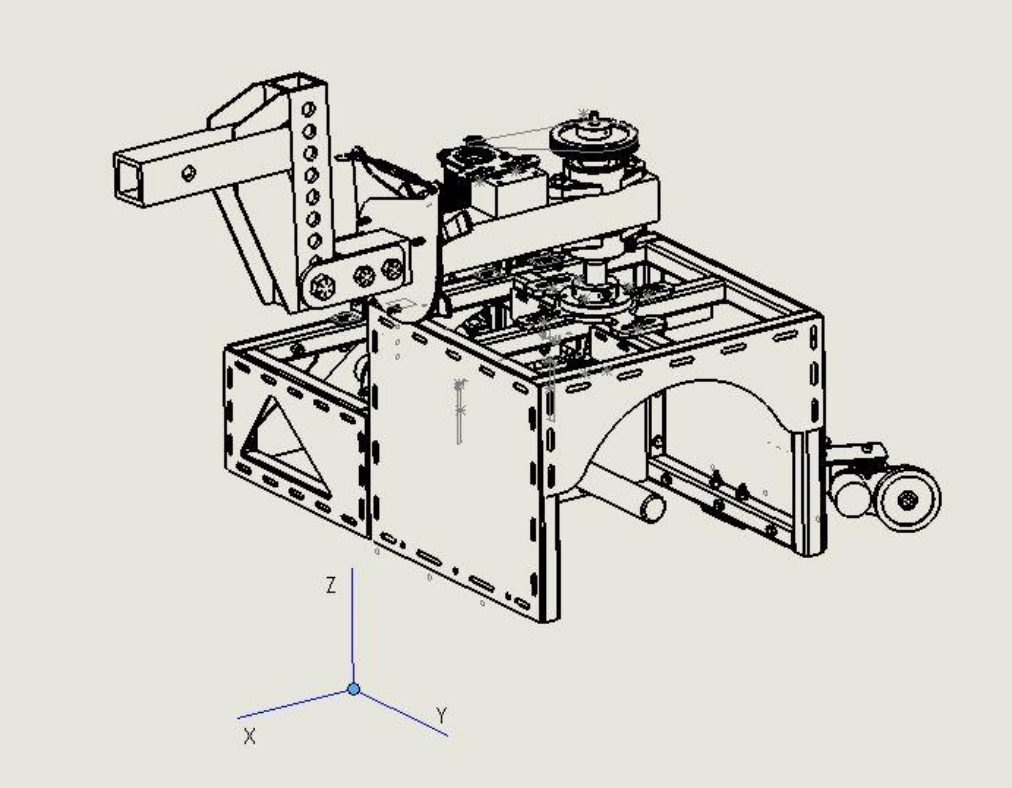

Figure 25: Coordinate System Full Assembly view b

The following major components will be referenced. The subassembly consisting of the load cell cage and tire cage is collectively referred to as the “rear assembly.”

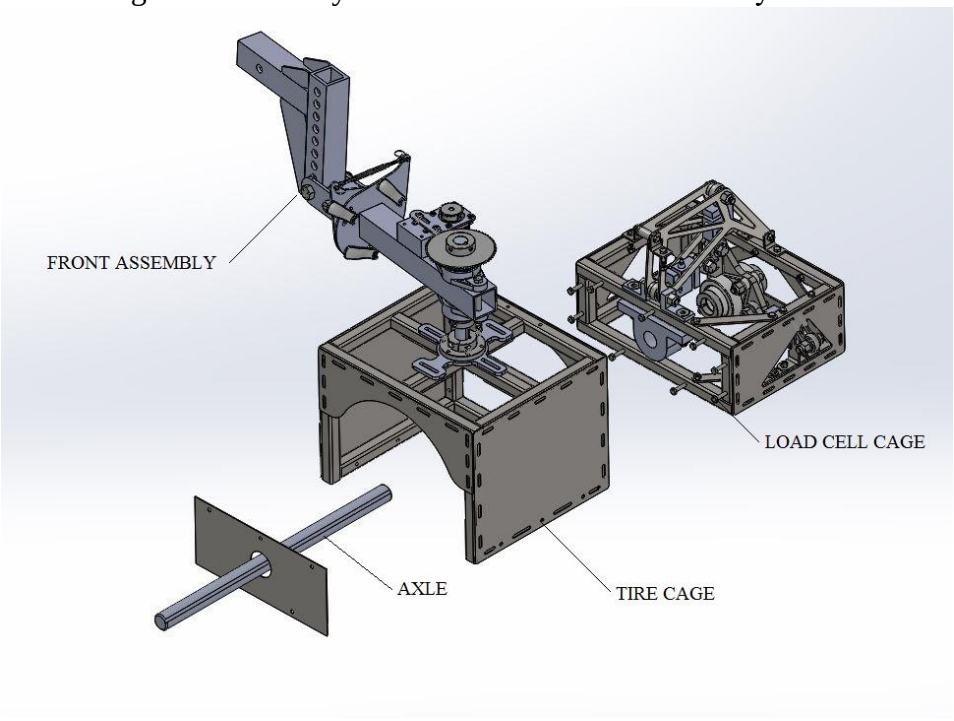

Figure 26: Sub-assembly Nomenclature

Tire Cage

The tire cage is constructed of welded 1 x 1 x .125” steel tube.
The tire is mounted to a go-kart hub on a 1-1/4” steel shaft.

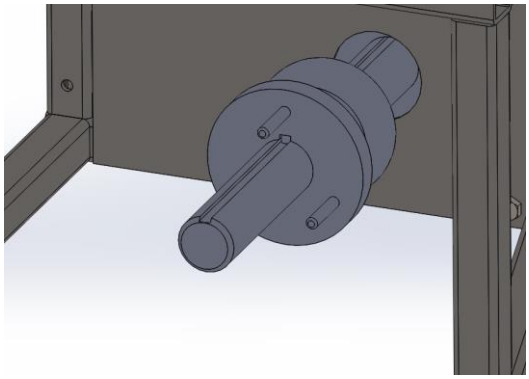

Figure 27: Tire Hub

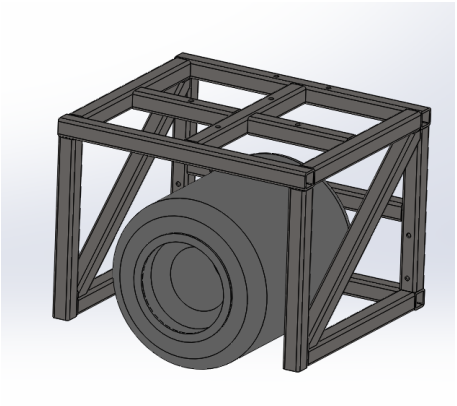

Figure 28: Tire in Tire Cage

The shaft is supported near the middle by a UCP206-20 pillow block bearing mounted to the load cell cage.

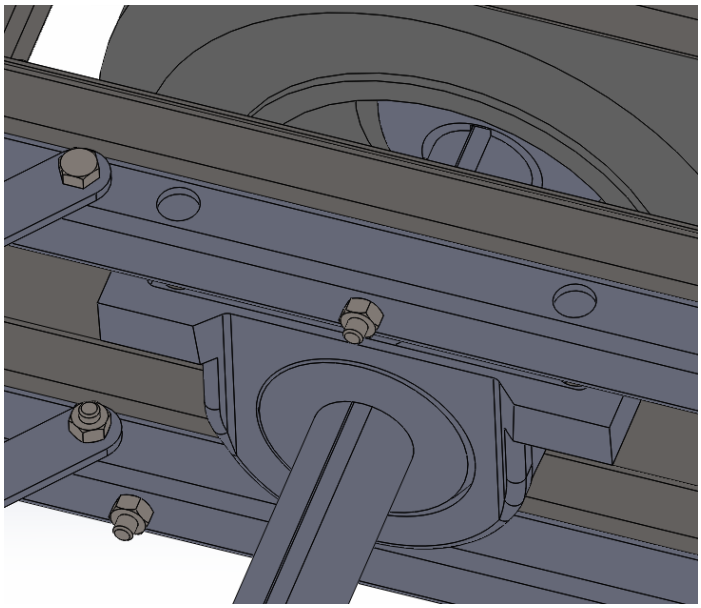

Figure 29: Pillow Block Bearing and Axle Interface

Load Cell Cage

The load cell (LC) cage is also constructed of welded 1 x 1 x .125” steel tube. 10 GA steel stiffener plates are plug welded to the front and back of the cage. The side of the cage has a 10 GA stiffener plate attached with 1/4-20 bolts for access.

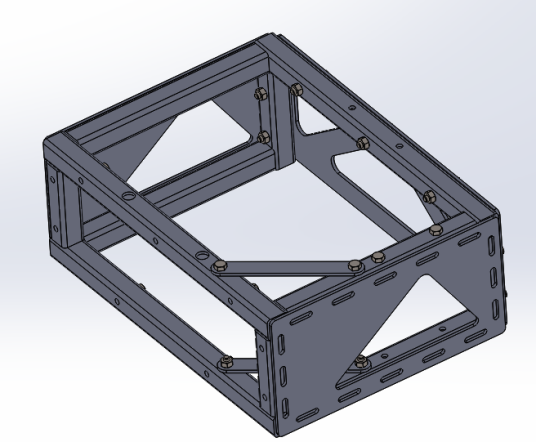

Figure 30: Load Cell Cage view a

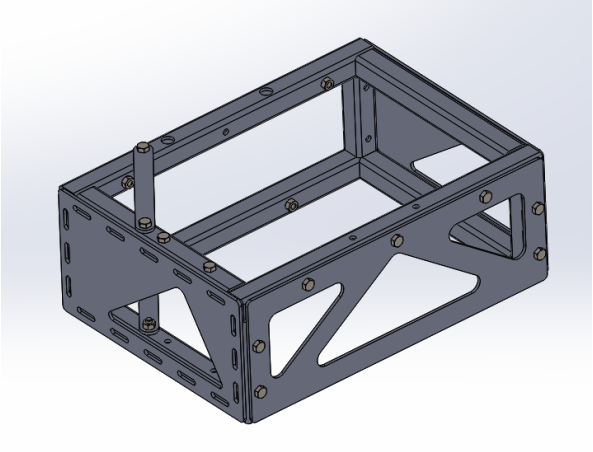

Figure 31: Load Cell Cage view b

Two 10 GA stiffening members are bolted to the top and bottom of the back inside corner of the cage with (4) 1/4-20 bolts

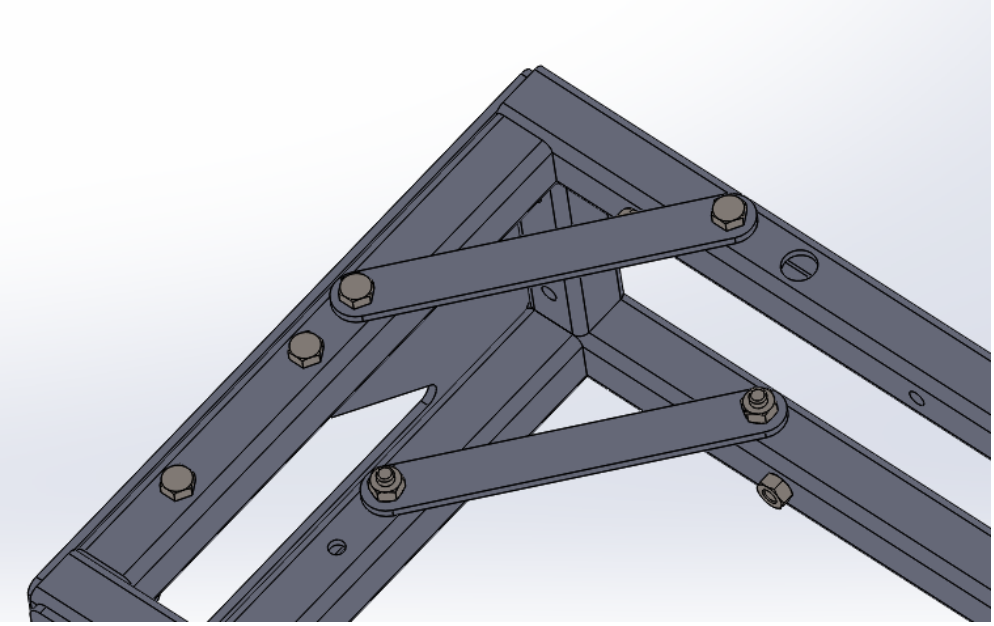

Figure 32: LC Cage Straps and Bolts

The load cell cage is bolted to the tire cage with (9) 1/4-20 bolts.

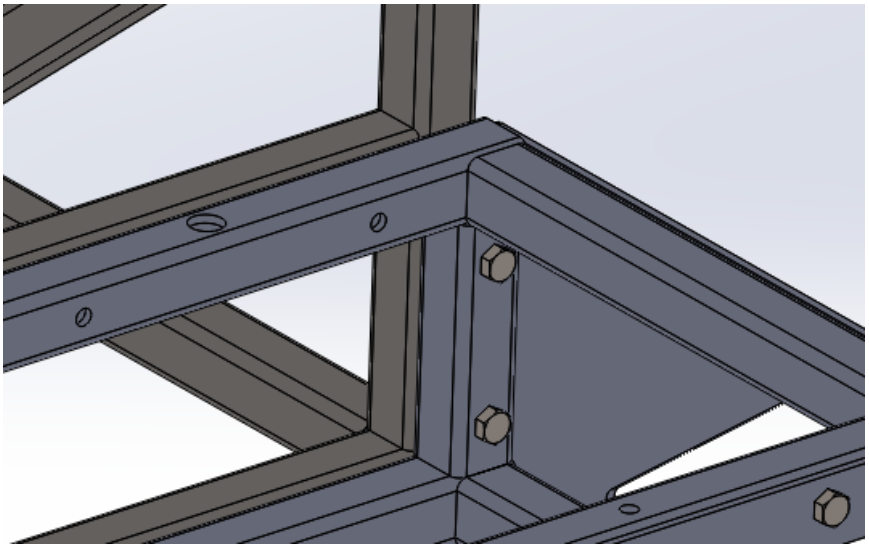

Figure 33: Tire Cage and LC Cage Bolt Interface

The pillow block bearing that supports the axle is mounted to the load cell cage with (2) 1/2”-13 bolts through two machined brackets.

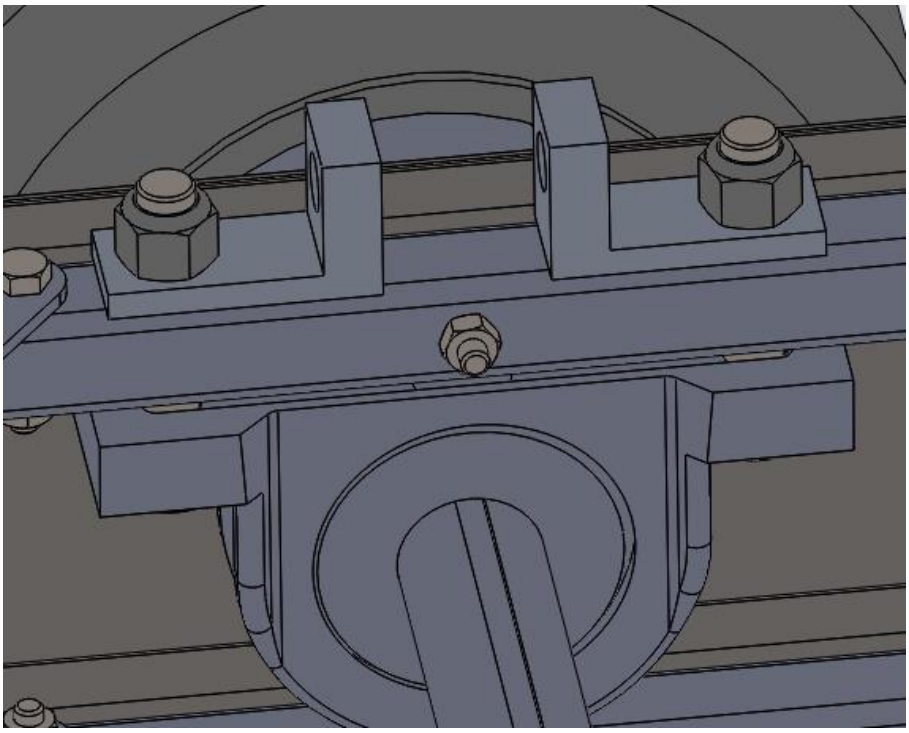

Figure 34: Axle Supported by Pillow Block Bearing

Load Cell Interface

The load cell interface is the point through which all loads from the tire are transferred. A main pillow block bearing supports the axle, ensures smooth shaft rotation, and acts like a spherical joint, allowing for 20 degrees of axial misalignment.

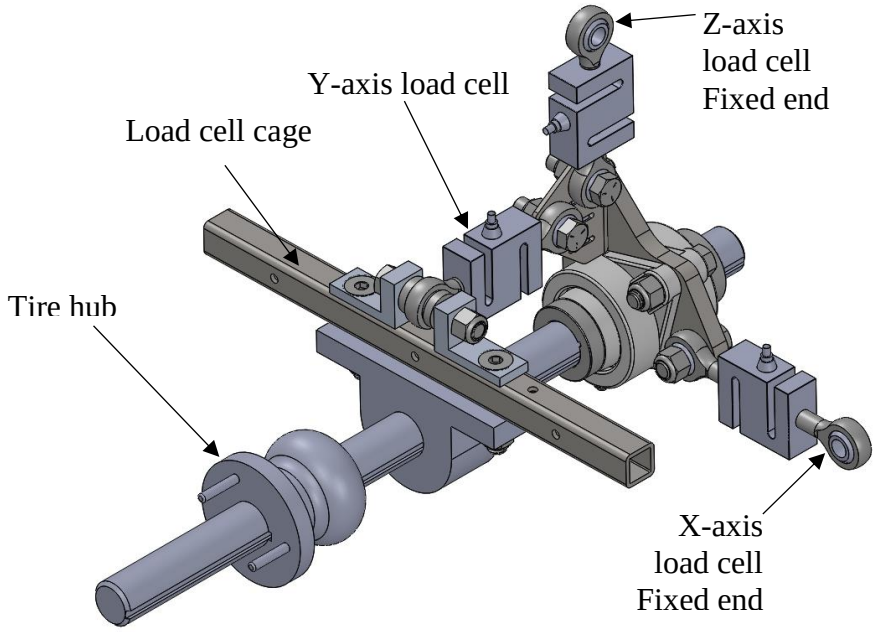

Figure 35: Load Cell Interface 1

The main bearing acts as the fulcrum and any load applied to one end of the axle will displace the axle on the other end. The load cell interface captures this displacement and uses load cells to measure the force applied. The hub is positioned on the axle so that main bearing is in the center. This ensures that the force input on one end of the axle is equal to the force output on the other end of the axle.

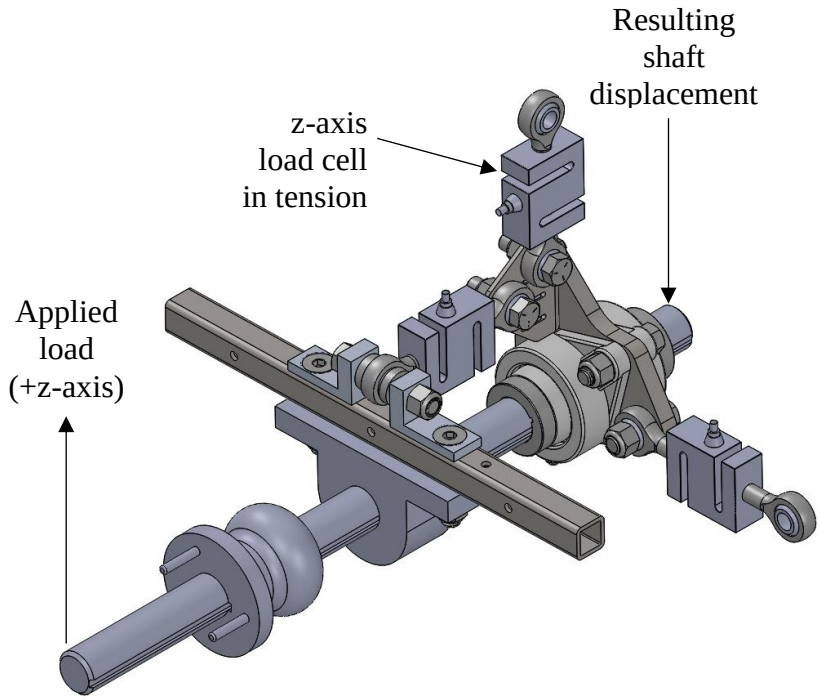

Figure 36: LC Interface 2

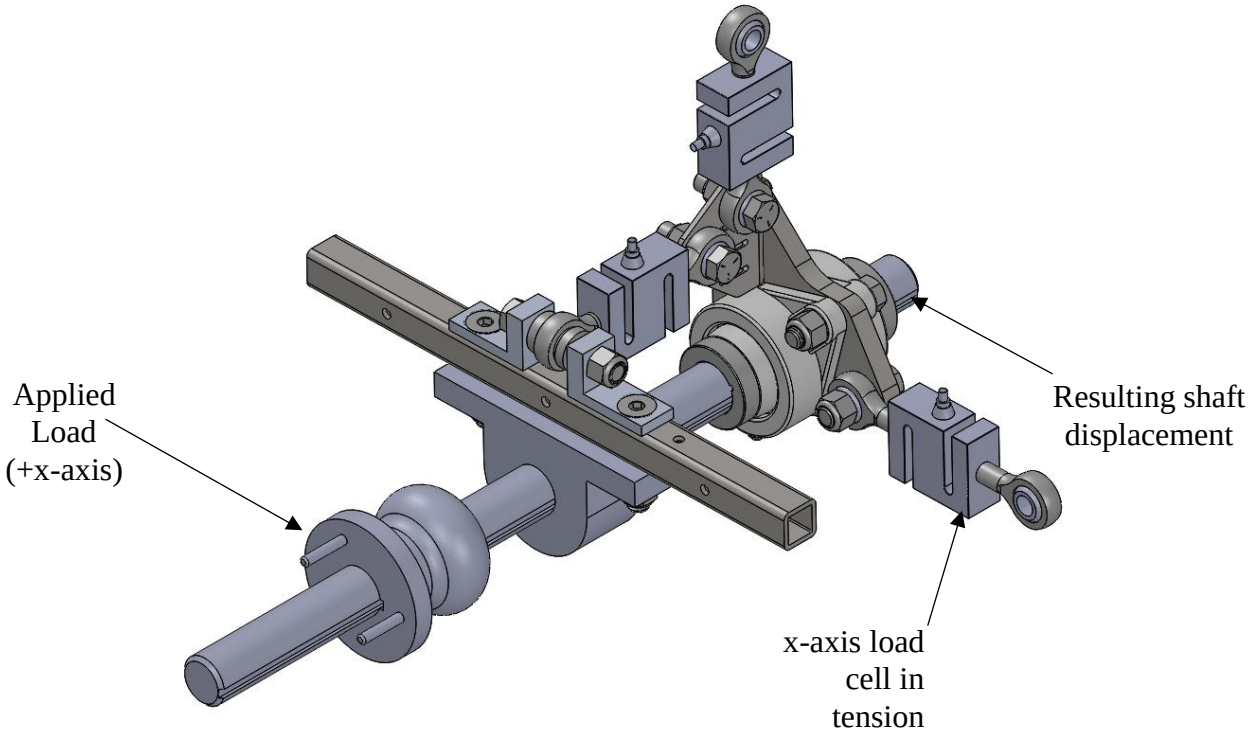

Figure 37: LC Interface 3

In order for the loads to transfer to the y-axis load cell, the shaft is free to slide through the main bearing axially. However, the actual displacement is very low since the load cells only deflect .005” maximum.

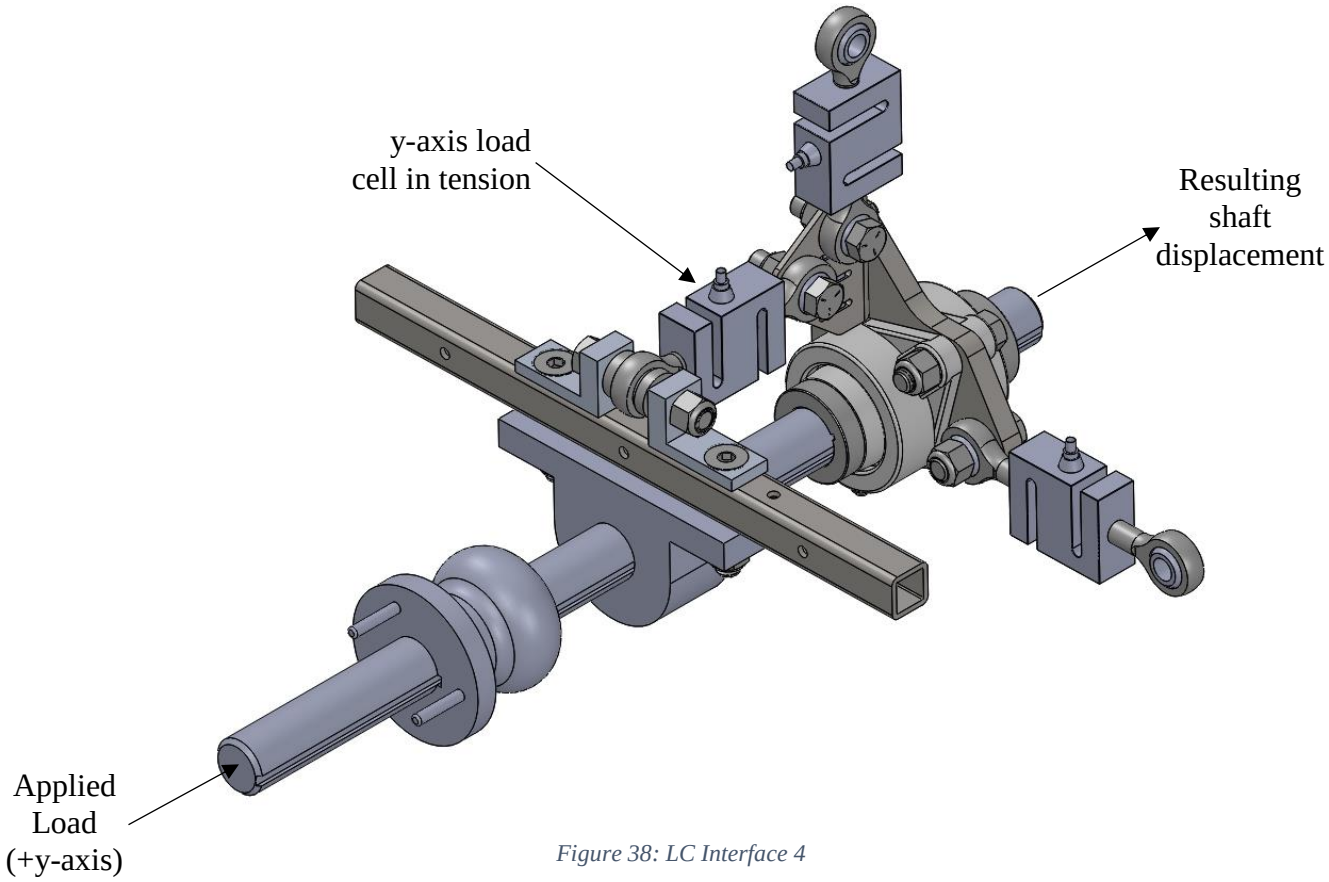

Figure 38: LC Interface 4

The load cell interface assembly attaches three load cell assemblies to the axle. Each load cell assembly consists of a s-beam load cell with a rod end on either side.

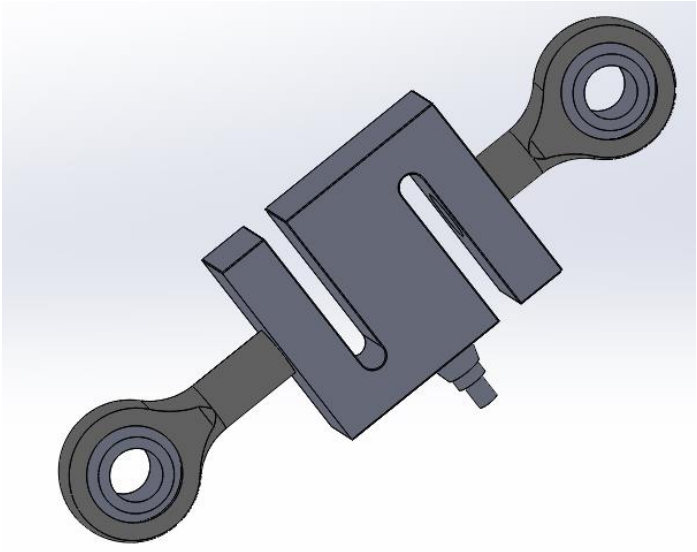

Figure 39: LC with Rod Ends

The load cell interface consists of a ½" thick laser cut, steel plate sandwiched between two flange mount bearings. The assembly is anchored to the end of the shaft with split clamps on either side.

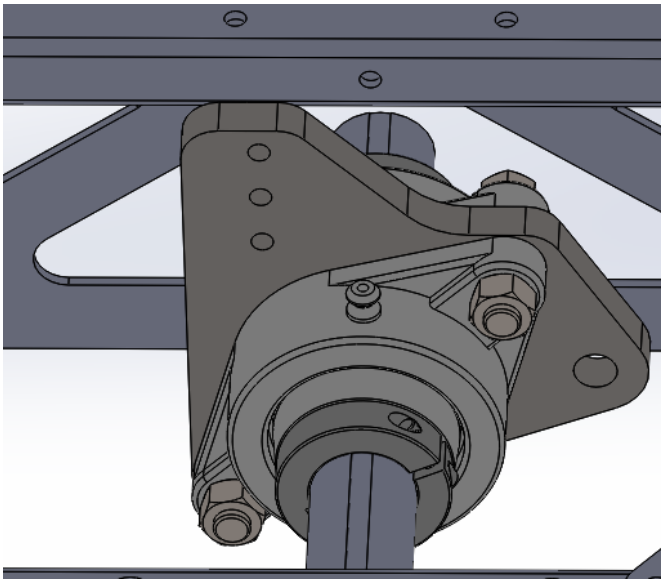

Figure 40: Steel Plates and Bearings view a

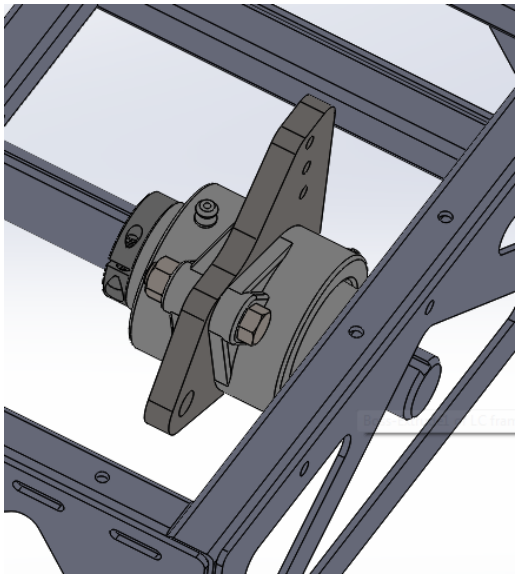

Figure 41: Steel Plates and Bearings view b

The x-axis load cell is bolted to the inside of the load cell interface plate with a 1/2"-13 bolt. The other side of the load cell is supported by two 10 GA laser cut sheet steel brackets.

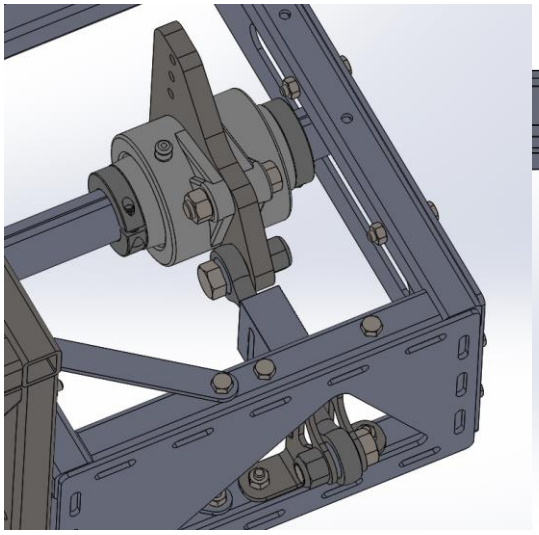

Figure 42: Steel Plates and Bearings view c

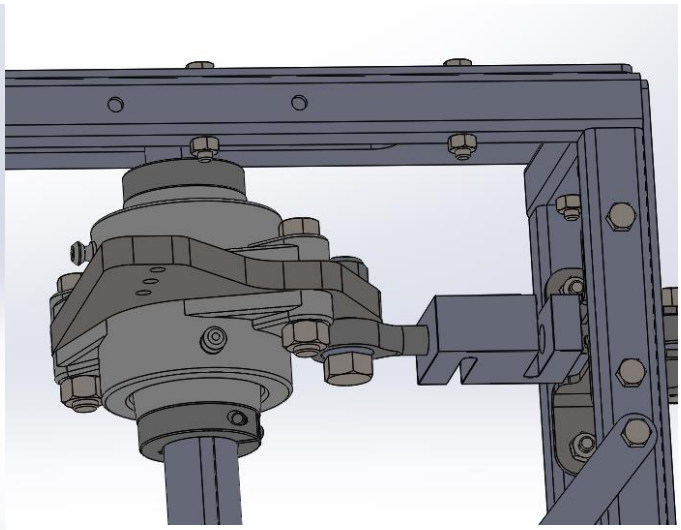

Figure 43: Steel Plates and Bearings view d

The brackets are bolted to the top and bottom of the load cell cage with 1/4" bolts. A 1/2" bolt through the two brackets anchors the load cell in place.

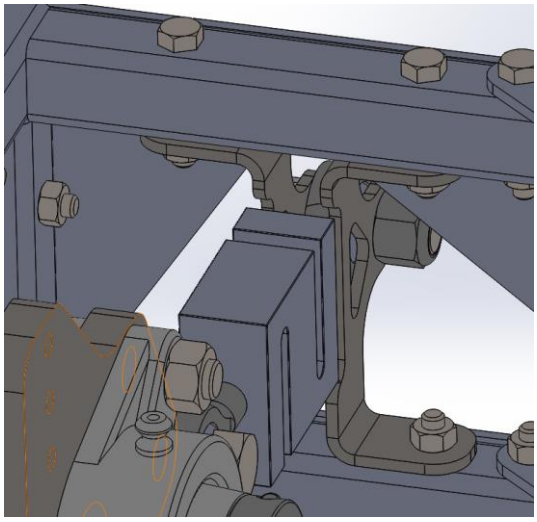

Figure 44: x-axis LC Interface

The y and z-axis load cells are both bolted to a weldment made of a piece of bent 10GA sheet steel and three 10GA gussets. This weldment bolts to the load cell interface plate with (3) 1/4" bolts. The y and z-axis load cells are bolted to the weldment with 1/2" bolts.

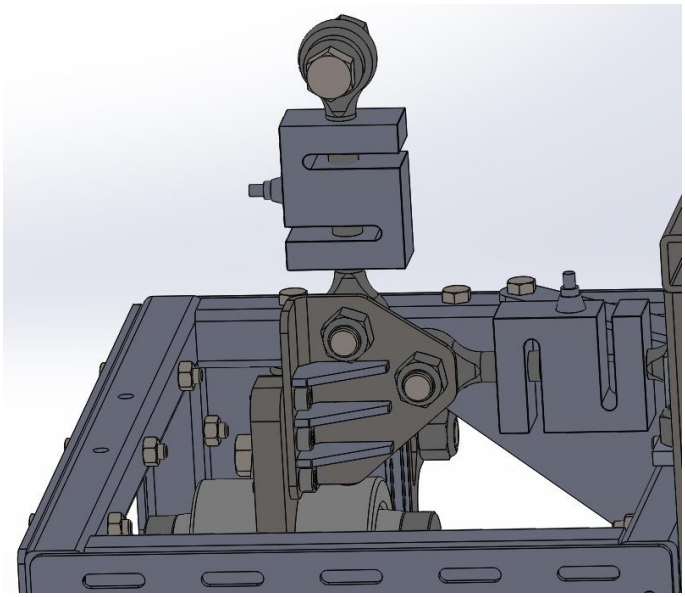

Figure 45: LC Weldment Interface view a

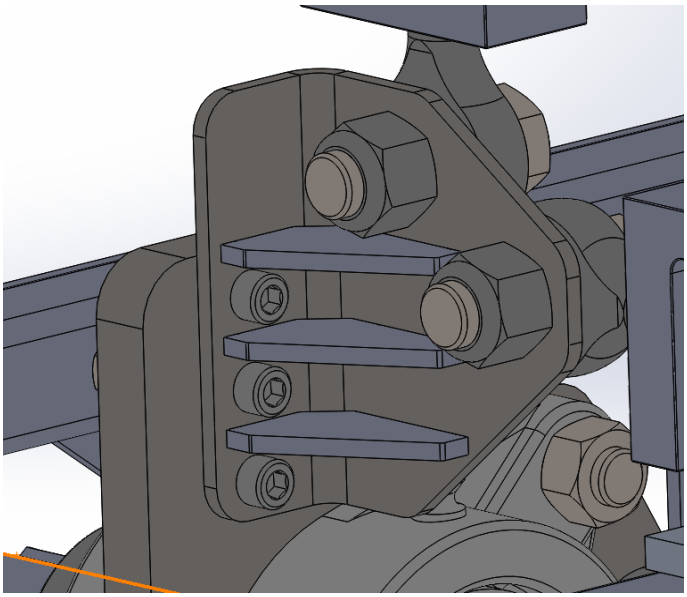

Figure 46: LC Weldment Interface view b

The other end of the y-axis load cell is bolted to the frame with the machined aluminum brackets that also attach the pillow block bearing to the frame. A 1/2" bolt goes through the brackets, vertical support gusset, spacers, and load cell assembly.

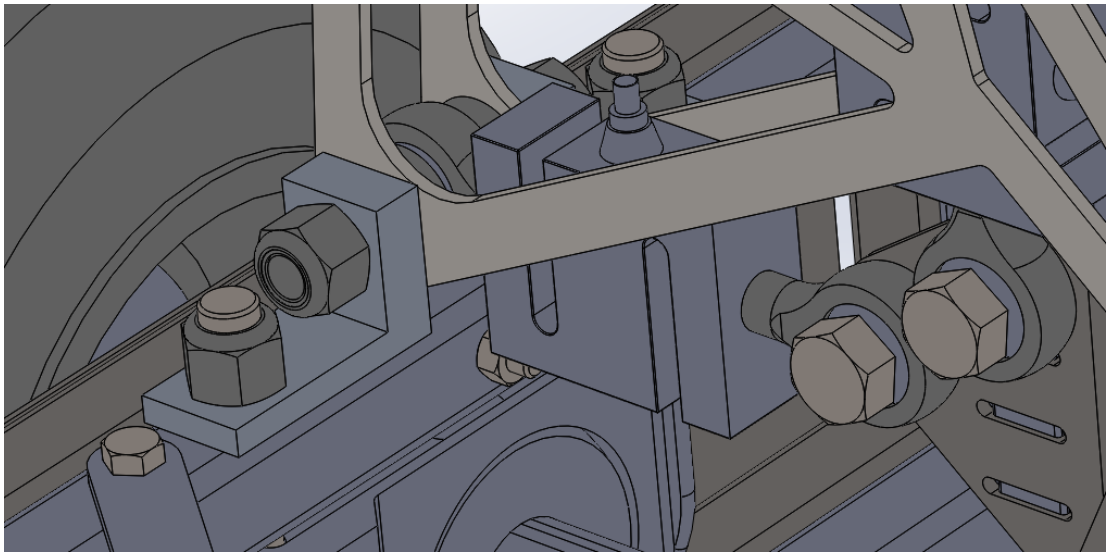

Figure 47: y-axis LC Interface

The vertical support gussets are laser cut 10 GA steel brackets which stiffen the rig and also supply a point to attach the z-axis load cell. The gussets attach to the rig at three points.

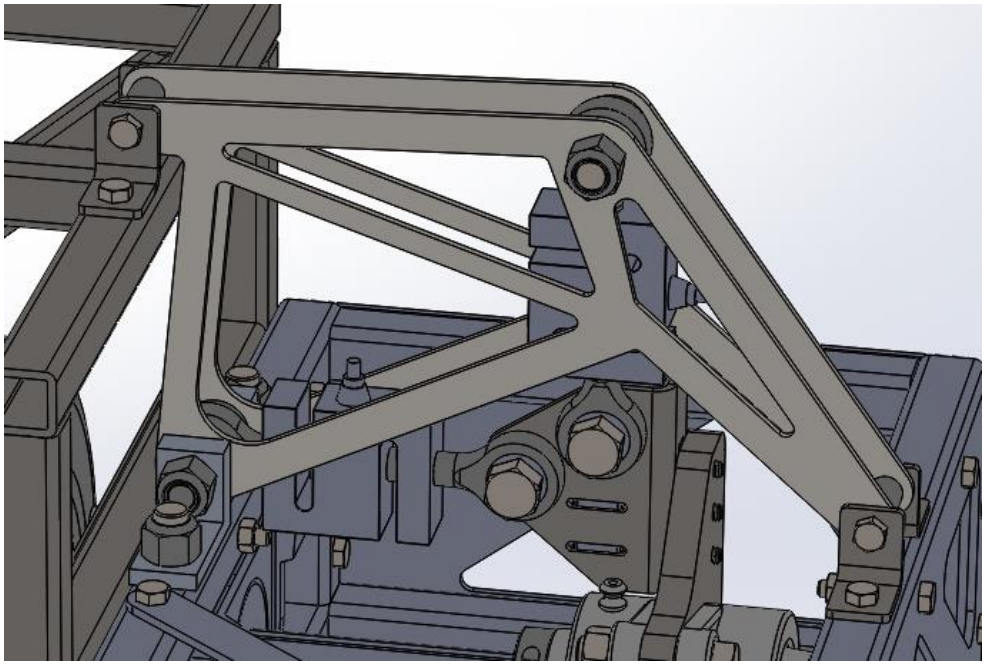

Figure 48: Vertical Support Gussets

One corner attaches to the load cell frame with the machined brackets. Another corner attaches to the top of the tire cage with two 10GA sheet steel brackets and 1/4” bolts. The other corner of the vertical brackets attaches to the outside of the load cell cage with the same 10GA sheet metal brackets. One end of the z-axis load cell is bolted to the vertical support gussets with a ½” bolt. The other end is bolted to the load cell interface weldment bracket.

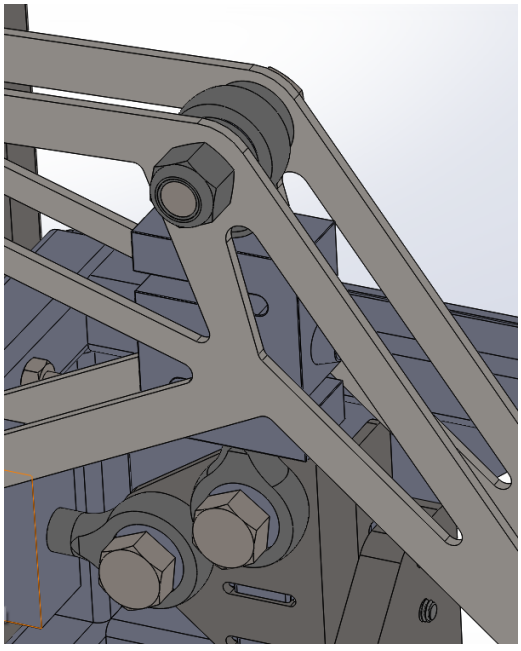

Figure 49: z-axis LC Interface

Front Assembly

Hitch Adapter Sub-Assembly:

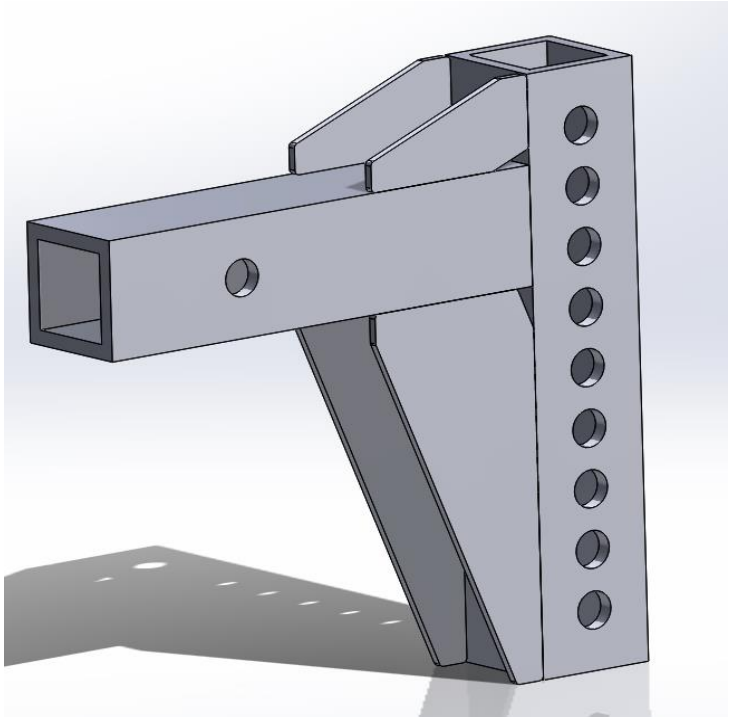

Figure 50: Hitch Adapter Assembly

This hitch adapter assembly was determined to be the best and most efficient design for the needs of the tire rig. The front contains 2” square tube, 1020 Steel, 8” long with a pin hole to easily attach to a square hitch from a pickup truck that is used to pull the tire rig. The gussets are 10-gauge mild steel and are used to reduce the amount of stress and displacement found in this sub-assembly when forces are applied. These gussets are welded into place. A previous design had much shorter gussets that did not make contact with the whole 10” long tube which resulted in high displacement and stress. The vertical square tube is 10” long and features multiple holes. This allows for the remainder of the front assembly to be pinned at different heights based on the distance a truck’s hitch connection is above the ground.

Pivot Plates:

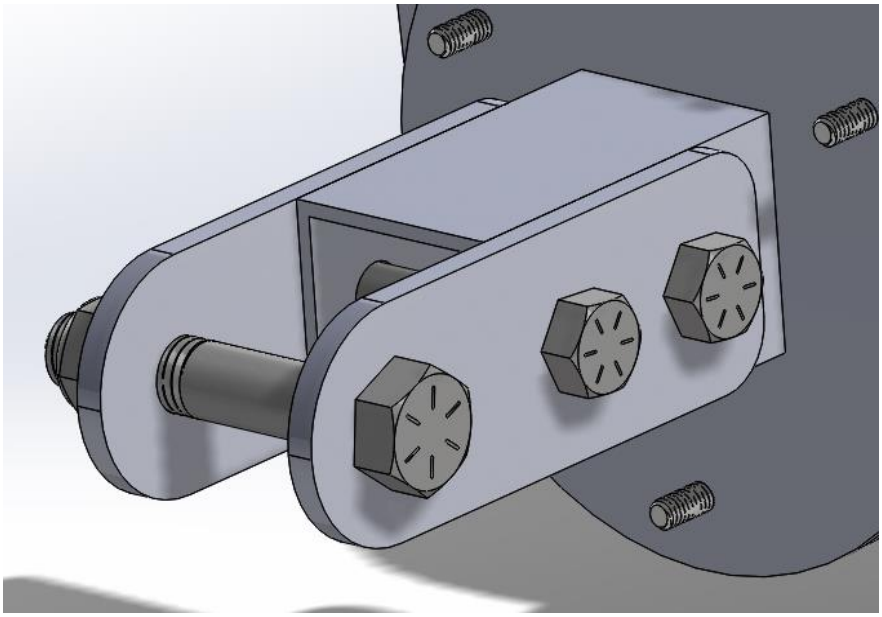

Figure 51: Pivot Plate Interface

The pivot plates interface between the hitch adapter and the rest of the rig. The larger 5/8” bolt acts as a pin joint between the pivot plates and the hitch adapter, allowing the test tire to move vertically over bumps without influence from the truck yet preventing lateral motion. The two smaller bolts near the camber cat are 1/2”. The pivot plates are .25” thick mild steel.

Camber Adjuster:

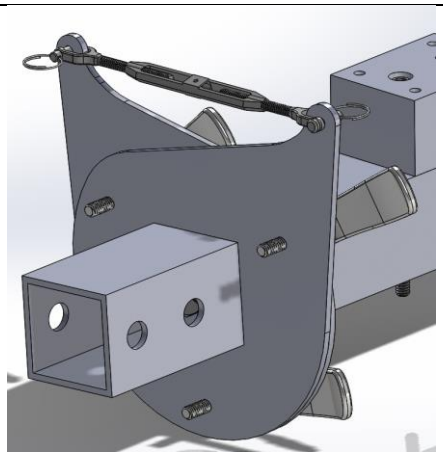

Figure 52: Camber Adjuster view a

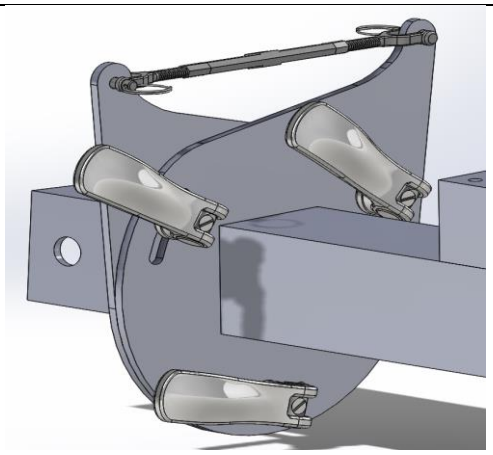

Figure 53: Camber Adjuster view b

The “Camber Cat” had two sheet metal plates rotating about the same axis with a turnbuckle to control the camber angle. The stationary plate had three tapped holes at 90 degree intervals centered around the center hole. The rotating plate had three slots at 90 degree intervals that were concentric with its center hole and at the same radius as the four tapped holes in the stationary plate. During testing, cam locks would sandwich the plates together creating a solid link between the front and rear parts of the testing rig. For camber adjustment, the cam locks would be released allowing the plates to rotate about a pin or bolt through their center axis. The turnbuckle would then allow control of the angle between the front and rear parts of the rig, setting the camber angle. The camber angle itself would be measured by using a standard camber gage on the test rig’s axle. Once the desired angle was reached, the cam locks would be engaged again locking the rig to that angle.

Slip Angle Drive:

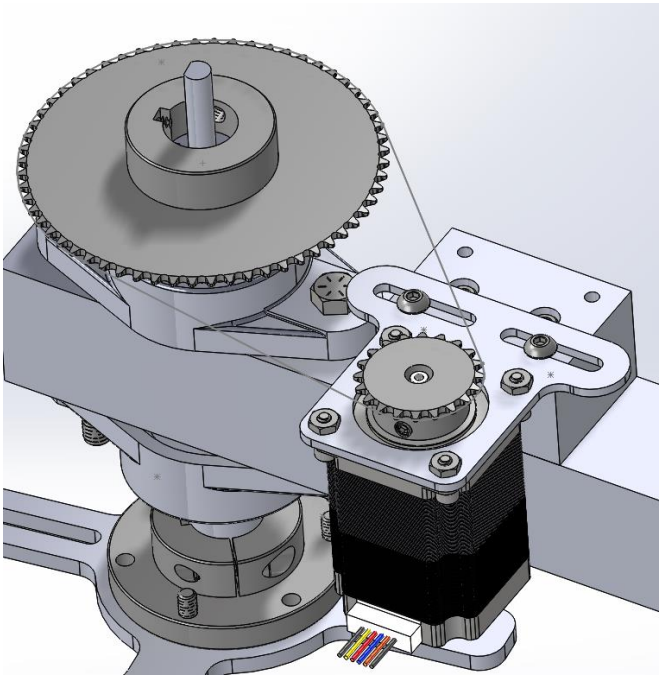

Figure 54: Slip Angle Drive Motor/Sprocket Interface

This system allows the slip angle of the rig to be automatically adjusted while running a test. The initial concept for the slip angle drive was timing pulleys and a toothed belt. This was chosen based on the assumptions made in the initial concept phase. Once the rig was built the motor output and pulley drive were not sufficient to slip the rig. To quantify the torque required to slip the rig, a pair of vice grips was clamped to the slip angle shaft.

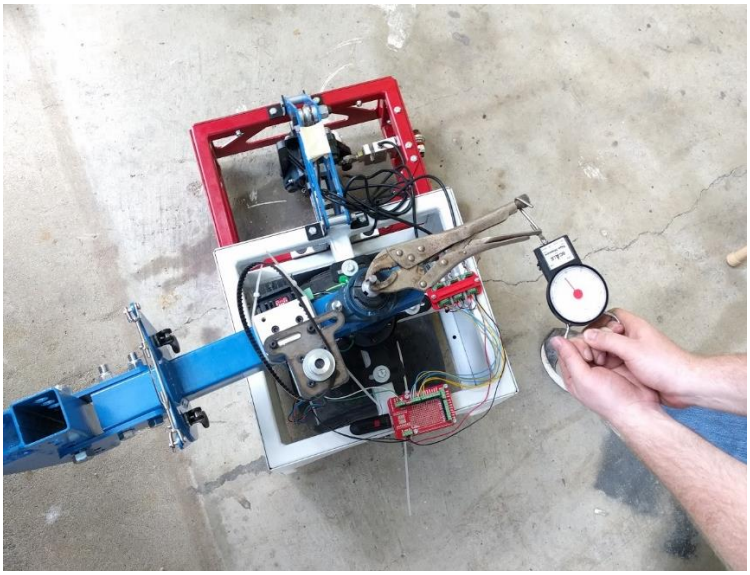

Figure 55: Fish Scale Testing

A fish scale was used to pull on the end of the vice grips. The result was a 25lb load at a moment distance of 8.5 inches. This resulted in a required applied torque of 21.5 in-lb or 17.7 ft-lb to slip the rig (on a concrete surface with the tire at 1 psi). A motor with a 47:1 gearhead was chosen. This motor outputs a running torque of 8.5 ft-lb and a hold torque of 17.7 ft-lb. The drive gear ratio was kept at 3:1 but the pulleys were replaced with a 20 tooth drive sprocket and a 60 tooth driven sprocket. With the 8.5ft-lb motor output and the 3:1 gear reduction, the drive applies a torque of 25.5 ft-lb to the rig. This results in a safety factor of 1.4. The belt was replaced with ANSI 25 chain. According to ANSI standard B29.1-2011, ANSI 25 chain has a minimum ultimate tensile strength of 780lb. The drive sprocket has a OD of 1.73 in (R .865 in). At motor holding torque the chain could experience 245.6 lbs tension. This results in a safety factor of 3.

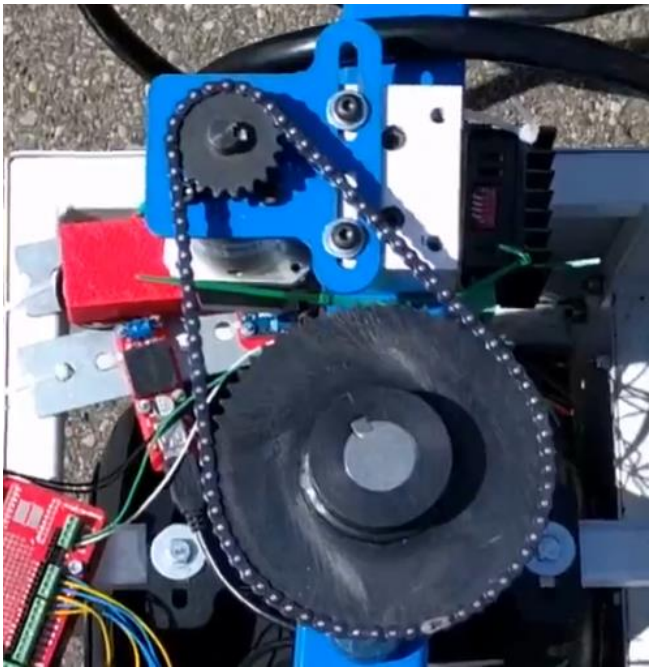

Figure 56: Finished-bore Sprocket Interface

The driver finished-bore sprocket specifications are: #25 Chain, 1/4” pitch, 20 Teeth, and 3/8” bore. ANSI #25 Roller Chain is used which has ¼” pitch and is 2 feet long. The driven sprocket sits directly above the tire cage and is connected to a keyed shaft which is connected to the top of the tire cage. The driven finished-bore sprocket configurations are: #25 Chain, 1/4” pitch, 60 Teeth, and 1” bore. The motor is a 2.8A NEMA 23 stepper motor with a 47:1 planetary gearhead. There is 1.5x backlash at gearhead output. The motor is connected to a mounting plate which is bolted to a block which is centered on the square tube. The mounting block is symmetric which allows another motor to be attached to the other side if needed. This sprocket system is beneficial because it allows the slip angle to be automatically adjusted during test runs.

Slip Angle Drive Cross and Collar:

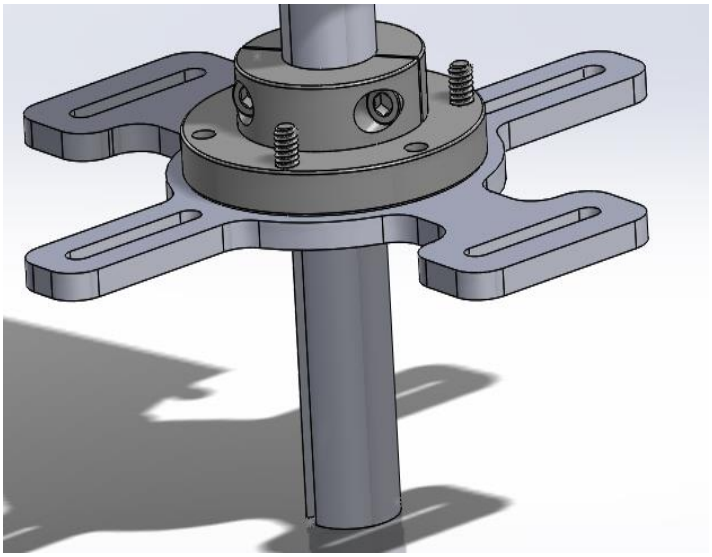

Figure 57: Slip Angle Drive Cross

The slip angle drive shaft connects to the top of the tire cage through a purchased shaft flange. The laser cut drive cross interfaces between the slip angle drive system and the tire cage weldment. The drive cross is bolted to the shaft flange with (3) 1/4-20 flat head screws. Four 1/4” bolts connect the drive cross to the tire cage at the four slots. The slots allow for adjustment of the rig’s mechanical trail to counteract self-aligning torque from the lateral force generated while testing the tire reducing the burden on the slip angle drive system.

Weight Interface

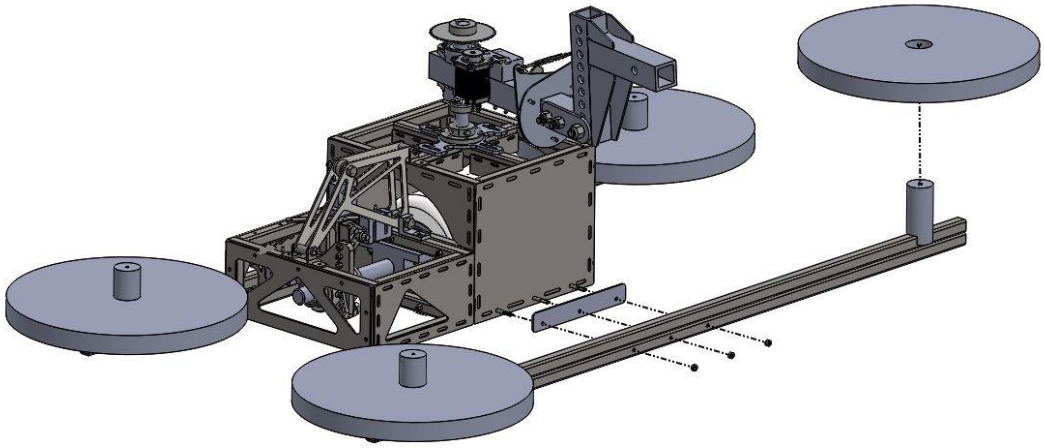

Figure 58: Weight Interface

A welded tube can be bolted to the front and rear of the tire cage allowing weight plates to be added to the rig for incremental adjustment of the test tire's normal load. The weight tube itself is two lengths of the same 1x1x.125" square tube used to construct the tire and load cell cages skip welded together along one side. A laser cut 10GA spacer is added between the weight tube and the tire cage to account for the slightly different overall lengths of the load cell and tire cages. Each weight tube is secured to the tire cage using three ¼-20 bolts. Lengths of 1 and 15/16" round stock standing on end are bolted to the ends of the weight tube using a single ¼-20 bolt to secure the added weight. The weights themselves are standard weight lifting plates and commonly available in sizes from 2.5 to 45 pounds.

DESIGN ANALYSIS

Preliminary Frame Design

After the size constraints and hard mounting points for the load cells and pillow block bearing were determined the initial shape of the tire and load cell cages were roughed in using square tubing. From there the cages were simulated separately to reduce simulation solve time. Gussets, cross tubes, and other sheet metal stiffeners were added and iterated to try and optimize each weldment's stiffness while adding as little weight as possible.

Starting with just the tubes in the general shape of the tire cage, a 500 pound-force load was applied to simulate lateral loading from the tire distributed about the load cell cage mounting holes. The weldment was constrained at the front assembly mounting holes on the top of the tire cage:

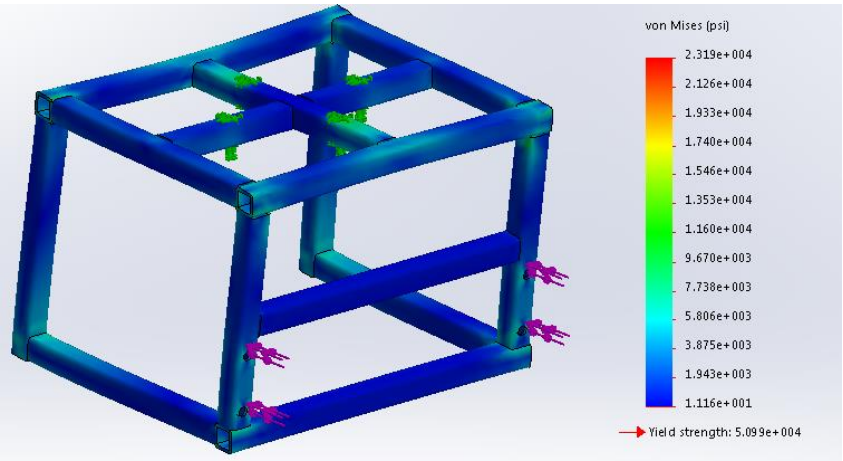

Figure 59: Basic Tire Cage Stresses

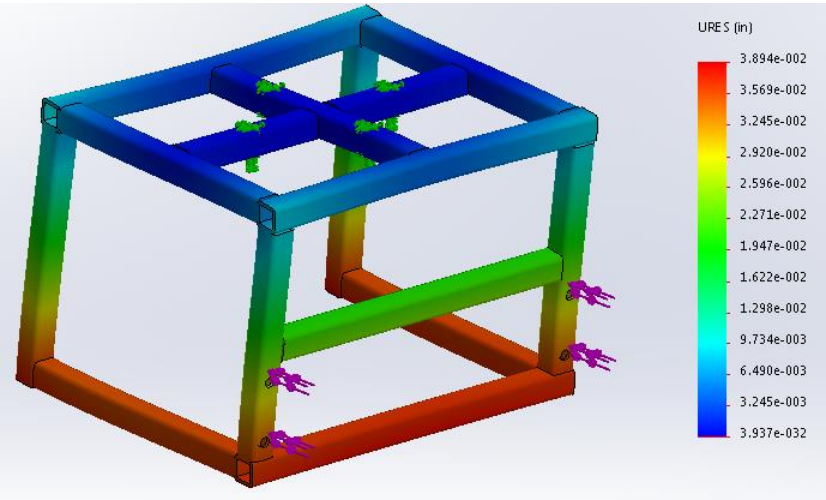

Figure 60: Basic Tire Cage Deflection

Adding in diagonal tubes:

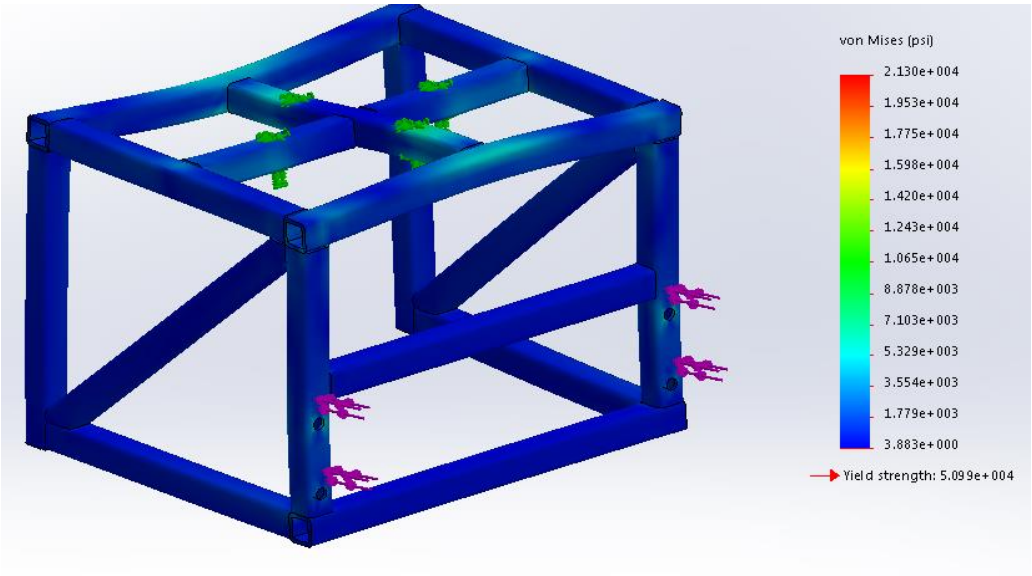

Figure 61: Diagonal Tubes Stresses

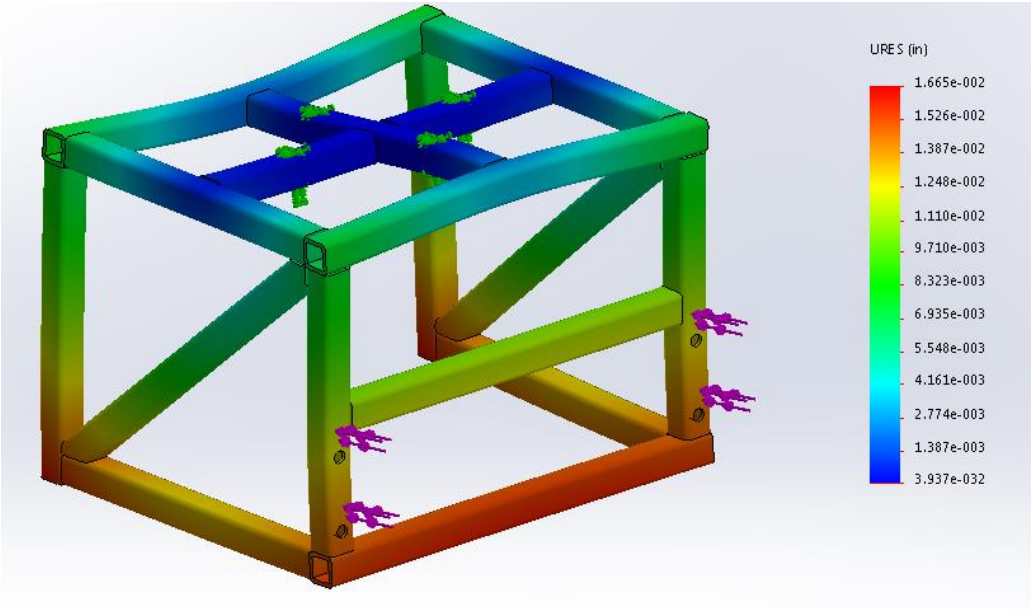

Figure 62: Diagonal Tubes Deflection

Evaluating stressed sheet metal panels:

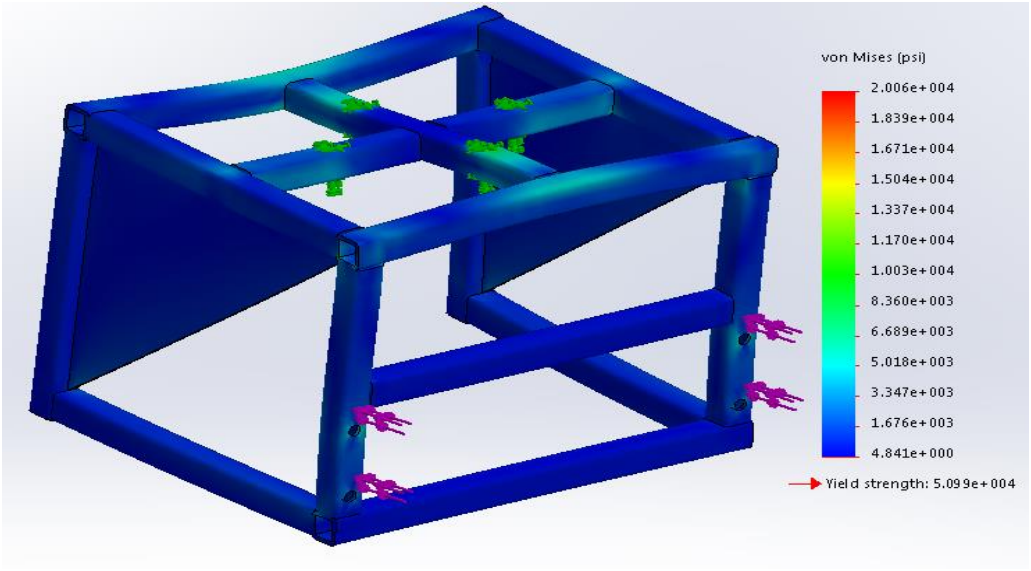

Figure 63: Sheet Metal Panels Stresses

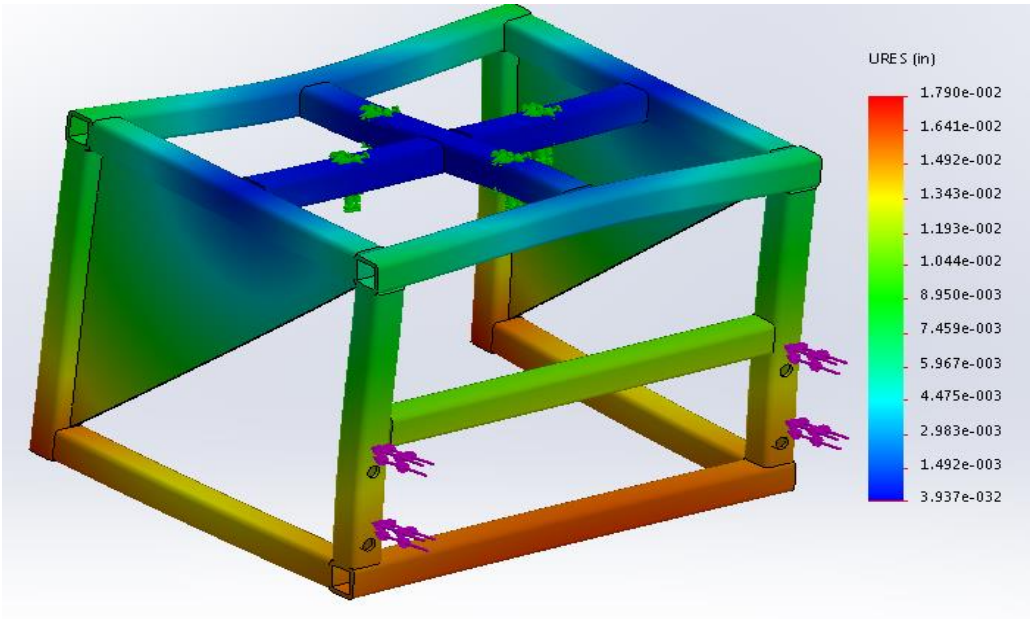

Figure 64: Sheet Metal Panels Deflection

Eventually it was decided to incorporate 16GA sheet metal panels welded to each end of the tire cage for their stiffness benefits. They also saved weight as closing out the entire end of the tire cage eliminated the need for separate close out panels.

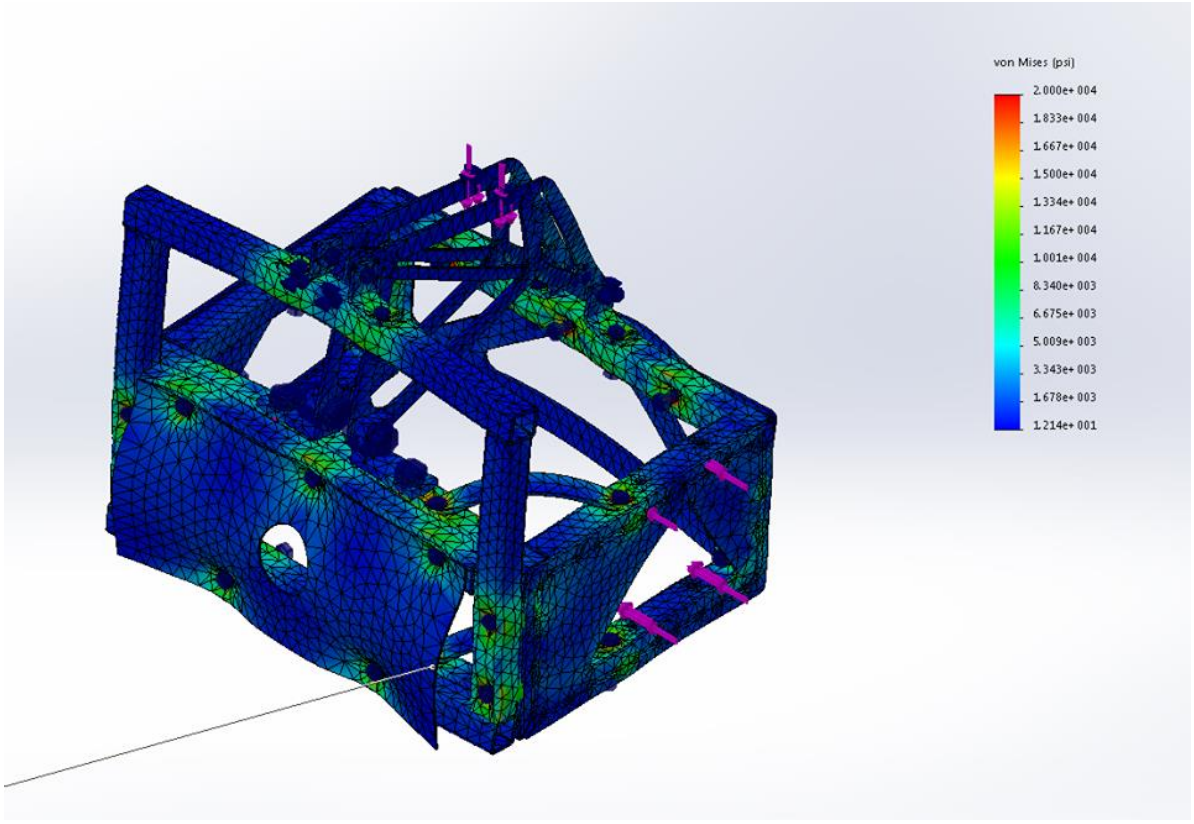

Figure 65: LC Cage with Sheet Metal Stresses

In order to optimize the stiffener plates on the load cell cage the vertical z-axis plates and their mounts were added to the assembly. Five tubes from the tire cage as well as the tire cage stiffener plate were also added as they contributed to the overall stiffness of the load cell cage, especially in resolving the y and z-axis loads. For this test the assembly was constrained at the four outermost holes where the tire cage and load cell cages bolt together. 500 pound-force loads were applied at each load cell mount. The bolted connection feature within SolidWorks Simulation was used to connect the weldments and the other components. All of the bolts were ¼ inch except for ½ inch bolts at the two machined aluminum brackets which interface between the y-axis load cell, z-axis gussets, and pillow block bearing. All bolt preloads were set to 1500 pounds. The interfacing faces between the bolted components were set as no penetration contact with a friction coefficient of .15.

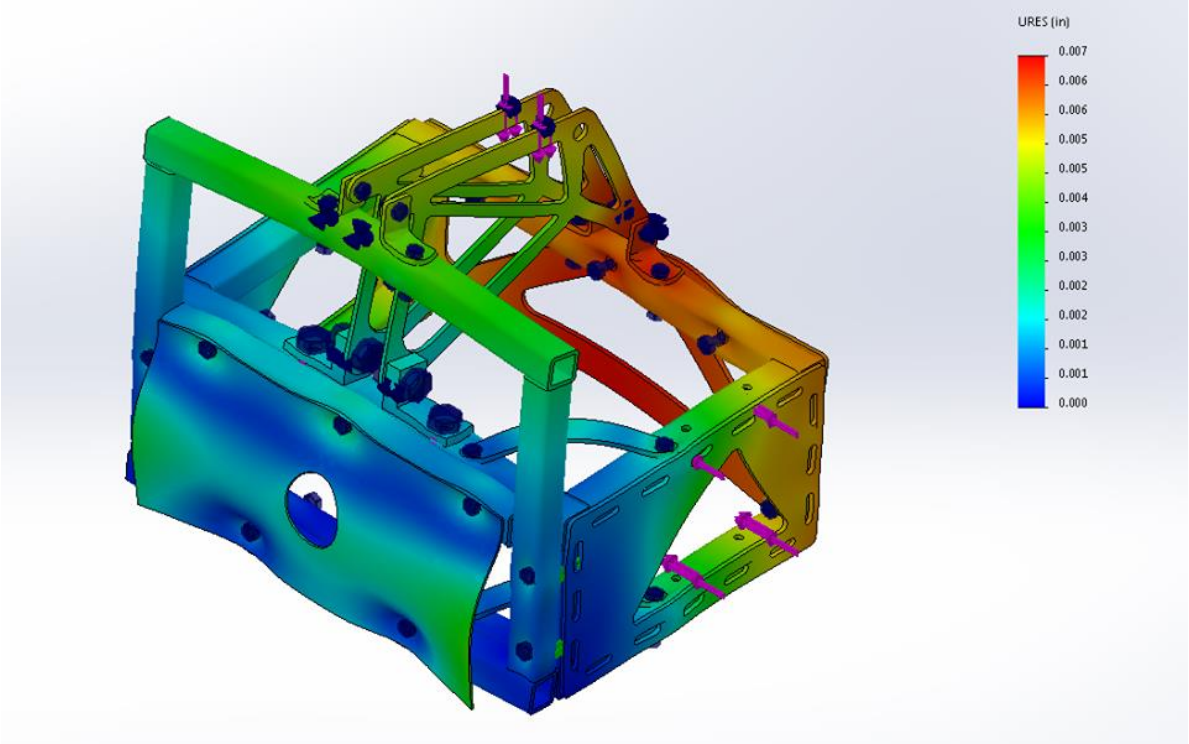

Figure 66: LC Cage with Sheet Metal Deflection

Rear Assembly

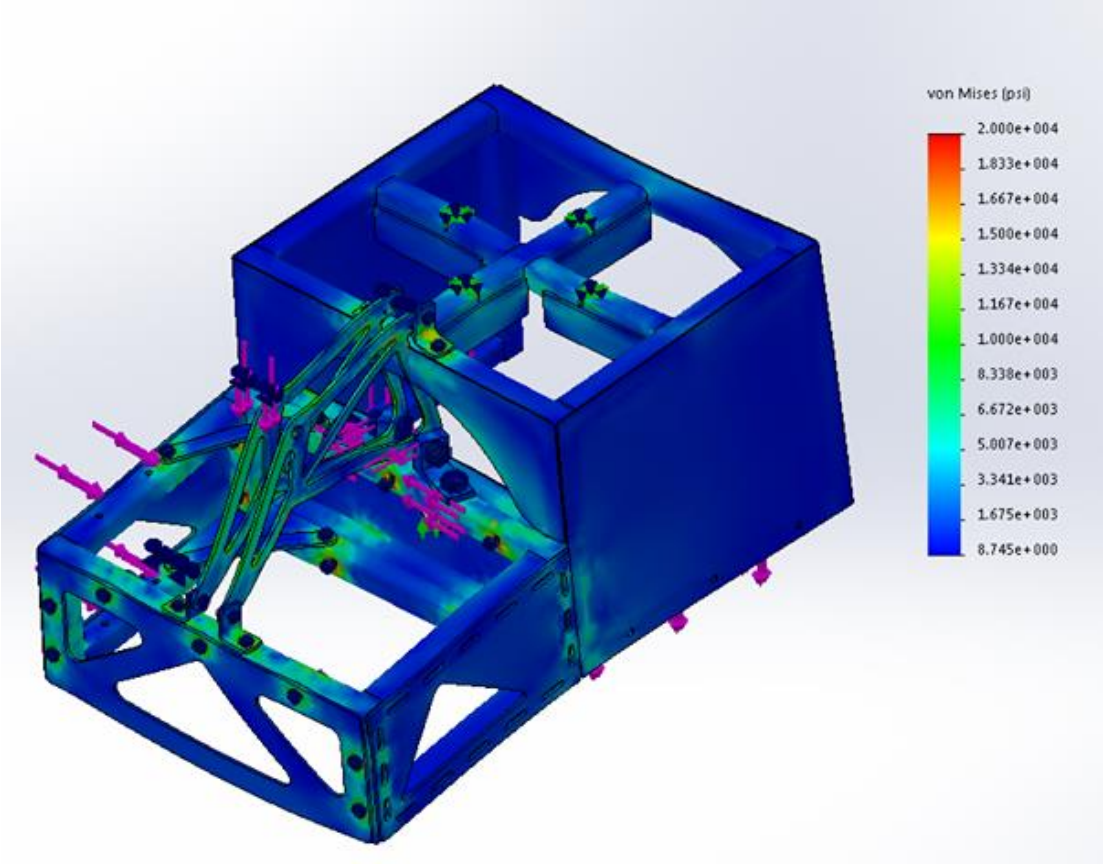

Figure 67: Rear Assembly Stresses view a

After the individual components were optimized the entire rear assembly was simulated to verify that the components worked together as anticipated. As discussed previously for the load cell cage analysis, the bolted connection feature within SolidWorks Simulation was used to connect the weldments and the other components. All of the bolts were ¼ inch except for ½ inch bolts at the two machined aluminum brackets which interface between the y-axis load cell, z-axis gussets, and pillow block bearing. All bolt preloads were set to 1500 pounds. The interfacing faces between the components were set as no penetration contact with a friction coefficient of .15. The assembly was fixed from translating in the x and y-axes at the four holes where the front assembly bolts to the top of the tire cage. The assembly was fixed from translating in the z-axis at the two holes where the pillow block bearing bolts to the load cell cage. 500 pound-force loads were applied at the mounting holes for each load cell as if the x and z-axes were in tension and the y-axis were in compression, as anticipated during normal testing. 250 pound loads were also applied in the negative z direction at the front and rear weight bar mounting holes to simulate 100 pounds of added weight on each end with the same 2.5 design factor as used for the z-axis.

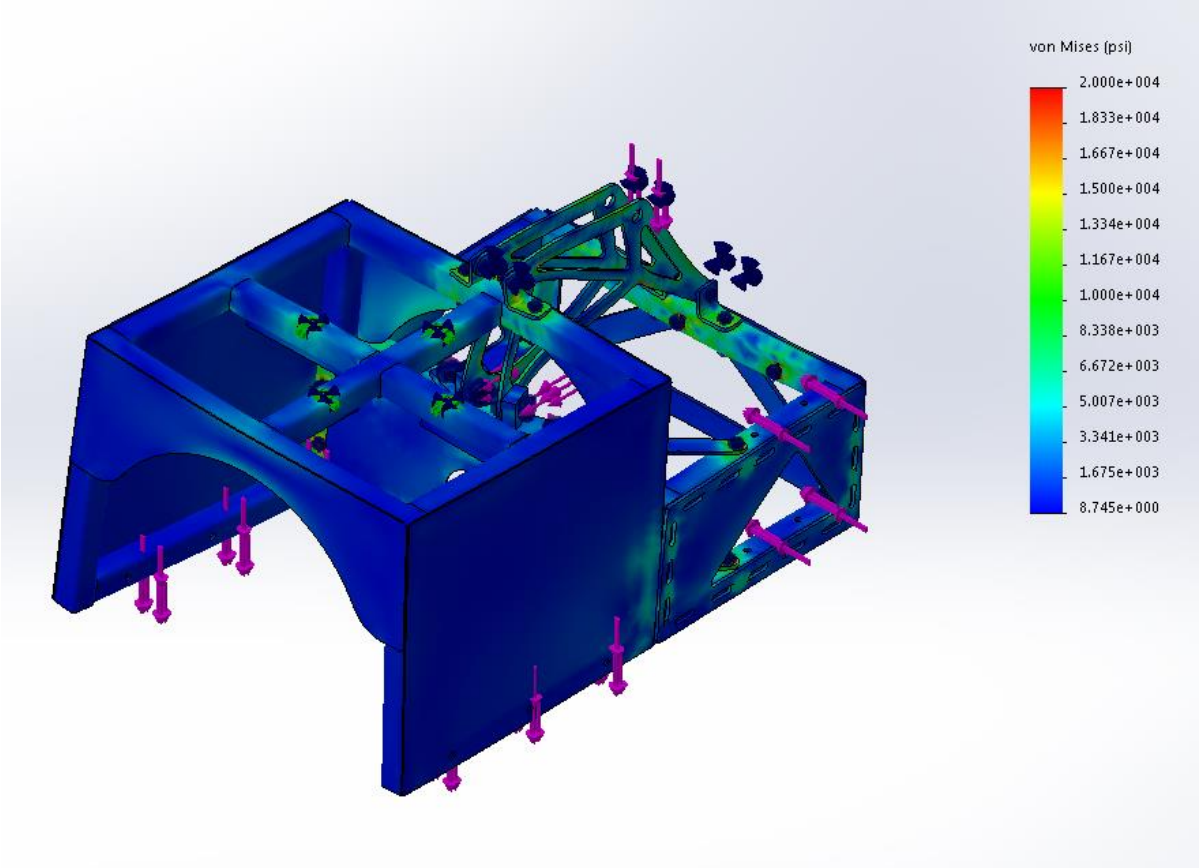

Figure 68: Rear Assembly Stresses view b

Note that the maximum stress on the color scale was fixed to 20,000psi to allow quick evaluation of changes. Peak stress was below 20,000psi. With a 1020 steel yield strength of about 43,000psi, this results in a factor of safety of about 2.1.

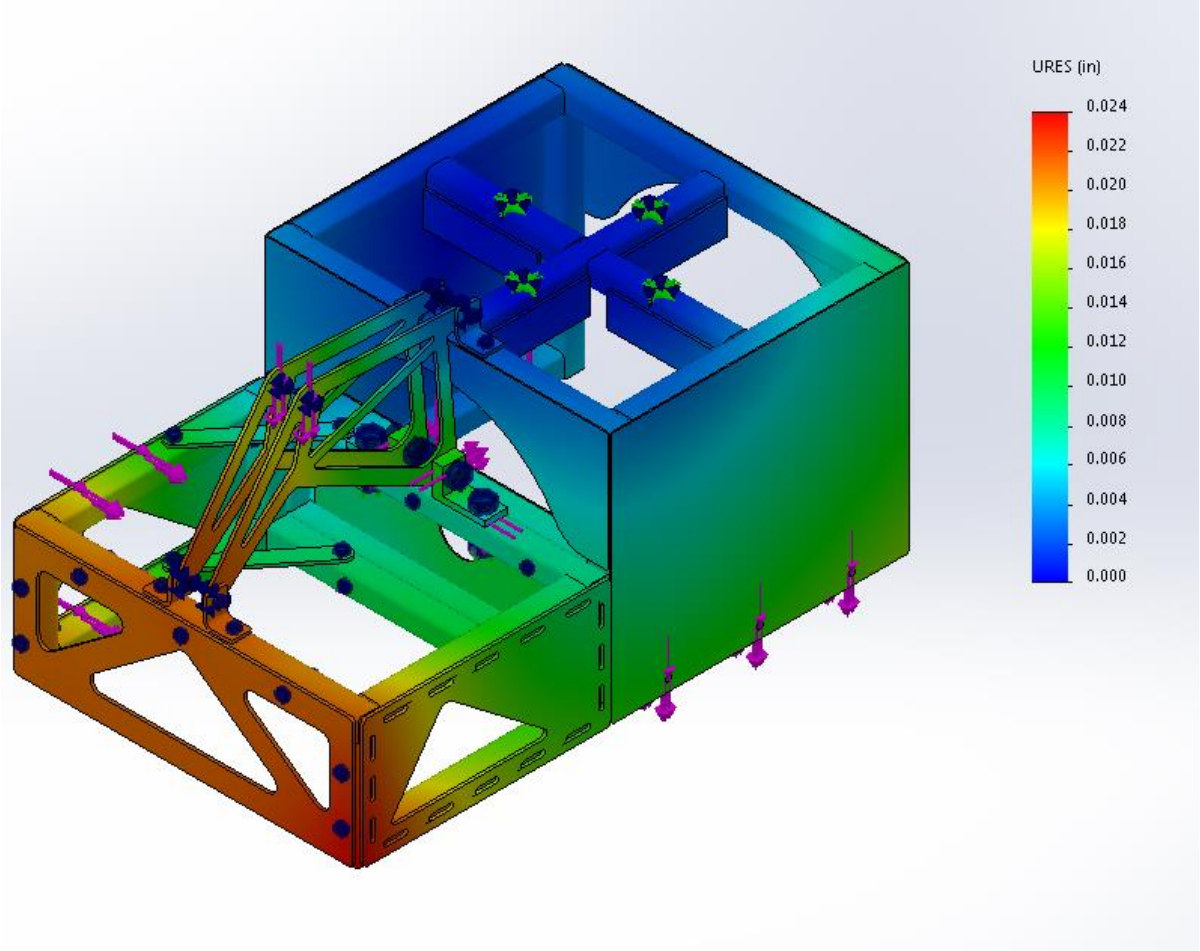

Figure 69: Rear Assembly Deflection view a

The displacement results show that none of the load cell mounting points deflect more than .02 inches at the worst case design load, meeting the requirements for slip and camber angle change due to rig deflection.

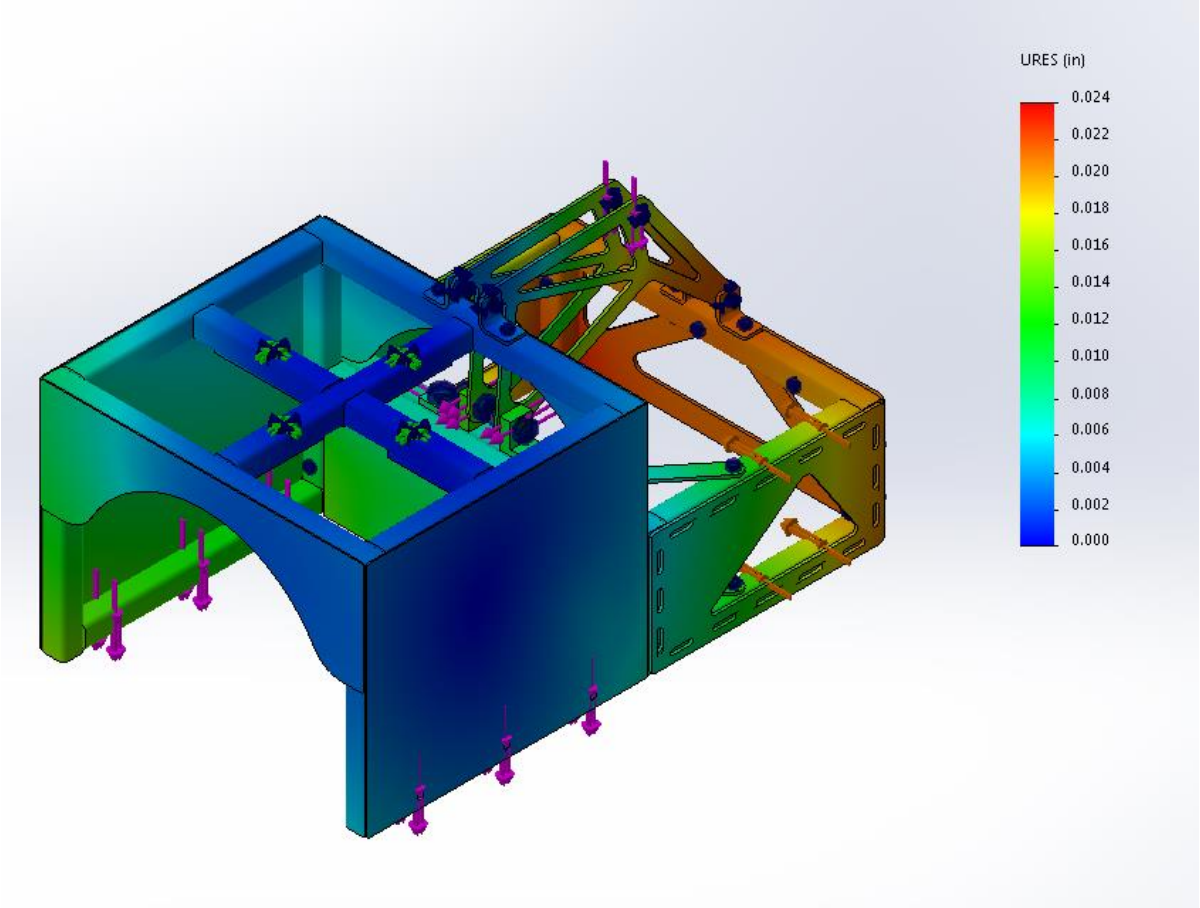

Figure 70: Rear Assembly Deflection view b

FABRICATION/ASSEMBLY

FABRICATION

Most of the sheet metal components used for the tire rig were laser cut at Cincinnati Incorporated.

Figure 71: Laser Cutting Sheet Metal

All machining and critical drilling was done at Victory Parkway.

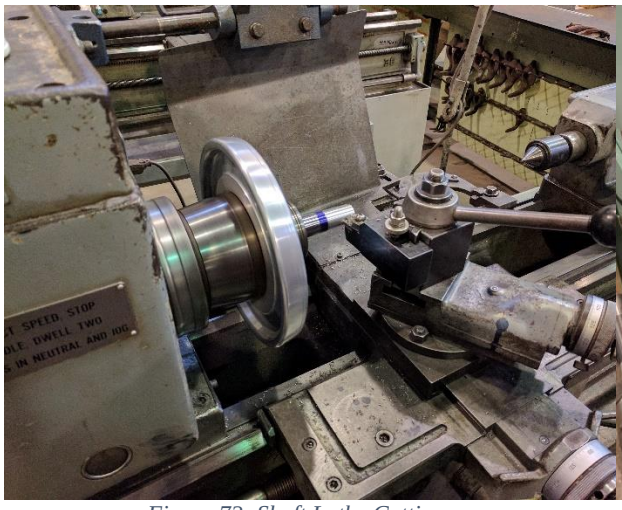

Figure 72: Shaft Lathe Cutting

Figure 73: LC Hole Drilling

ASSEMBLY

The stiffener plate and tire cage closeout plate were used as a guide to drill the necessary 1/4" mounting holes. The stiffener plate was then attached to the load cell cage.

Figure 74: Stiffener Plate Clamping

Figure 75: Tire Cage Drilling

The load cell cage/tire cage interface mounting holes were drilled into the load cell cage and the tire cage using a 3D printed guide.

Figure 76: Hole Drilling 3D Printed Guide

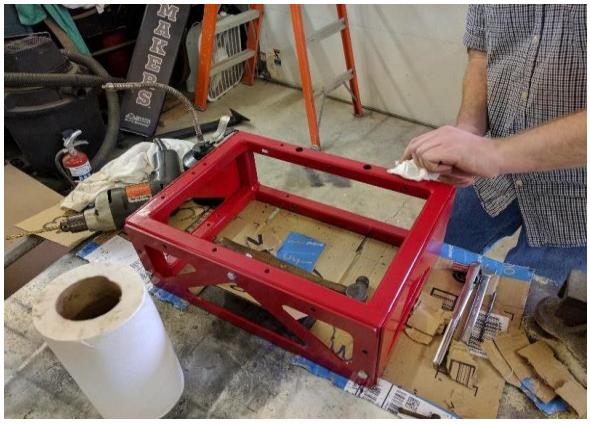

Figure 77: Cleaning LC Cage Drill Debris

The x-axis support straps and x-axis load cell brackets were added. The pillow block bearing and brackets were mounted.

Figure 78: x-axis Support Straps

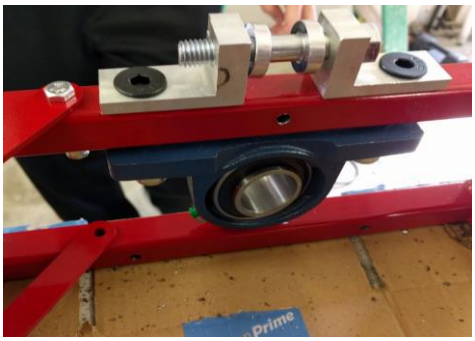

Figure 79: Pillow Block Bearing

The flange mount bearings for the load cell interface had to be drilled out. The flange bearing housing had the incorrect mounting hole size from the manufacturer.

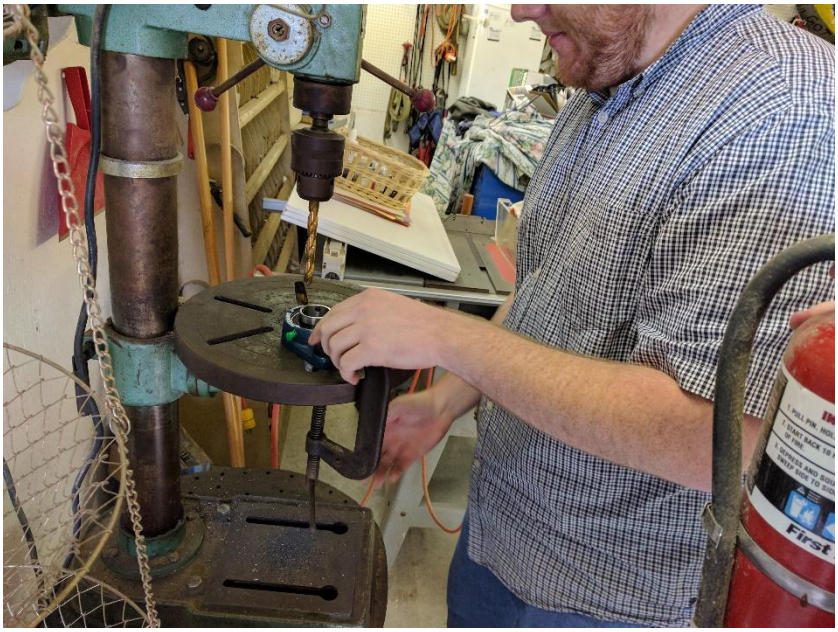

Figure 80: Drilling Out Flange Mount Bearings

After mounting the y and z-axis mounting bracket, the axle was aligned through the two flange mount bearings at the load cell interface.

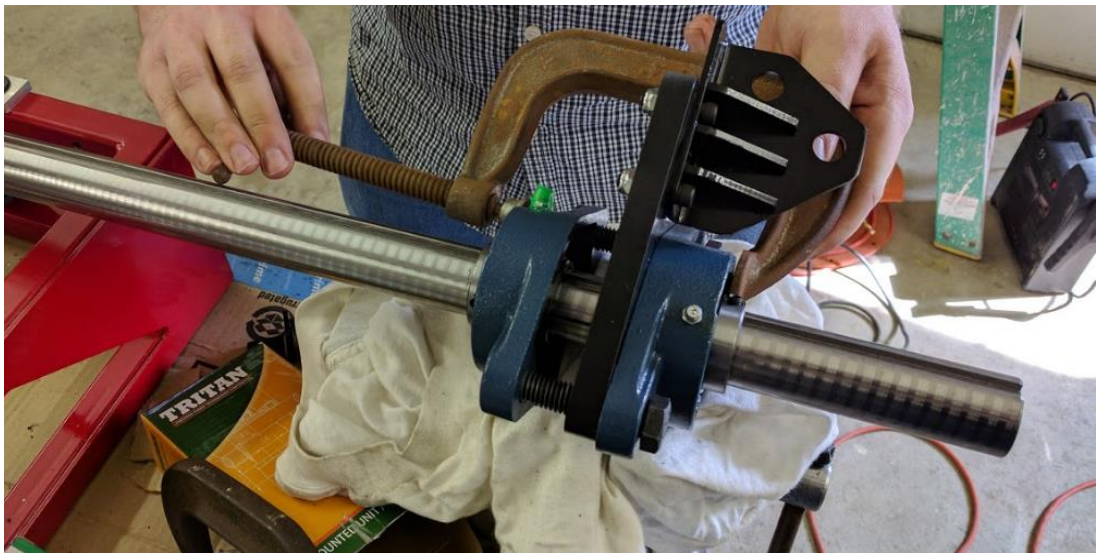

Figure 81: Aligning Flange Mount Bearings on Shaft

The shaft was then passed through the main pillow block bearing.

Figure 82: LC Cage with Shaft/Pillow Block Bearings

At this stage, the rod ends were cut to size to place the load cell interface in a centered position within the load cell cage. A nut was screwed onto the rod end to protect the thread form the vice grip and re-cut the marred threads. Load cell assembly dimensions are listed on assembly drawing.

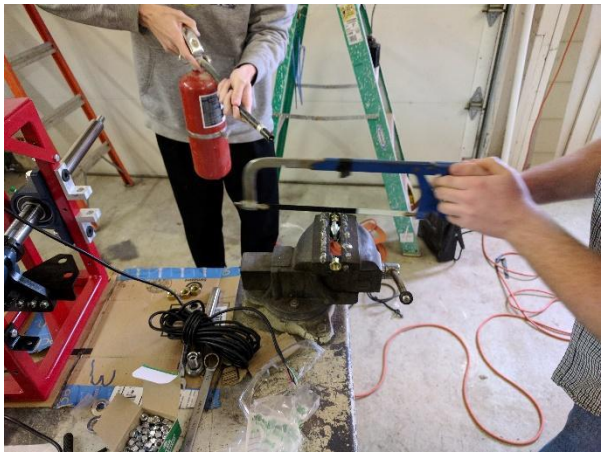

Figure 83: Cutting Rod Ends view a

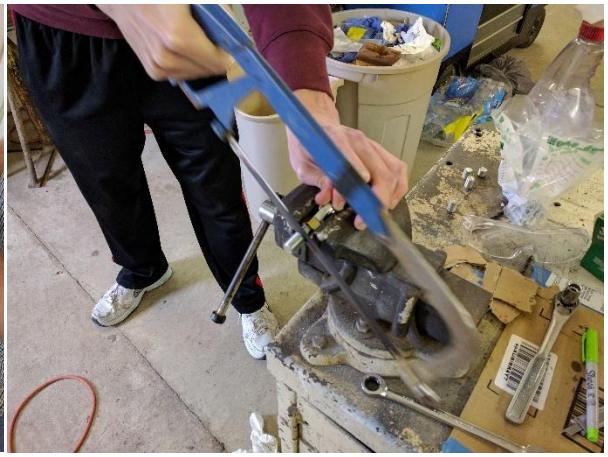

Figure 84: Cutting Rod Ends view b

The load cells were mounted to the three mounting locations on the load cell interface and their respective mounting locations on the load cell cage and the vertical support brackets. Once the load cell interface was centered and verified, everything was tightened.

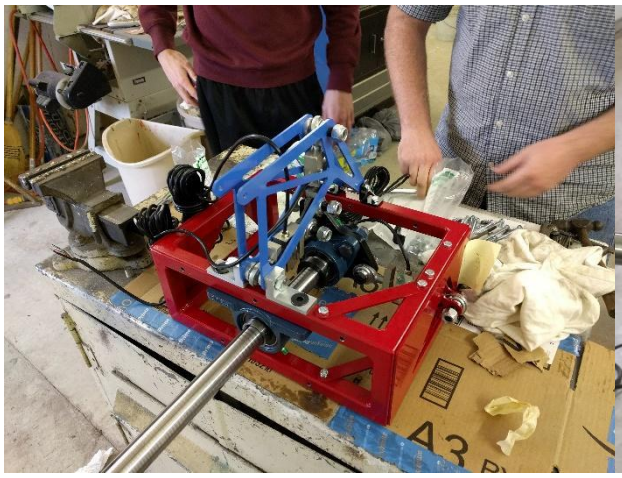

Figure 85: Load Cell Cage Assembled view a

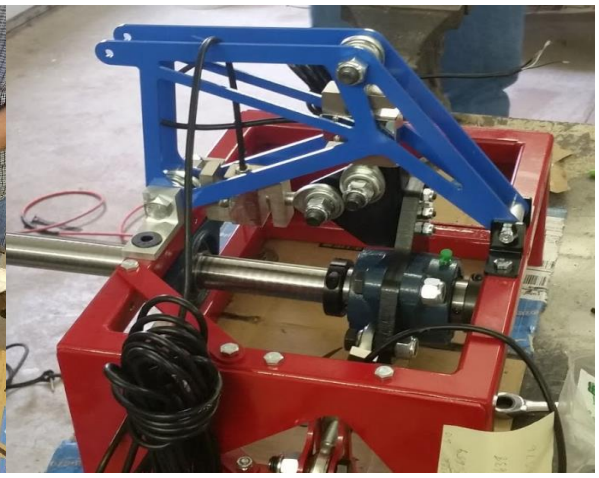

Figure 86: Load Cell Cage Assembled view b

The fit of the load cell cage to the tire cage was evaluated and the mounting holes had to be enlarged slightly to take manufacturing tolerances into account.

Figure 87: Aligning LC and Tire Cage Holes

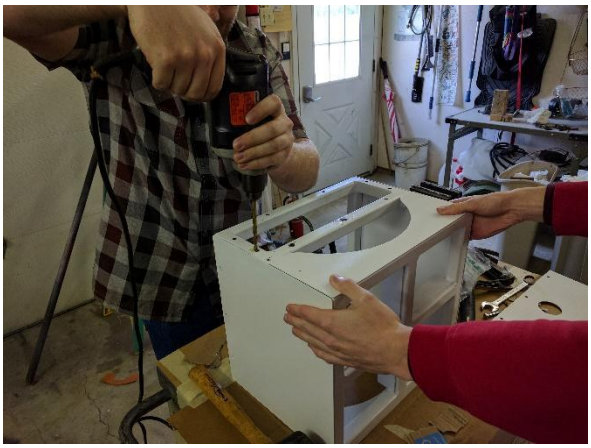

Figure 88: Enlarging Mounting Holes

The LC cage was then bolted to the tire cage. Placing the tire cage on its side and then setting the LC cage on top made it easier to bolt the two together.

Figure 89: Bolting LC Cage to Tire Cage on its Side

Mounting holes for the two brackets that connected the top of the vertical supports to the tire cage were drilled. The brackets were then fitted.

Figure 90: Fitting Vertical Support Brackets to Tire Cage

Four holes were drilled on the top of the tire cage. The slip angle drive cross and the flange-mount shaft collar were then positioned and bolted to the top of the tire cage.

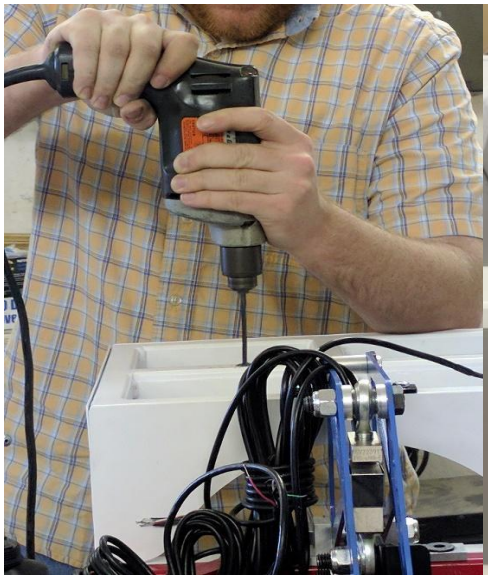

Figure 91: Drilling SA Drive Cross Mounting Holes

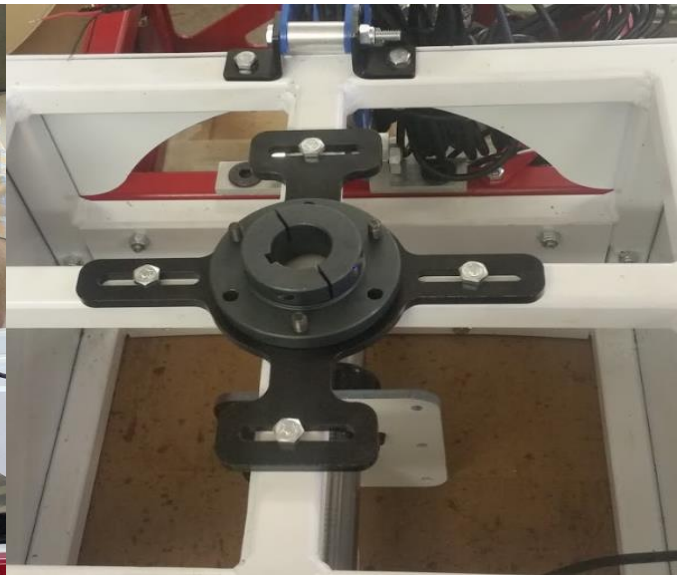

Figure 92: Mounting Shaft Collar of SA Drive

The Front Assembly was assembled to the 2 x 2 x.125 Tube separate from the cage assemblies like shown. The shaft was then fitted inside the flange-mount shaft collar on top of the tire cage. Once this was added, the motor was attached to the motor mounting block.

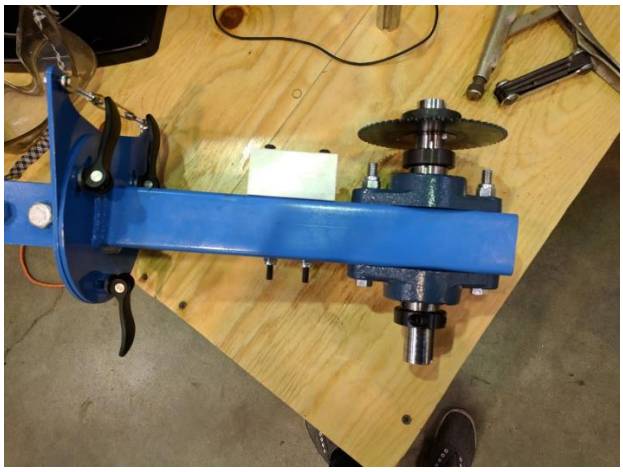

Figure 93: Front Assembly

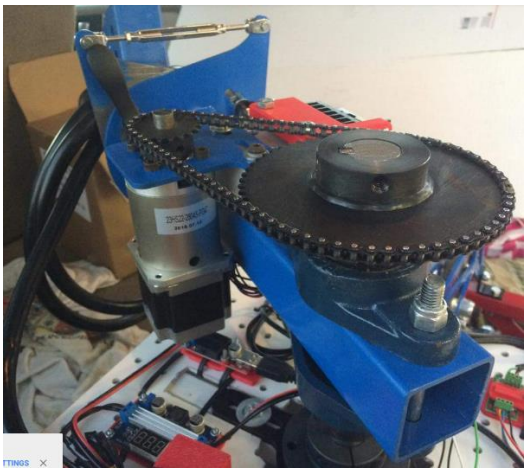

Figure 94: Motor/Sprocket Interface

The hitch adapter is attached to two pivot plates that allow for different hitch heights.

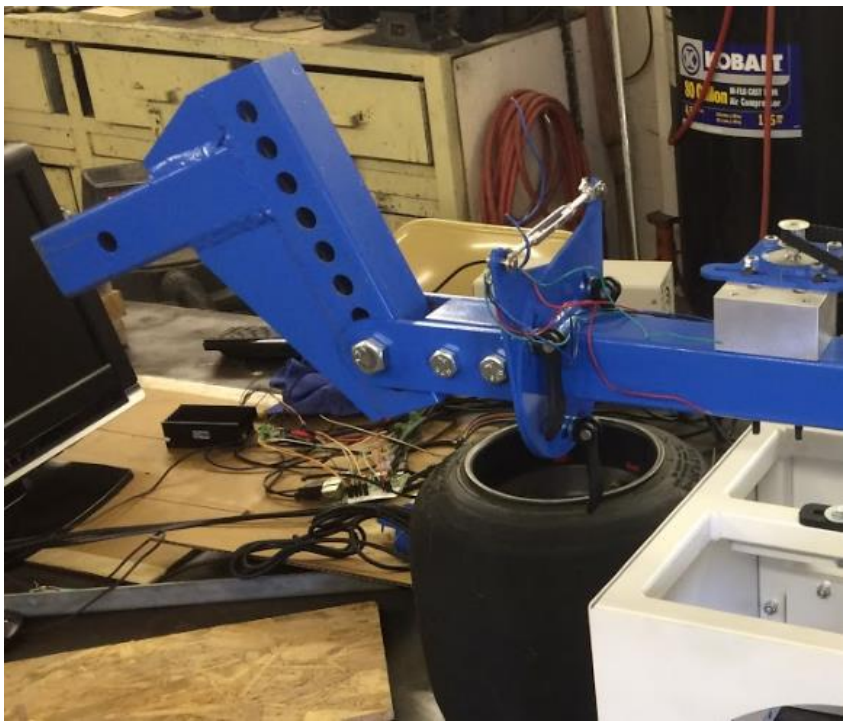

Figure 95: Hitch Adapter on Front Assembly

TESTING/VALIDATIONS

Testing was done in two stages: static validation and dynamic testing. Static validation was done to validate that the rig was outputting load readings of the correct axis and that the load readings were repeatable. Dynamic testing was then done to test the dynamic features of the rig and make sure the data that was captured matched expectations.

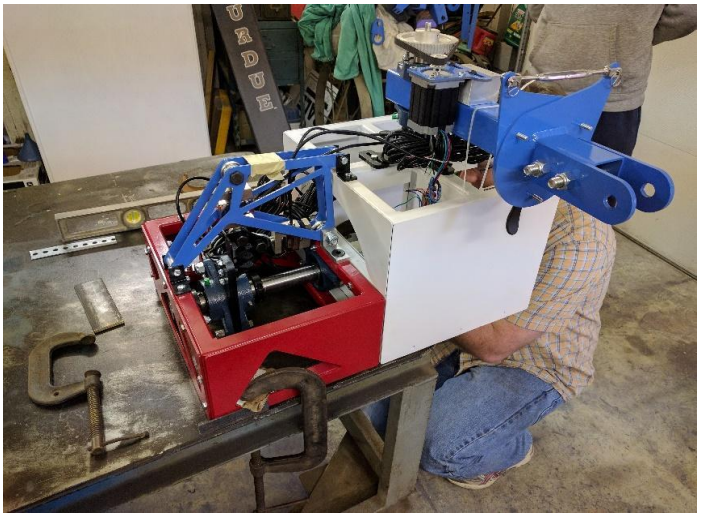

Figure 96: Full Assembly Prepped for Testing

STATIC VALIDATION

Static validation was done on each of the three axes individually. A laser cut test plate was bolted onto the hub and was used as an attachment point for the loads. The rig was leveled and clamped down to a heavy table. The RaspberryPi was set up to print the load cell readings on a display to provide real-time feedback. The details of applying the load varied for each axis but the general method was to load the shaft with iron weight plates in the axis being tested. The load readings would then be allowed to settle for 3 seconds and a load cell reading for all three axes was taken. Readings were taken for every axis, every time to catch any loads that were being transferred to axes other than the one being currently tested.

z-axis validation

The z-axis was validated first. The z-axis load cell captures the resultant normal force on the tire. Paracord was used to attach the load to the top of the test plate.

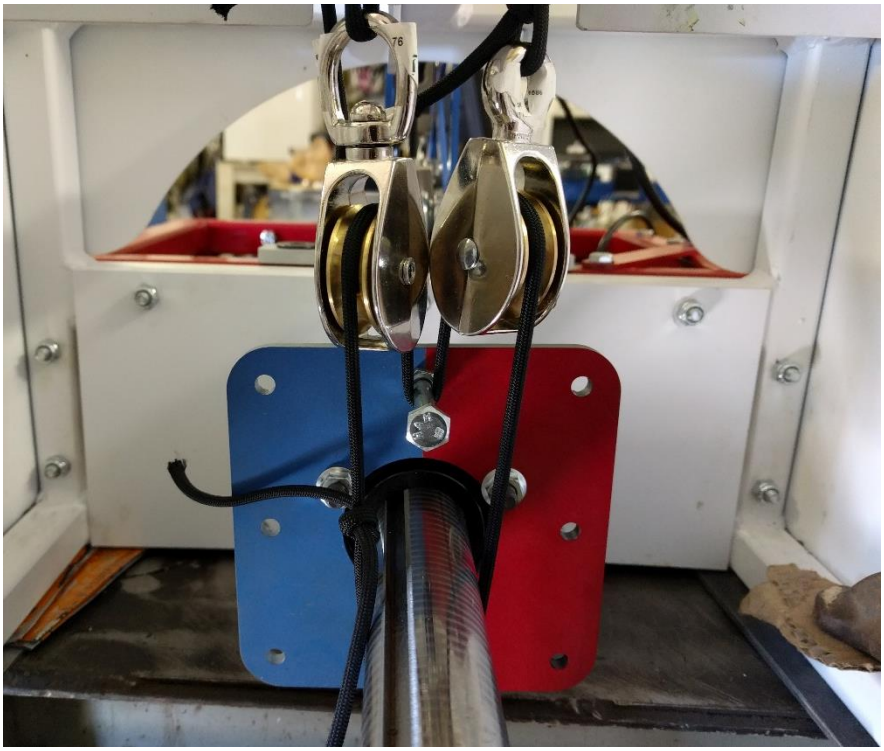

Figure 97: z-axis Testing Pulley Setup

The paracord was run through a pulley on each side and the weight plates were then attached to the ends.

Figure 98: z-axis Weight Held by Paracord

This setup allowed the suspended load to pull up on the shaft and transfer through the positive Z direction. The applied loads started at 77lbs and increased to 225.8lbs. These loads were based on assumptions about the type of loading that the z-axis would experience.

While setting up the test, the load cell readings showed a load in the y-axis when the z-axis was loaded. The solution to this problem was found after some testing. In order for the y-axis load cell to receive the loads from the tire, the axle must slide axially through the bearing race (less than .005”). A load applied in the z axis applies a radial load to the bearing. As the radial load increases, the friction between the shaft and the bearing race increases and the shaft resists sliding axially through the bearing. This phenomena was seen by pushing or pulling on the shaft in the y- direction when the z-axis was loaded. After the shaft was released, the y-load would not go back to zero. After some testing, it was found that rotating the shaft would break the static friction and reset the y-load to zero.

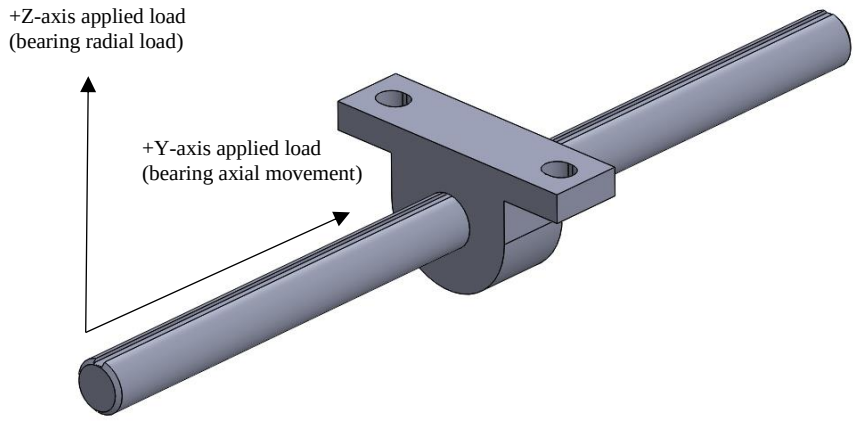

Figure 99: Load in y-axis when z-axis is loaded

A procedure to accurately test the z-axis was developed:

1. Apply the load to the z-axis
2. Take load cell readings from all three axes
3. Pull on shaft in –Y axis
4. Take load cell readings
5. Rotate shaft
6. Take load cell readings
7. Push on shaft in +y axis
8. Take load cell readings
9. Rotate shaft
10. Take load cell readings

This procedure was done to verify that the hypothesis (that the z-axis load increased bearing friction) was correct. The data is shown below.

Z-Axis Load Cell Validation Data						
Weight	77 lbs	Load	Pull -Y	Rotate	Pull +Y	Rotate
	X	1	2	2	1	2
	Y	0	-15	3	13	3
	Z	76	85	79	89	79
Weight	87 lbs	Load	Pull -Y	Rotate	Pull +Y	Rotate
	X	2	2	2	1	1
	Y	4	-13	3	20	3
	Z	87	98	87	77	86
Weight	97 lbs	Load	Pull -Y	Rotate	Pull +Y	Rotate
	X	2	2	2	2	1
	Y	3	-7	-7	24	1
	Z	96	102	102	87	98
Weight	107 lbs	Load	Pull -Y	Rotate	Pull +Y	Rotate
	X	2	2	2	2	1
	Y	3	-1	3	9	3
	Z	108	117	110	106	108
Weight	117 lbs	Load	Pull -Y	Rotate	Pull +Y	Rotate
	X	3	3	2	1	1
	Y	3	-11	4	20	4
	Z	118	125	118	105	118
Weight	127 lbs	Load	Pull -Y	Rotate	Pull +Y	Rotate
	X	2	2	1	1	1
	Y	0	-13	3	11	5
	Z	128	136	128	122	126
Weight	137 lbs	Load	Pull -Y	Rotate	Pull +Y	Rotate
	X	2	2	1	1	1
	Y	-1	-5	4	19	2
	Z	139	143	137	130	138
Weight	147 lbs	Load	Pull -Y	Rotate	Pull +Y	Rotate
	X	2	2	2	2	1
	Y	5	-4	0	31	5
	Z	148	156	151	136	150
Weight	149 lbs	Load	Pull -Y	Rotate	Pull +Y	Rotate
	X	3	2	1	1	1
	Y	-1	-20	0	23	2
	Z	149	163	158	147	157
Weight	174 lbs	Load	Pull -Y	Rotate	Pull +Y	Rotate
	X	3	3	2	2	2
	Y	-2	-21	2	22	2
	Z	179	191	182	172	184
Weight	201.6 lbs	Load	Pull -Y	Rotate	Pull +Y	Rotate
	X	3	2	2	3	2
	Y	-4	-21	0	22	0
	Z	202	211	207	195	208
Weight	225.8 lbs	Load	Pull -Y	Rotate	Pull +Y	Rotate
	X	4	3	2	2	2
	Y	-2	-34	-1	17	0
	Z	227	245	226	214	228

Table 2: z-axis Load Cell Validation Data

In every case, rotating the shaft broke the friction and allowed the y-axis load to resettle near zero. This validated the hypothesis and meant that no correction was necessary. Next, the error between the applied load and the load cell output was plotted and analyzed.

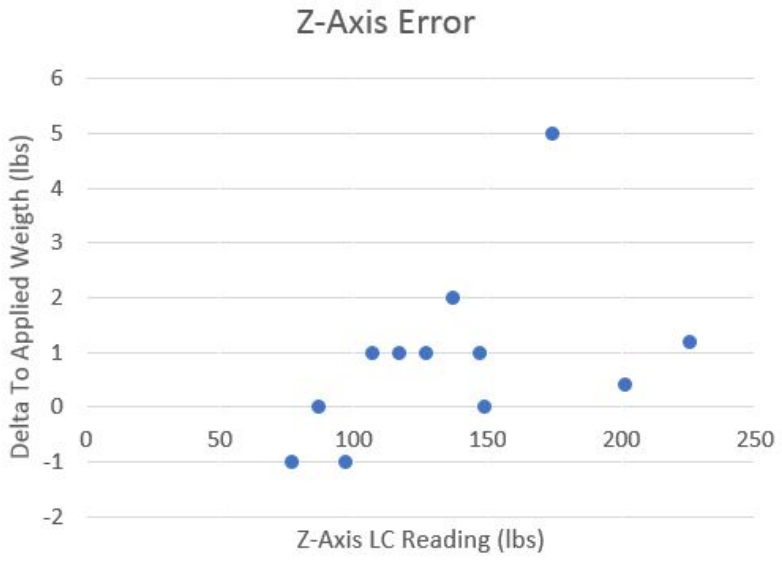

Figure 100: z-axis Error Graph

The maximum error between the applied load and the load cell reading was 5 lbs. This was deemed satisfactory.

x-axis validation

To load the z axis, the paracord was attached to the shaft. A support roller stand was used as a pulley so the weights could hang but the load would be applied in the x-axis.

Figure 101: x-axis Validation Setup with Support Roller Stand

The procedure for accurately validating this axis was the same as the procedure used to validate the z-axis. This was done to further validate our hypothesis about the bearing friction. The applied loads ranged from 24.2lbs to 129.4lbs. These loads were based on assumptions about the type of loading that the x-axis would experience. The data is shown below.

X-Axis Load Cell Validation Data						
Weight	24.2	Just Weight	Pull -Y	Rotate	Pull +Y	Rotate
	X	-23	-23	-25	-26	0
	Y	-2	-5	0	5	1
	Z	2	-5	0	-2	-25
Weight	51.8	Just Weight	Pull -Y	Rotate	Pull +Y	Rotate
	X	-49	-50	-51	-51	-50
	Y	0	-10	0	12	-1
	Z	2	8	2	-6	2
Weight	76	Just Weight	Pull -Y	Rotate	Pull +Y	Rotate
	X	-71	-70	-74	-74	-74
	Y	-5	-13	0	6	0
	Z	5	10	2	-3	1
Weight	105.2	Just Weight	Pull -Y	Rotate	Pull +Y	Rotate
	X	-101	-99	-100	-96	-96
	Y	0	-11	0	-22	-2
	Z	4	12	5	19	7
Weight	129.4	Just Weight	Pull -Y	Rotate	Pull +Y	Rotate
	X	-125	-124	-126	-126	-125
	Y	0	-18	-3	22	-1
	Z	7	20	10	-5	9

Table 3: x-axis Load Cell Validation Data

Next, the error between the applied load and the load cell output was plotted and analyzed.

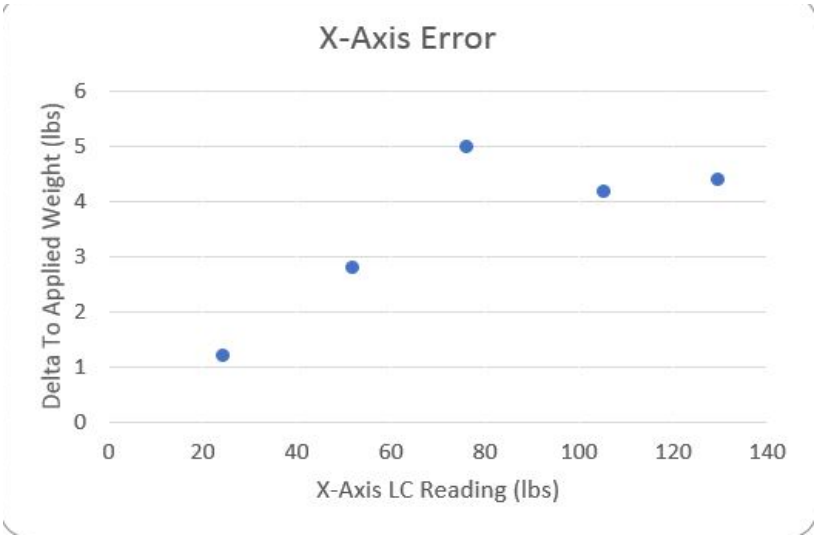

Figure 102: x-axis Error Data

The maximum error between the applied load and the load cell reading was 5 lbs. This was deemed satisfactory.

y-axis validation

To load the y axis, paracord was attached to two points on either side of the test plate and run over the support roller.

Figure 103: y-axis Validation Setup with Support Roller Stand

This allowed the weight plates to hang but apply a load in the y-axis. The procedure was different for the y-axis testing. The shaft was not rotated because it couldn't be. This did not affect the readings because there was no load applied in the other axes and the shaft could slide axially through the bearing with not problem. Loads were applied from 24.2lbs to 225.8lbs. This was based on the loading expected in the y axis. The data is shown below.

Y-Axis Load Cell Validation Data		
Weight	24.2	Load
	x	3
	y	-24
	z	12
Weight	52.6	Load
	x	4
	y	-52
	z	27
Weight	76.8	Load
	x	-7
	y	-71
	z	39
Weight	97.2	Load
	x	-9
	y	-92
	z	52
Weight	125	Load
	x	-10
	y	-111
	z	63
Weight	149.8	Load
	x	-10
	y	-137
	z	76
Weight	174	Load
	x	-9
	y	-156
	z	86
Weight	201.6	Load
	x	-7
	y	-183
	z	101
Weight	225.8	Load
	x	-5
	y	-197
	z	108

Table 4: y-axis Load Cell Validation Data

From the data it is clear that loading the y axis also imparts a load into the z-axis. This is because of the location of the y-load cell.

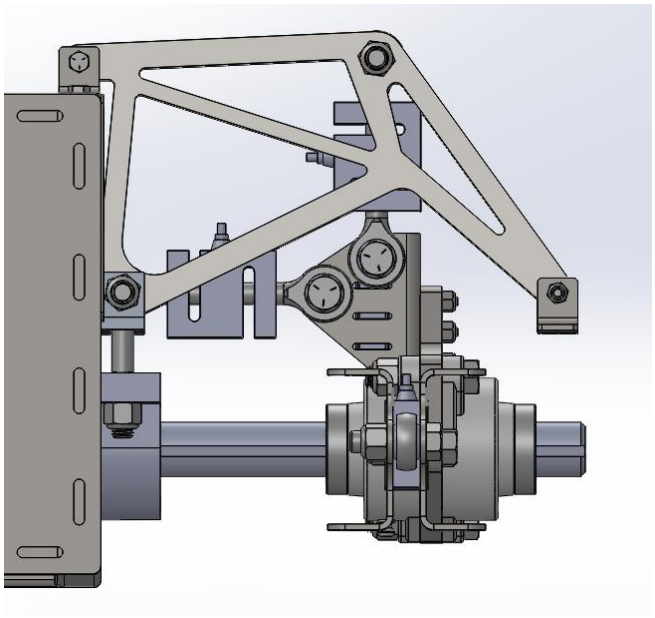

Figure 104: x and y Load Cell Positioning

As shown above, the x, and z load cells are positioned so that they act directly in line with the line of action of the load. The y-axis load cell is offset from the line of action of the load which generates a moment. This moment imparts a load into the z-axis. To correct for this the z and y readings were plotted as shown below.

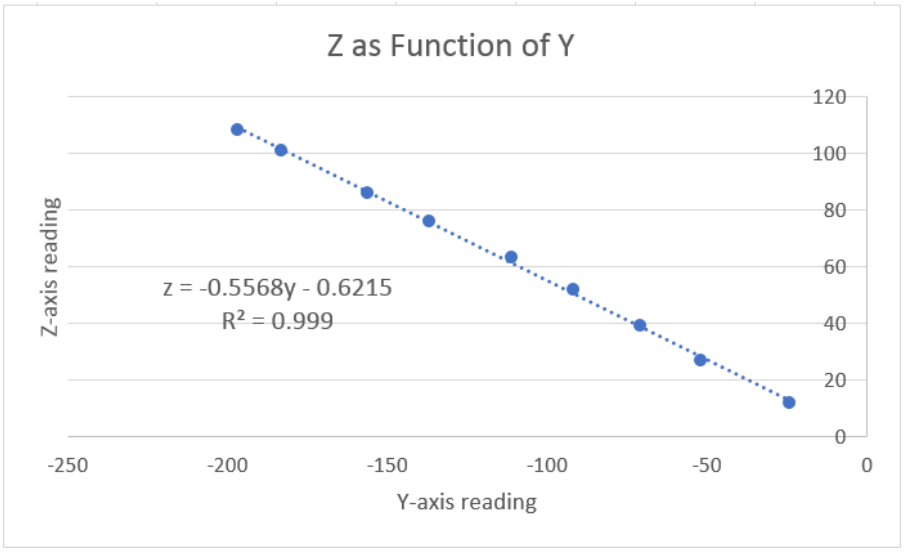

Figure 105: z as a Function of y Data

This plot shows a very strong (R^2=.999) linear correlation between the y and z axes. The z-axis was corrected using the resulting line-of-best-fit equation.
The y-axis was re-validated after this z-axis correction. The data and error plot is shown below.

Y-axis re-validation		
Weight	52.6	Load
	x	0
	y	-51
	z	-1
Weight	105.2	Load
	x	-5
	y	-104
	z	0
Weight	157	Load
	x	-10
	y	-155
	z	1
Weight	211.4	Load
	x	-10
	y	-193
	z	0
Weight	25	Load
	x	0
	y	-25
	z	-1
Weight	77.6	Load
	x	-9
	y	-79
	z	1
Weight	130.2	Load
	x	-14
	y	-125
	z	3
Weight	184.6	Load
	x	-11
	y	-175
	z	3
Weight	134.8	Load
	x	5
	y	-135
	z	3
Weight	187.4	Load
	x	6
	y	-175
	z	2
Weight	211.4	Load
	x	2
	y	-201
	z	2
Weight	256	Load
	x	1
	y	-236
	z	2
Weight	304	Load
	x	6
	y	-274
	z	1
Weight	354	Load
	x	4
	y	-310
	z	0

Table 5: y-axis Re-validation Data

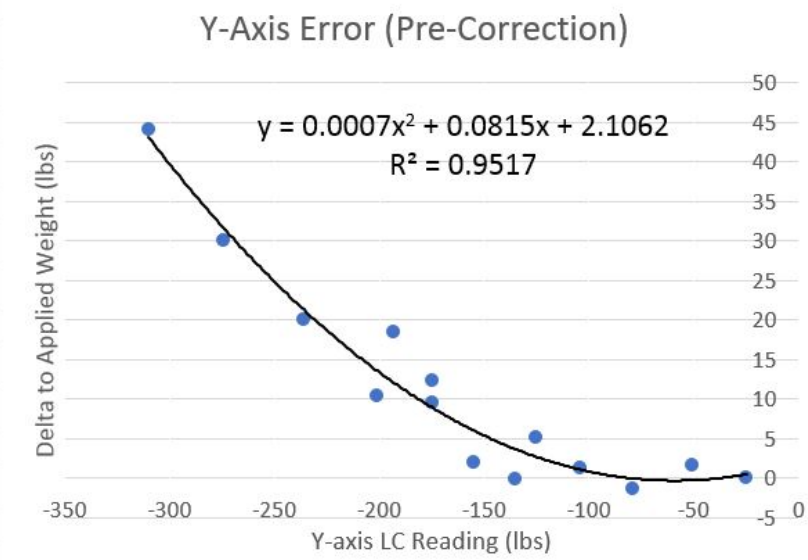

Figure 106: y-axis Error (Pre-Correction)

The errors increased as the y axis load increased. The y-axis load cell generates a moment that imparts a load on the z-axis. Now this is a combined loading case as was seen during the z-axis validation. The load imparted into the z-axis applies a radial load to the bearing which resists the axle sliding axially. This meant that the y-axis load cell readings were not accurate. In the z-axis validation this friction problem was overcome by rotating the shaft. Because of the setup of the y-axis loading, the shaft could not be rotated. To validate the y-axis readings, a trend line was fit to the data (R^2=.952) and the resulting line-of-best-fit equation was used to correct the y-axis data. The y-axis was validated again and the errors were plotted.

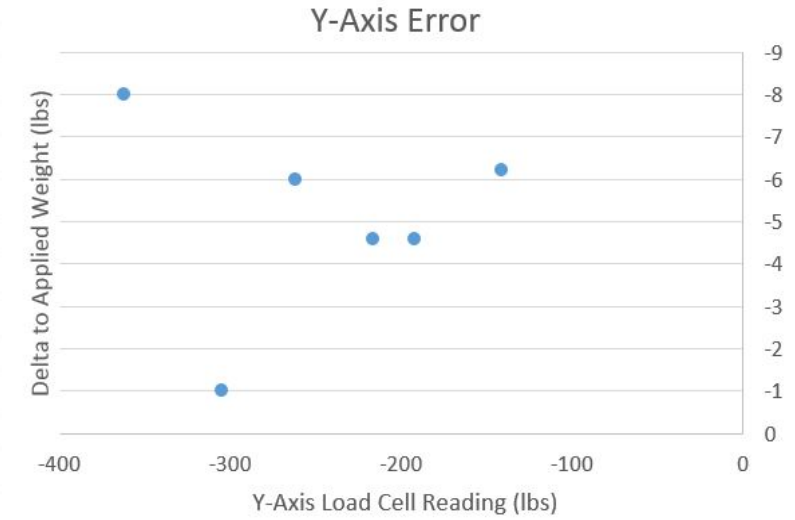

Figure 107: y-axis Error after Correction

The result was much better than the uncorrected errors. This completed the static analysis.

DYNAMIC TESTING

The graph below shows the forces in the x, y, and z axes while the rig was being towed behind a vehicle. The testing surface was asphalt and contained a lot of bumps (clearly visible in the z-axis data)

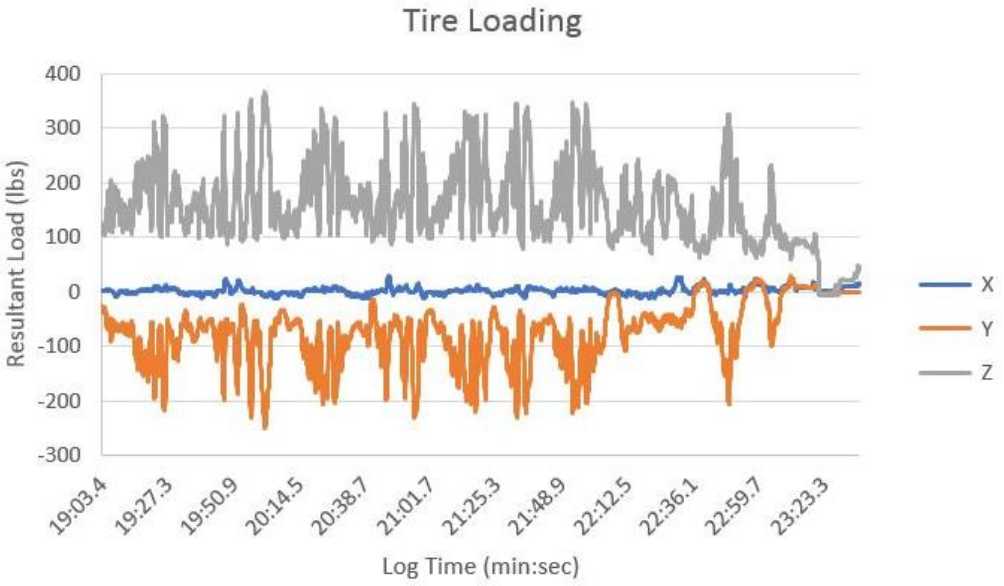

Figure 108: Dynamic Tire Loading Data

The graph below shows the tire surface and ambient temperatures logged during the test run. The tire surface temperatures are positioned behind the tire at the inside, middle, and outside along the tire surface. The ambient temperature was also logged during the run.

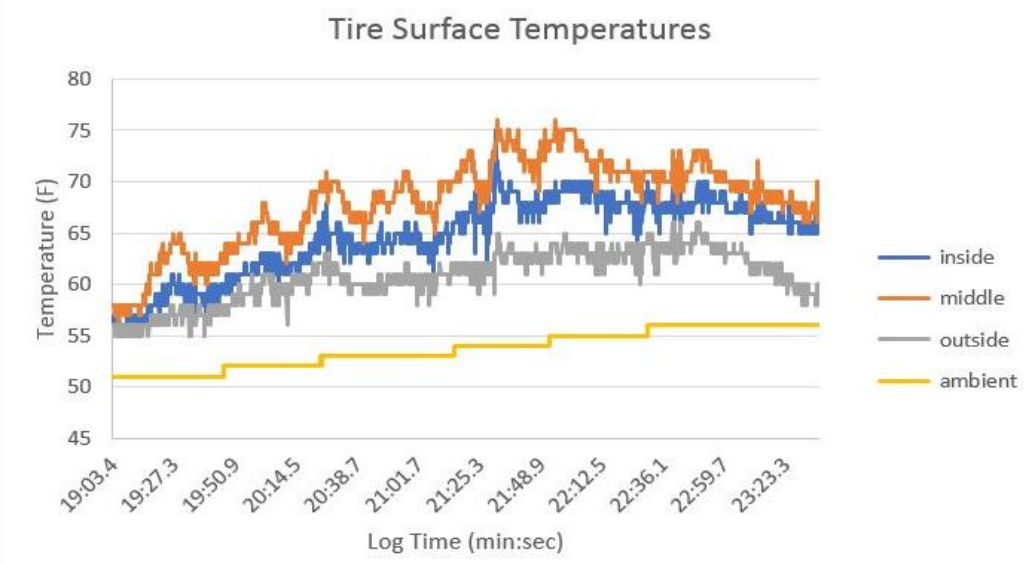

Figure 109: Dynamic Tire Temperatures

PROJECT MANAGEMENT

SCHEDULE

Original/Proposed

Task Name	Duration	Start	Finish
Tire Data Collection Rig	**175 days**	**Mon 8/22/16**	**Fri 4/21/17**
⊟ **Design 1**	**38 days**	**Mon 8/22/16**	**Wed 10/12/16**
Start Design 1	1 day	Mon 8/22/16	Mon 8/22/16
Design Report Rough Draft	24 days	Tue 8/23/16	Fri 9/23/16
Final Proposal Report	13 days	Mon 9/26/16	Wed 10/12/16
Design 1 Complete	0 days	Wed 10/12/16	Wed 10/12/16
⊟ **Design 2**	**70 days**	**Mon 10/17/16**	**Fri 1/20/17**
Start Design 2	1 day	Mon 10/17/16	Mon 10/17/16
Concept Sketches	10 days	Mon 10/17/16	Fri 10/28/16
Select Best Concept Design (ad	5 days	Mon 10/24/16	Fri 10/28/16
Design Rig	51 days	Mon 10/31/16	Mon 1/9/17
Prepare for Design Presentatio	5 days	Mon 1/9/17	Fri 1/13/17
First Design Presentation	**5 days**	**Mon 1/16/17**	**Fri 1/20/17**
Design 2 Complete	1 day	Fri 1/20/17	Fri 1/20/17
⊟ **Design 3**	**65 days**	**Mon 1/23/17**	**Fri 4/21/17**
Start Design 3	1 day	Mon 1/23/17	Mon 1/23/17
Manufacture Rig	21 days	Mon 1/23/17	Mon 2/20/17
Perform Testing/Collect Data	30 days	Mon 2/20/17	Fri 3/31/17
Tech Expo	**5 days**	**Mon 4/3/17**	**Fri 4/7/17**
Project Presentation	**5 days**	**Mon 4/10/17**	**Fri 4/14/17**
Submit Report to Library	5 days	Mon 4/17/17	Fri 4/21/17

Table 6: Original Schedule

Actual

Task Name	Duration	Start	Finish
Tire Data Collection Rig	175 days	Mon 8/22/16	Fri 4/21/17
Design 1	**38 days**	**Mon 8/22/16**	**Wed 10/12/16**
Start Design 1	1 day	Mon 8/22/16	Mon 8/22/16
Design Report Rough Draft	24 days	Tue 8/23/16	Fri 9/23/16
Final Proposal Report	13 days	Mon 9/26/16	Wed 10/12/16
Design 1 Complete	0 days	Wed 10/12/16	Wed 10/12/16
Design 2	**81 days**	**Mon 10/17/16**	**Mon 2/6/17**
Start Design 2	1 day	Mon 10/17/16	Mon 10/17/16
Concept Sketches	10 days	Mon 10/17/16	Fri 10/28/16
Select Best Concept Design (advisor)	5 days	Mon 10/24/16	Fri 10/28/16
Design Rig	70 days	Mon 10/31/16	Fri 2/3/17
Prepare for Design Presentation	9 days	Fri 1/20/17	Wed 2/1/17
First Design Presentation	**1 day**	**Thu 2/2/17**	**Thu 2/2/17**
Design 2 Complete	1 day	Mon 2/6/17	Mon 2/6/17
Design 3	**60 days**	**Mon 2/6/17**	**Fri 4/28/17**
Start Design 3	1 day	Mon 2/6/17	Mon 2/6/17
Design/Manufacture Rig	35 days	Mon 2/6/17	Fri 3/24/17
Perform Testing/Collect Data	12 days	Fri 3/17/17	Sun 4/2/17
Tech Expo	**1 day**	**Thu 4/6/17**	**Thu 4/6/17**
Project Presentation	**1 day**	**Fri 4/14/17**	**Fri 4/14/17**
Submit Report to Library	11 days	Sat 4/15/17	Fri 4/28/17

Table 7: Actual Schedule

One of the most time consuming parts was the actual designing aspect of the rig. Originally the goal was to have the tire rig designed by the end of January, but there were still design changes being made in mid-March. This delay was due to multiple redesigns including more FEA validation than originally assumed. Preliminary testing of the rig resulted in some design changes too. Originally there was about a month planned for testing but less than half a month was actually used due to the extended design process. There are currently still *plans to finish* some testing and analysis before the rig will be deployed and data will be used.

BUDGET

Original/Proposed

Category	Item	Unit Price ($)	Quatntity	Total ($)
Structure	Raw materials	250	1	250
	Fabrication	250	1	250
				0
Data Aq	Raspberry Pi	35	1	35
	Temperature Sensors	13	4	52
	Load Cells	40	3	120
	Rotary encoder	17	4	68
	Ambient temp, press	24	1	24
	Sensor Mounting	20	1	20
	misc electron wrangling	50	1	50
Tire interface	Hub	16	1	16
	Axle	45	1	45
	bearings and mounts	100	1	100
				0
Controls	stepper	50	1	50
	stepper driver	20	1	20
	belt+sprockets	35	1	35
				0
Total				1135

Table 8: Original Budget

Actual

Item	Unit Price ($)	Quantity	Total ($)
village hardware	41.74	1	41.74
drive sprocket	11.39	1	11.39
driven sprocket	32.84	1	32.84
roller chain	10.28	1	10.28
master link	1	1	1
SA shaft	27.6	1	27.6
SA flange mount	62.03	1	62.03
cam lock handle	12.43	3	37.29
tire shaft	52.43	1	52.43
rod ends	6.58	6	39.48
.50 spacer	6.97	4	27.88
.25 spacer	3.77	2	7.54
turnbuckle	15.93	1	15.93
encoder spring	10.35	1	10.35
SA bearings	12.43	2	24.86
tire bearings	15.32	2	30.64
LC amps	9.99	2	19.98
screw terminal	16.99	1	16.99
1" shaft collar	10.8	1	10.8
stepper motor	92	1	92
voltage step up	12.49	1	12.49
12v to USB	7.99	1	7.99
IR sensor	18.5	4	74
rotary encoders	20.98	4	83.92
pillow block	28.67	1	28.67
encoder hub	4	1	4
encoder wheel	3	1	3
stepper driver	15.5	1	15.5
LCs	69.75	3	209.25
raspi	35	1	35
LC Stiffener Plate	18	2	36
Tire Closeout	26	1	26
Stiffener	8	4	32
Stiffener 1	14.44	2	28.88
Stiffener 2	12.27	2	24.54
Raw Materials	0	1	0
Fabrication	0	1	0
Total			1194.29

Table 9: Actual Budget

By just looking at the total amount for both the projected and actual budget, they would appear to be very similar. The original had estimates for raw materials and fabrication. The raw materials were donated for the rig, sheet metal components were mostly cut and bent without charge, and the welding was done free-of-charge. The fabrication was self-done with assistance from Victory Parkway's machine shop. All of these things greatly reduced the amount spent but there were a lot more components needed for the rig than previously assumed which increased the budget.

CONCLUSION

After assembling, testing, and obtaining data that verifies the functionality of the tire rig, there is still more progress to be made. The rig fulfills our customer requirements, however, one of the main goals for the rig was to be able to run it on a dirt track. Currently, the only data taken was on a bumpy asphalt parking lot due to a lack of time or track availability to obtain data on dirt. One of the main goals for the future is testing is how different tire compounds, tire manufactures, chemical preps, and rim widths affect the forces and temperatures being recorded. An auxiliary probe will also be added to the rig assembly to log the moving speed, true heading, and rolling radius. Some additional temperature sensors will also be added to the rig so that the track surface and ambient air temperature can also be recorded simultaneously with the tire surface temperatures and tire cage ambient temperature.

WORKS CITED

1. ***Caesars Creek Speedway.*** [Online] [Cited: October 12, 2016]. https://www.caesarscreekspeedway.com/schedule

2. G, Yogesh. Track Testing: LeCont tyre compounds. *Karting magazine.* [Online] Karting Magazine, February 13, 2013. [Cited: September 25, 2016]. http://www.kartingmagazine.com/features/track-testing-lecont-tyre-compounds/

3. Godwin, Todd. Balance Achievement Part Three: Weights and Percentages. *Oval Kart Magazine.* [Online] Dynamics of Speed, January 2007. [Cited: October 12, 2016]. http://www.dynamicsofspeed.com/articles/PercentagesP3.pdf

4. Godwin, Todd. Bite… Makin' It. *Oval Kart Magazine*. [Online] Dynamics of Speed, December 2005. [Cited: October 12, 2016]. http://www.dynamicsofspeed.com/articles/Bite_Dec-05

5. ***Larry Jones Motorsports.*** [Online] [Cited: September 25, 2016]. http://www.larryjonesmotorsports.com/price.html

6. Milliken, William F. and Douglas L. Milliken. Race Car Vehicle Dynamics. Society of Automotive Engineers, 1995.

7. Tomasi, Davide. Fitting of tire's experimental data. [Online] multibody.net. [Cited: March 26, 2017]. http://www.multibody.net/teaching/dissertations/2011-tomasi/

8. Tsubakimoto Europe. ANSI G7 Standard Roller Chain. [Online] [Cited: March 28, 2017]. http://tsubaki.eu/chain/ansi-standard-roller-chain/#Single

9. Wehrheim, Chris. Kart360 Product Test: Vega FH Tires. *Kart360*. [Online] Kart360, September 24, 2013. [Cited: September 25, 2016]. http://kart360.com/features/kart360-tire-test-vega-fh

APPENDIX A

FRONT ASSEMBLY DRAWINGS

2” square tube by 8” long

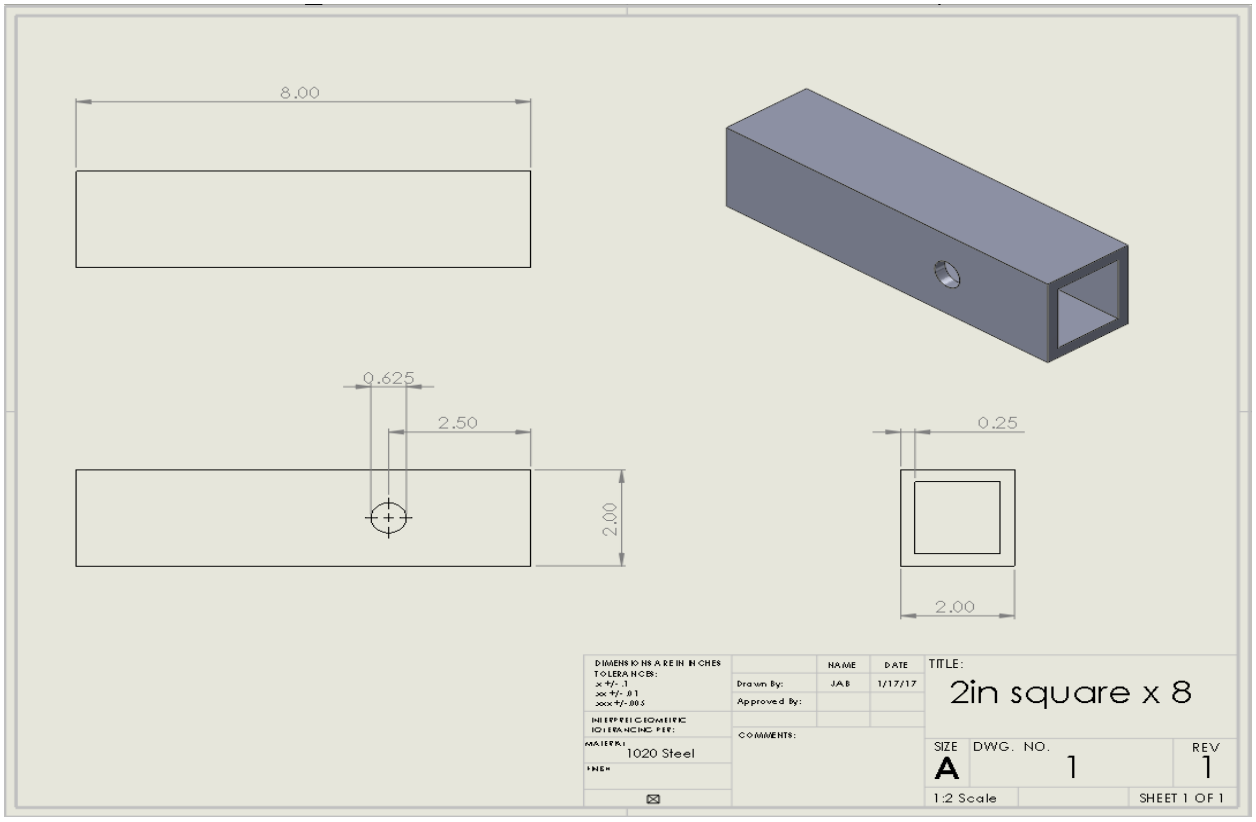

2” square tube by 10” long

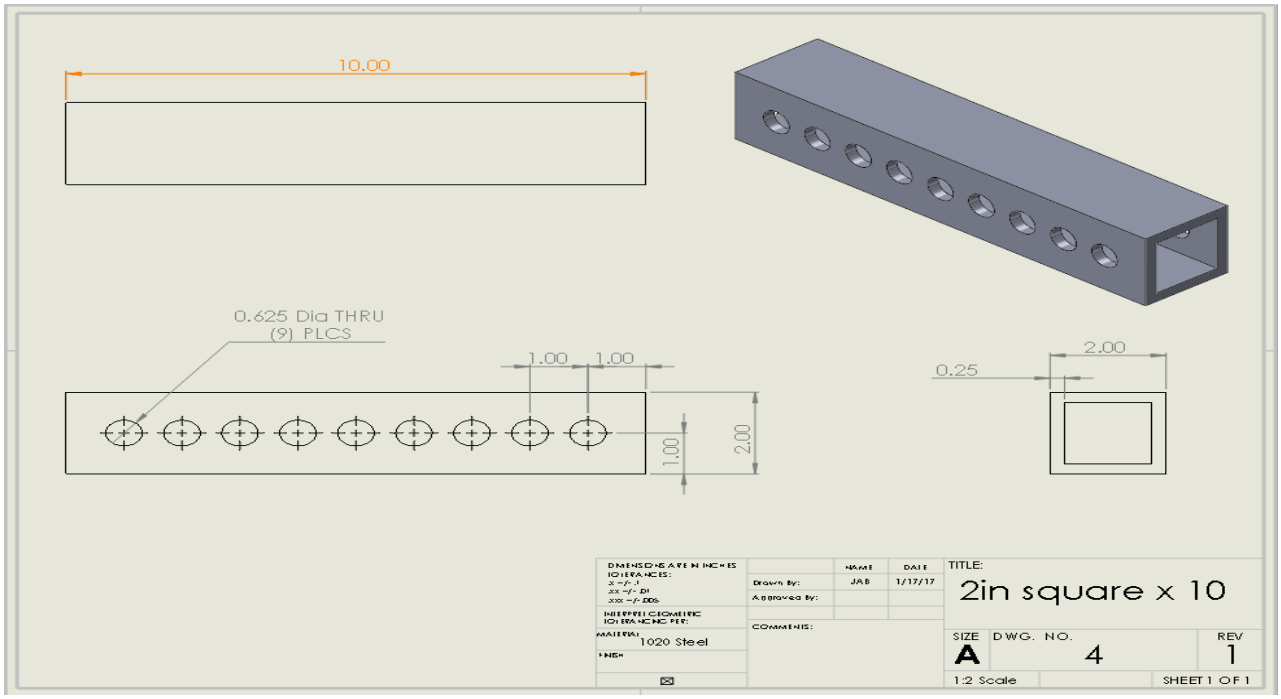

3” wide by 1.5” tall gusset

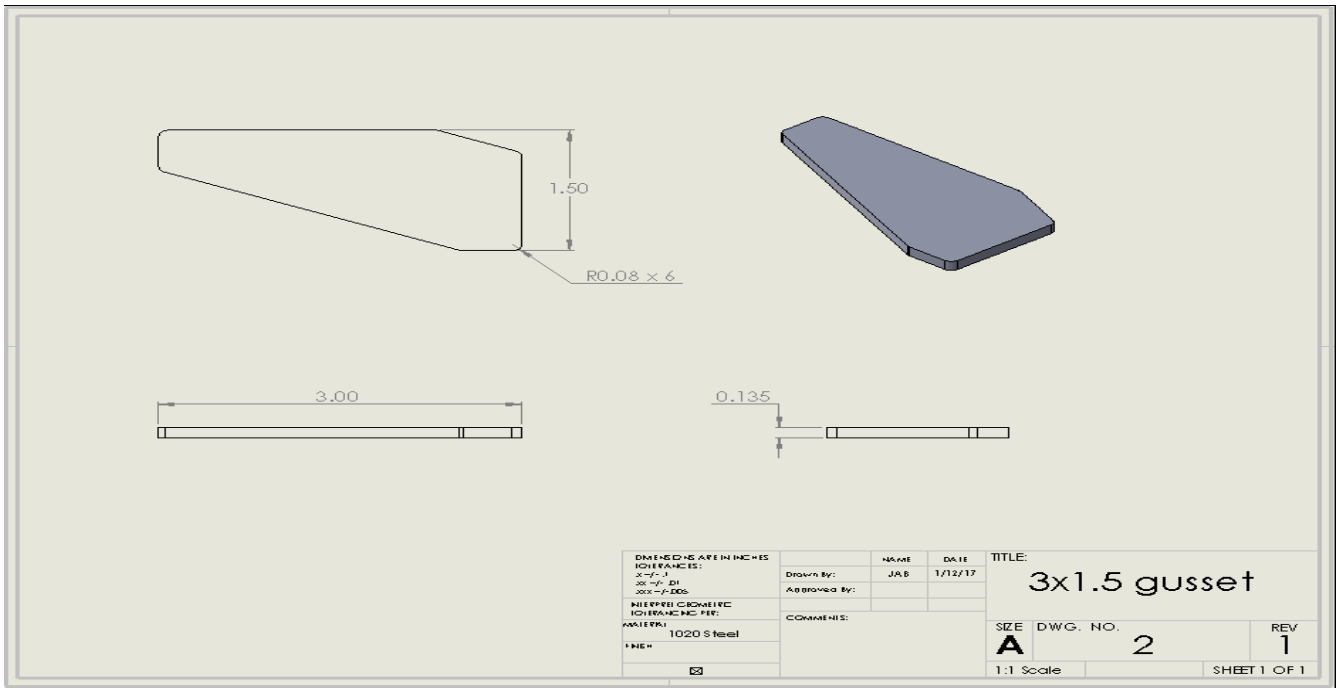

3” wide by 6.5” tall gusset

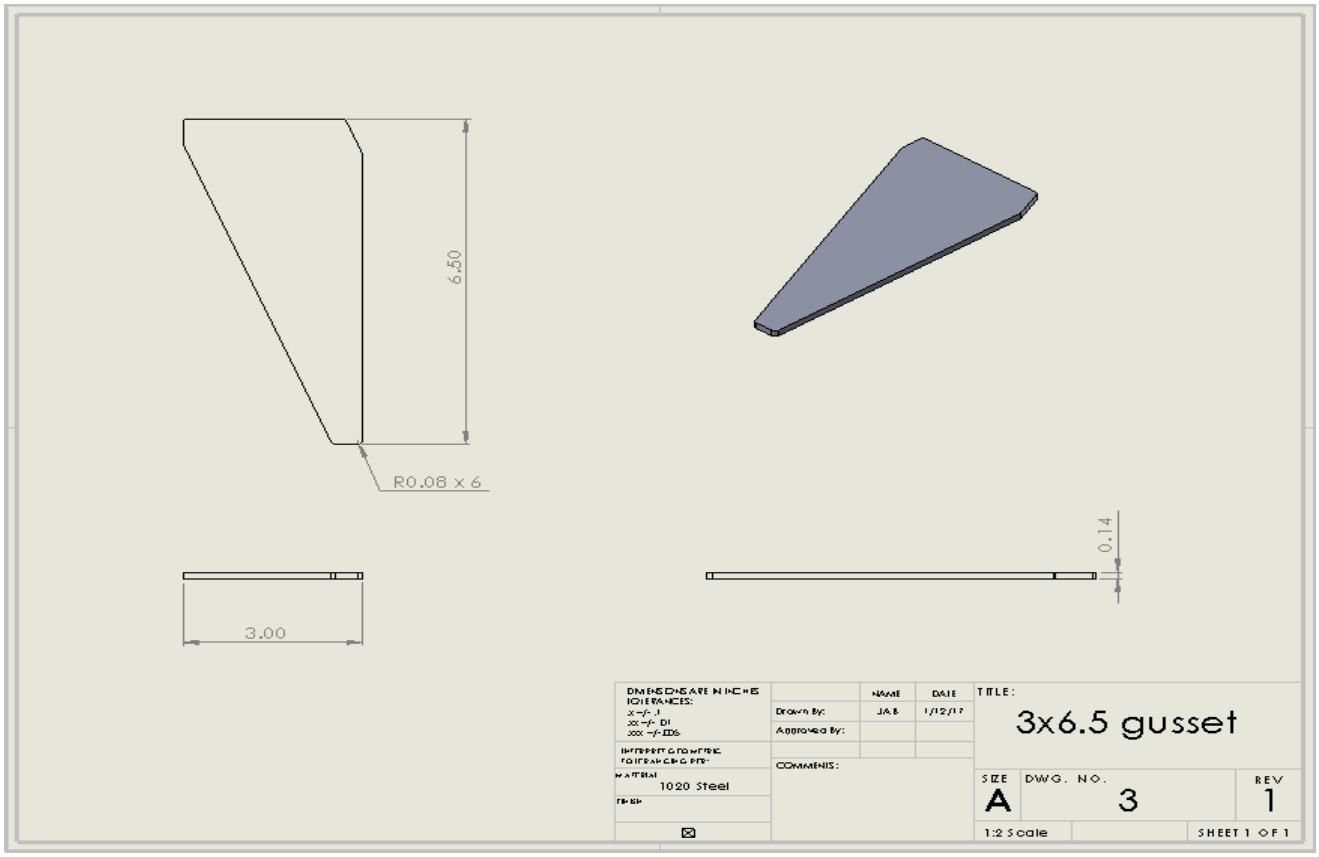

Hitch Adapter Sub-Assembly

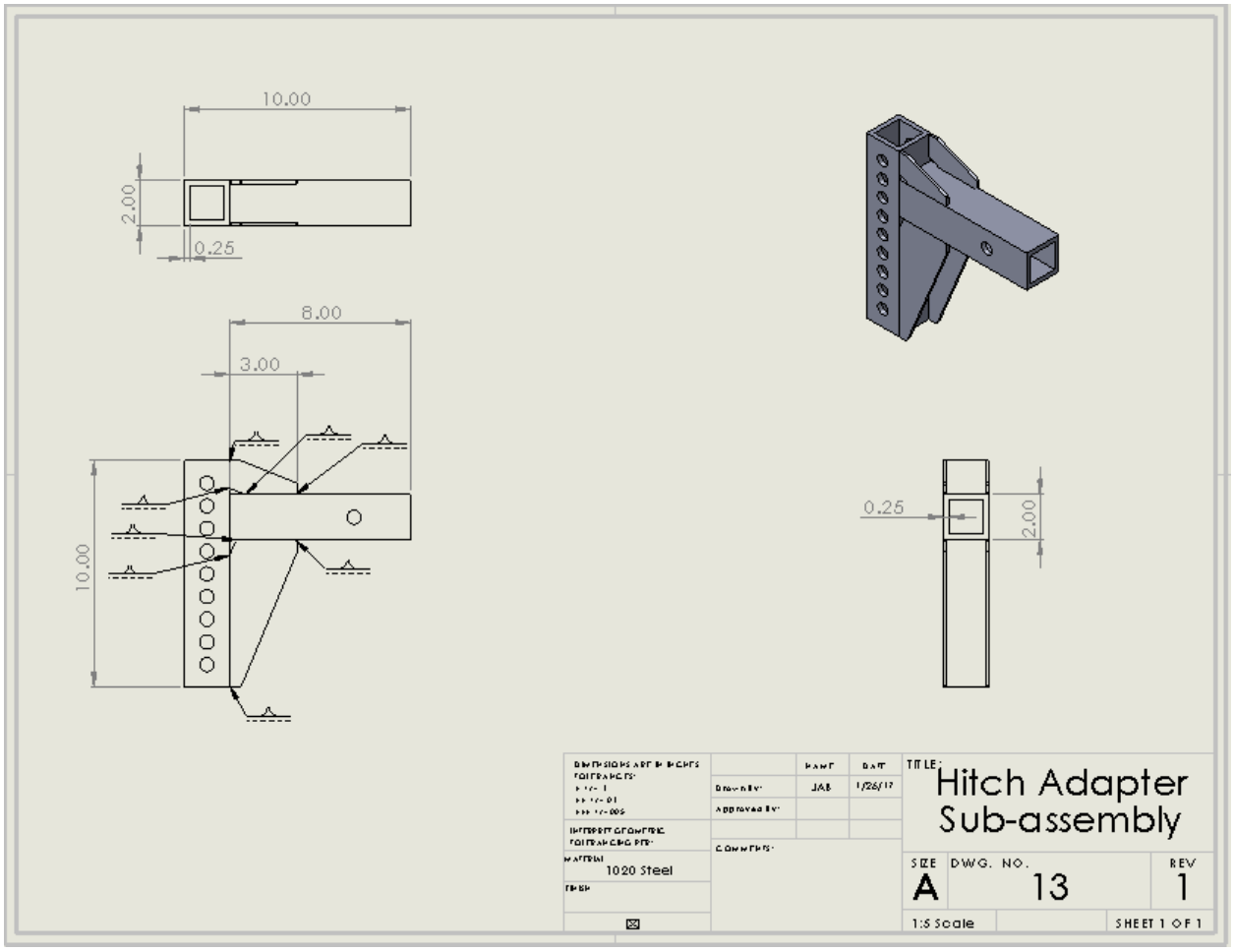

Pivot Plate

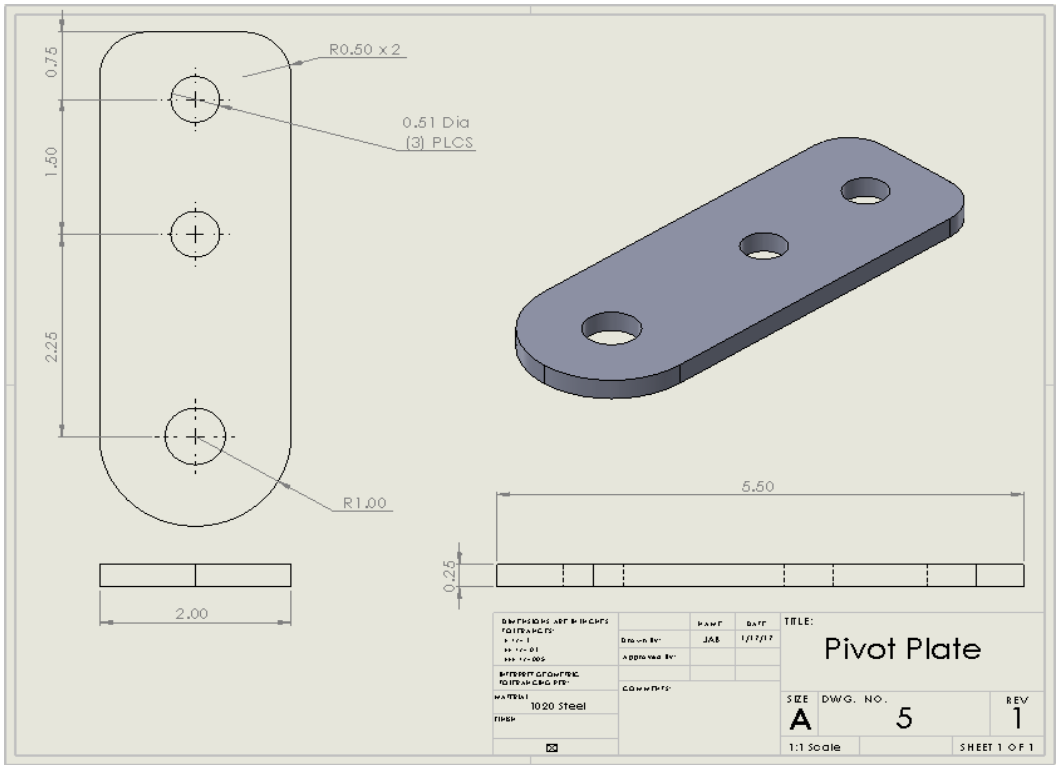

Pivot Tube

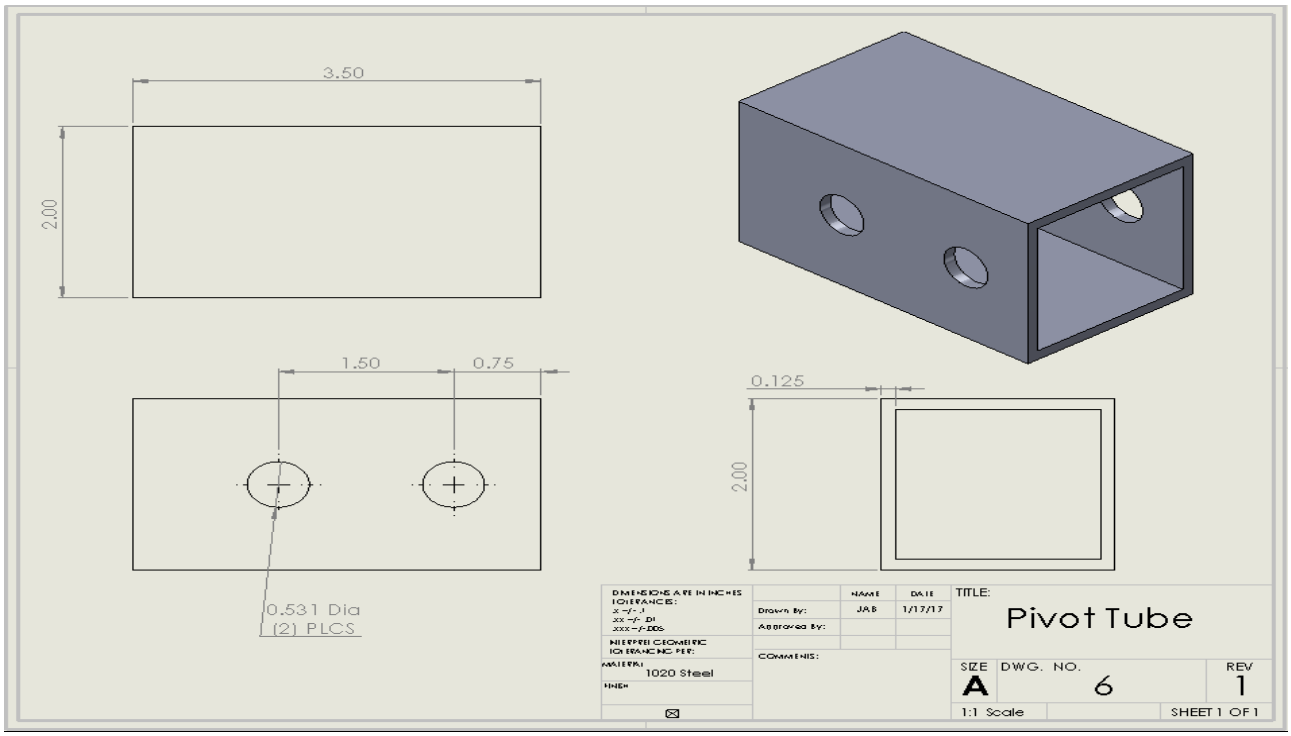

Camber Tube

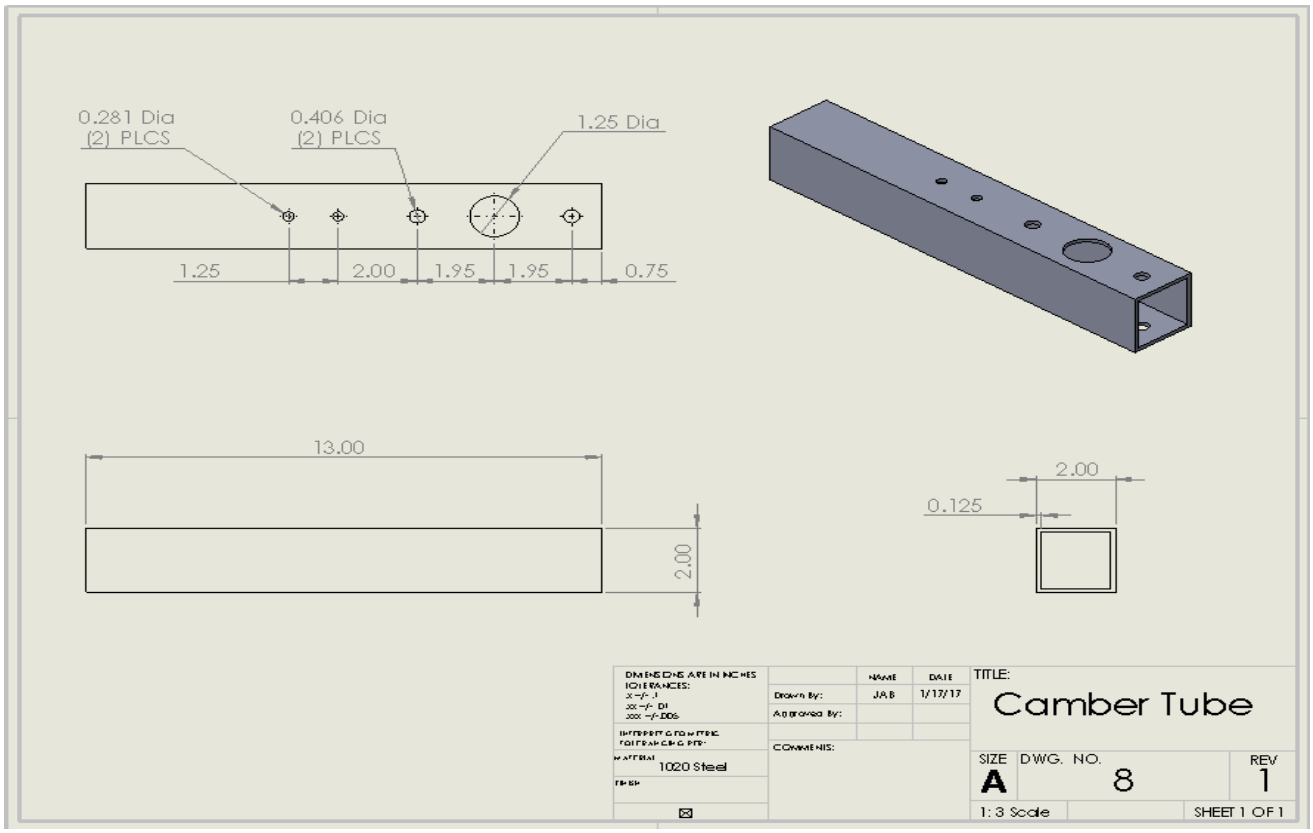
0.281 Dia
(2) PLCS
0.406 Dia
(2) PLCS
1.25 Dia
1.25
2.00
1.95
1.95
0.75
13.00
2.00
2.00
0.125
DIMENSIONS ARE IN INCHES
TOLERANCES:
NAME
DATE
Drawn By:
JAB
1/17/17
Approved By:
COMMENTS:
1020 Steel
TITLE:
Camber Tube
SIZE
A
DWG. NO.
8
REV
1
1: 3 Scale
SHEET 1 OF 1

Fixed Plate

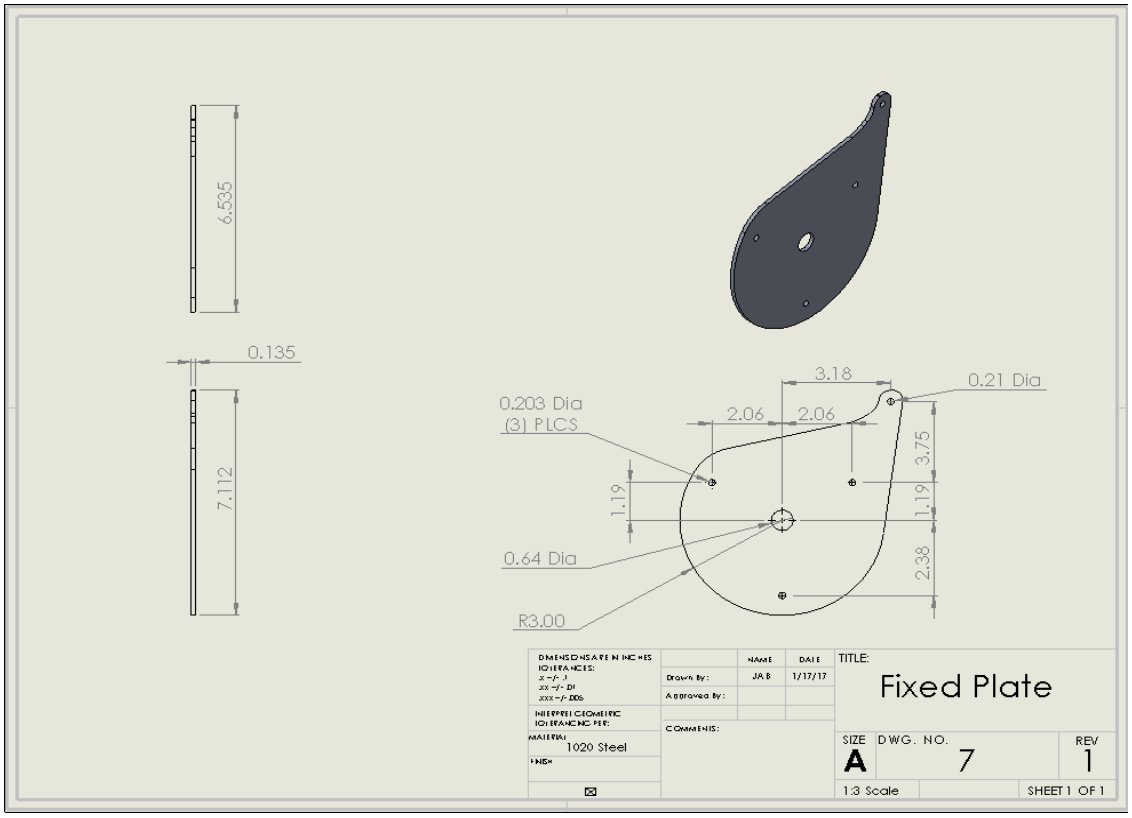

Sliding Plate

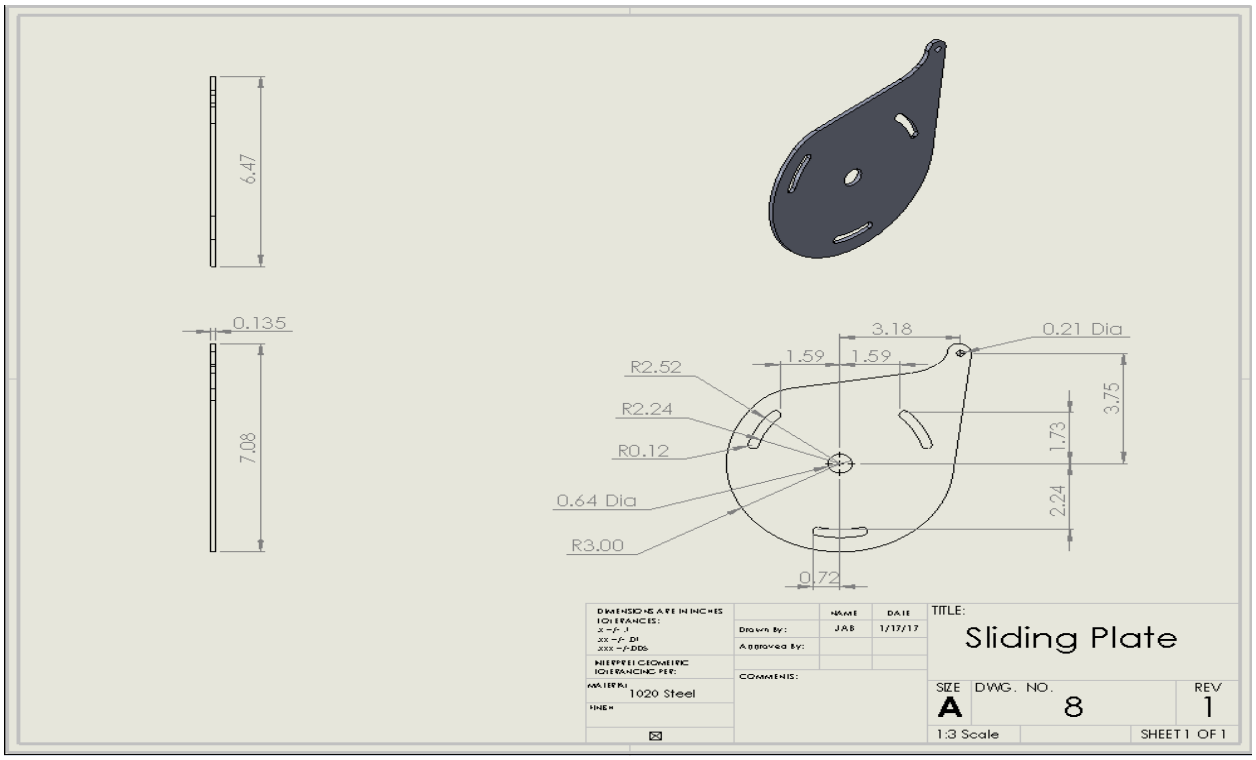

Slip Angle Drive Cross

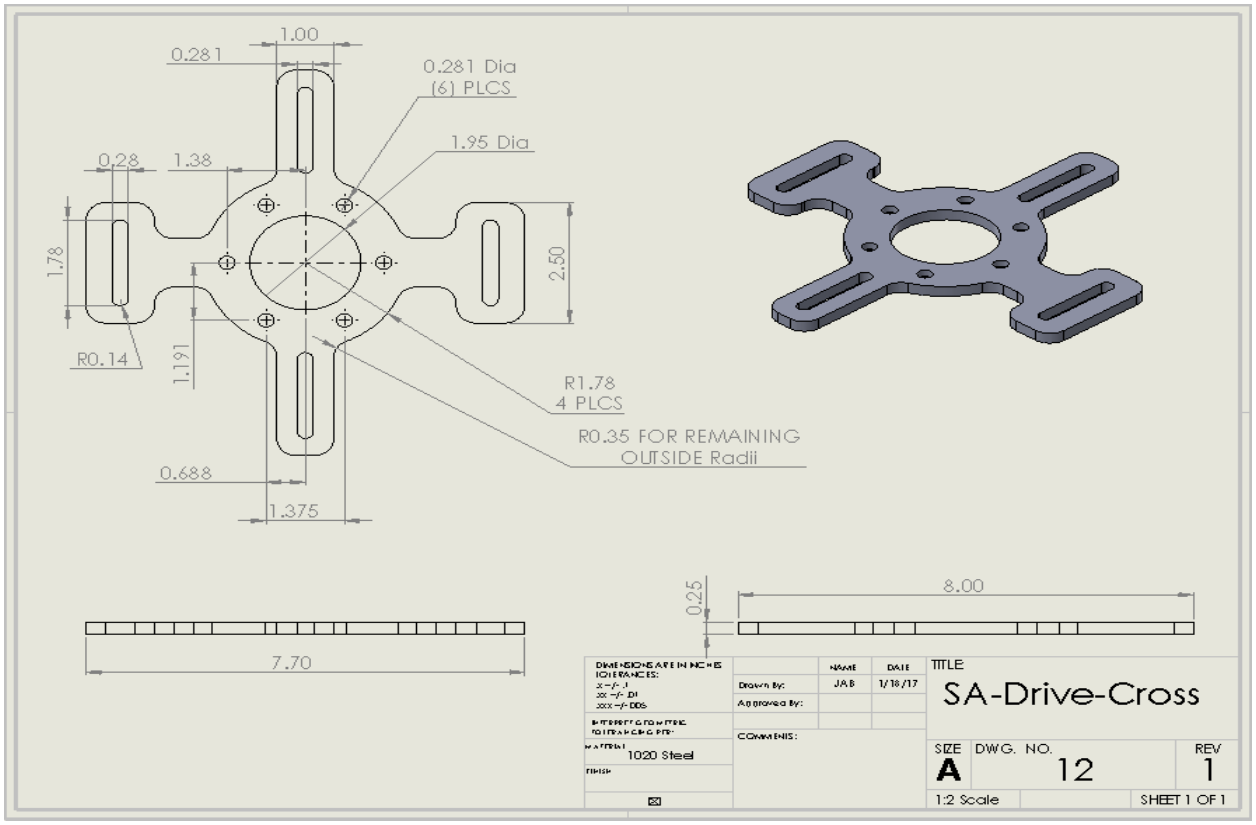

Motor Block

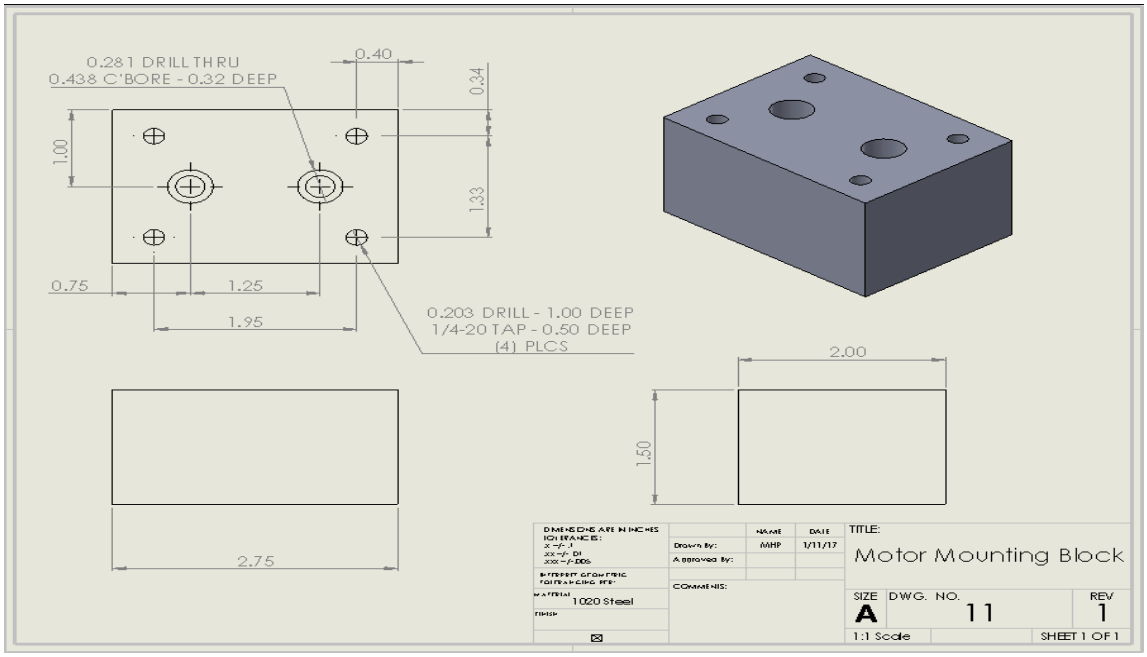

Motor Mounting Plate

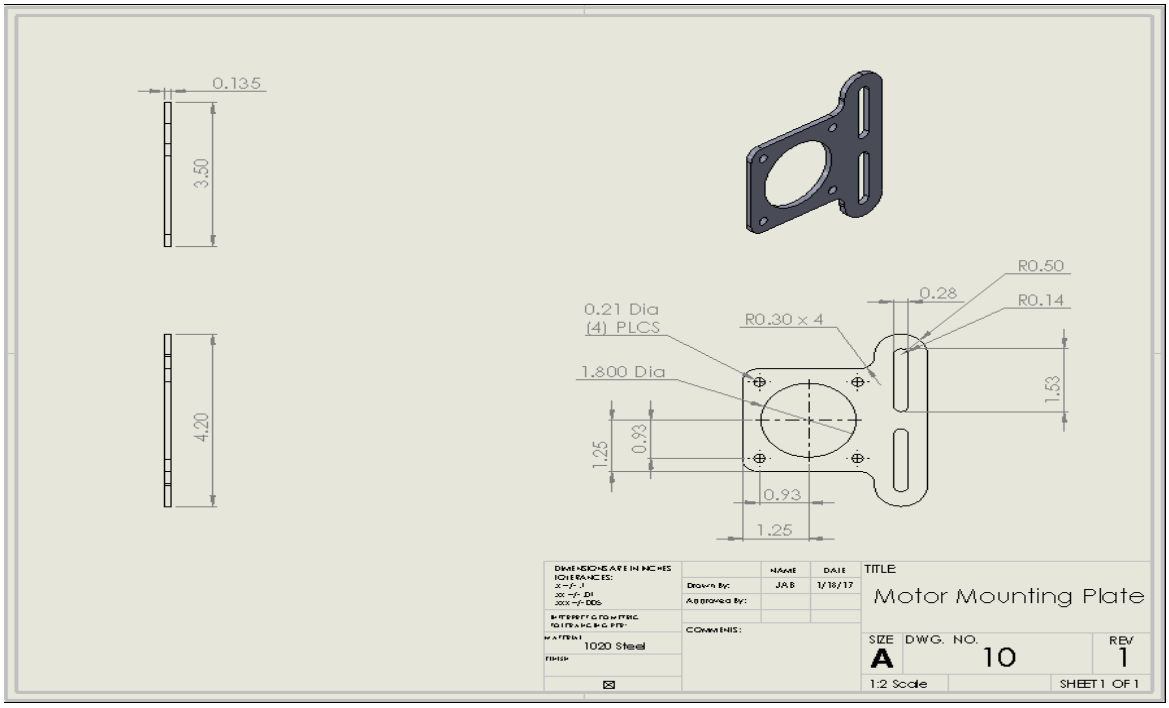

Front Assembly

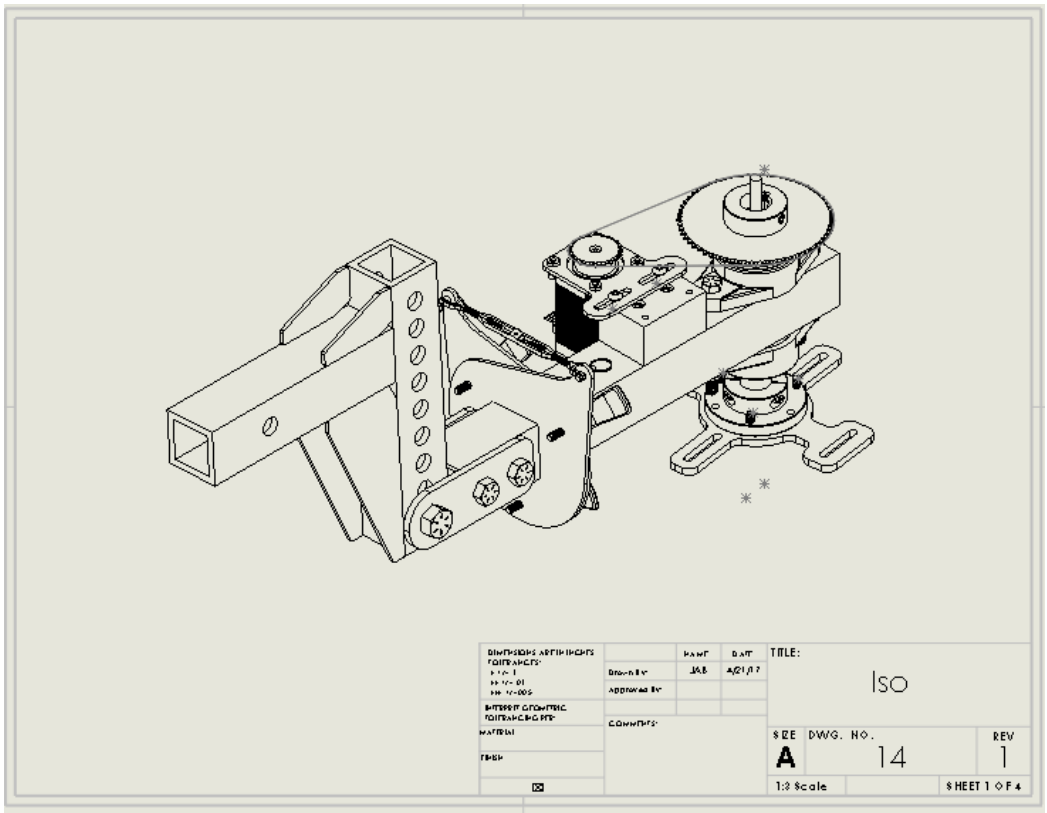

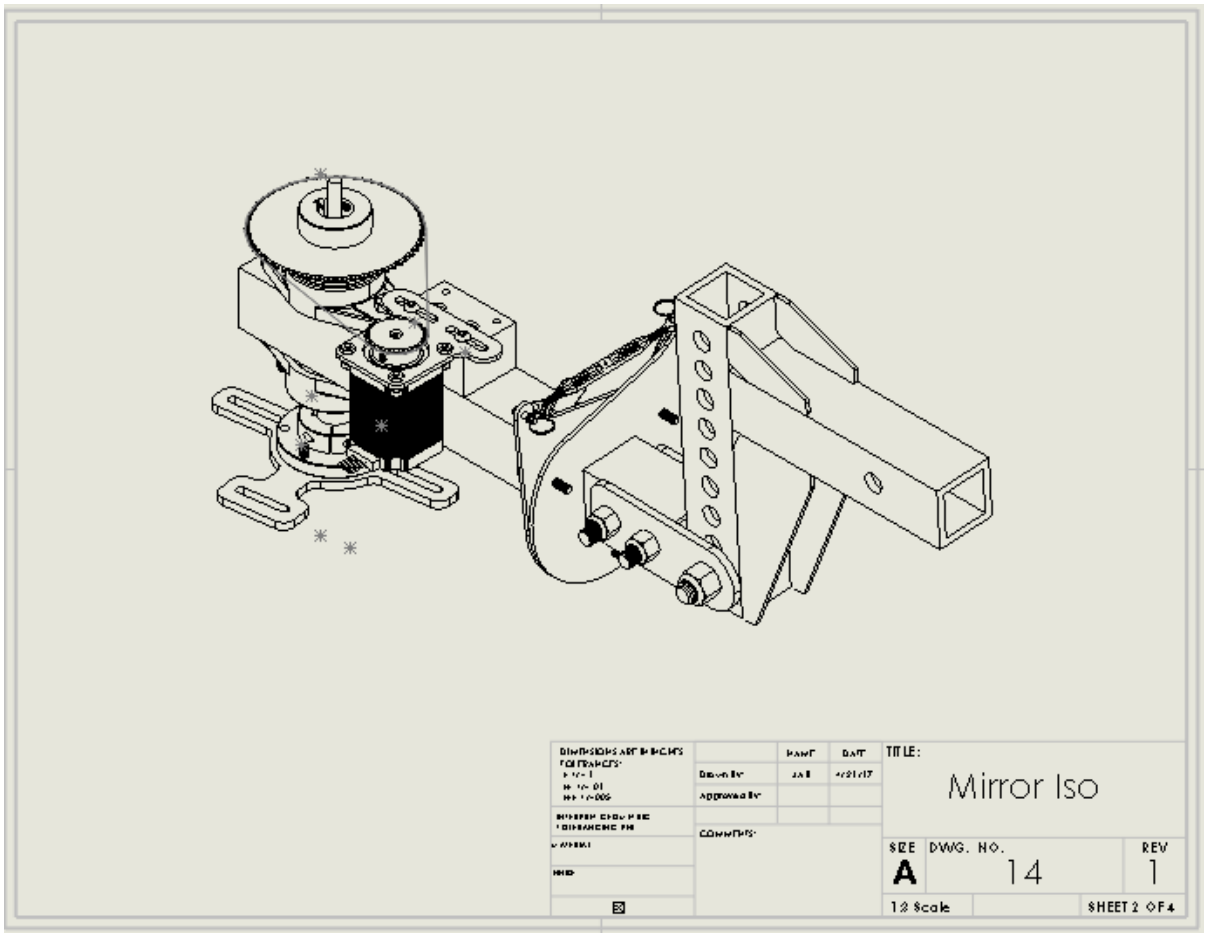
Mirror Iso
SIZE
A
DWG. NO.
14
REV
1
SHEET 2 OF 4

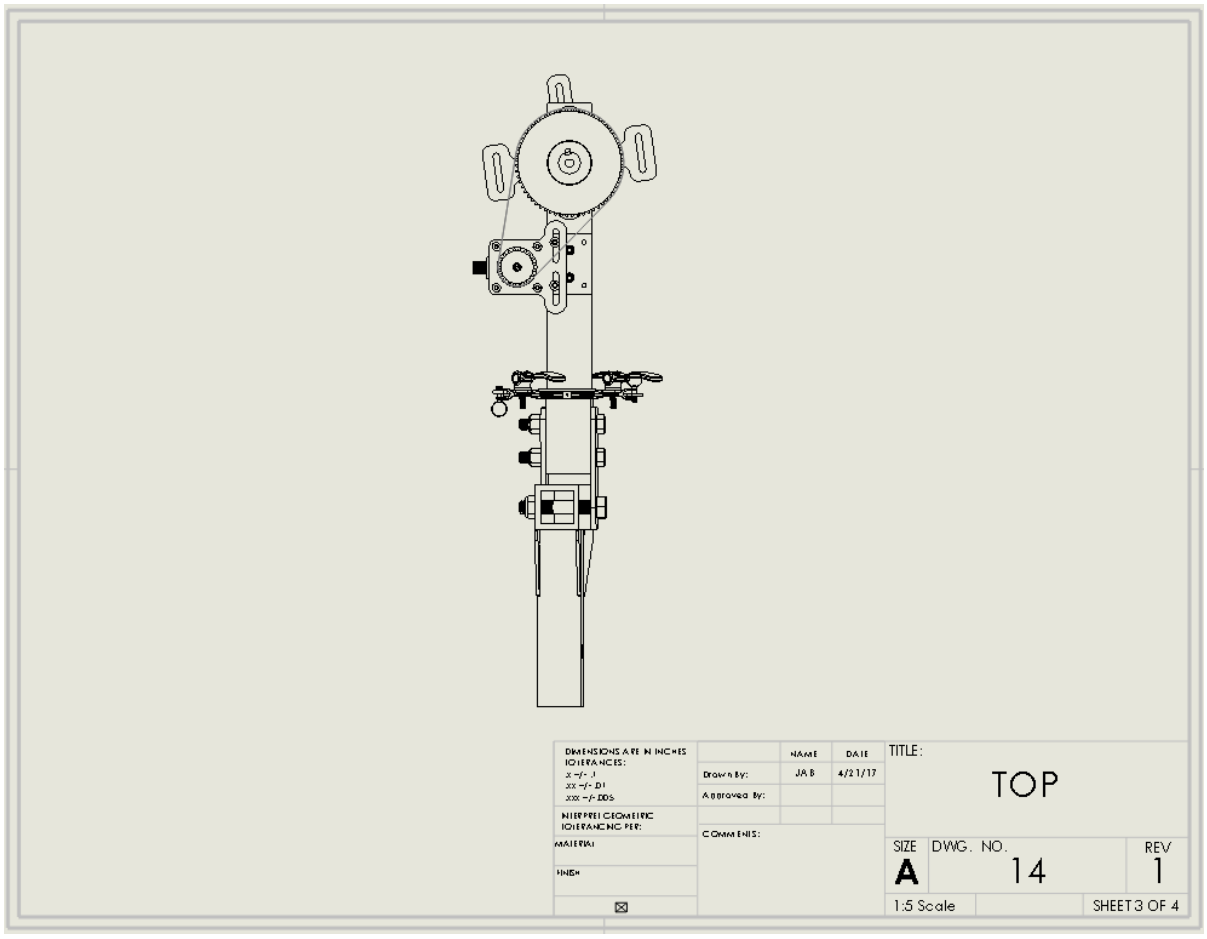
DIMENSIONS ARE IN INCHES
TOLERANCES:
x +/- .1
xx +/- .01
xxx +/- .005
INTERPRET GEOMETRIC TOLERANCING PER:
MATERIAL
FINISH
NAME
DATE
Drawn By:
JAB
4/21/17
Approved By:
COMMENTS:
TITLE:
TOP
SIZE
A
DWG. NO.
14
REV
1
1:5 Scale
SHEET 3 OF 4

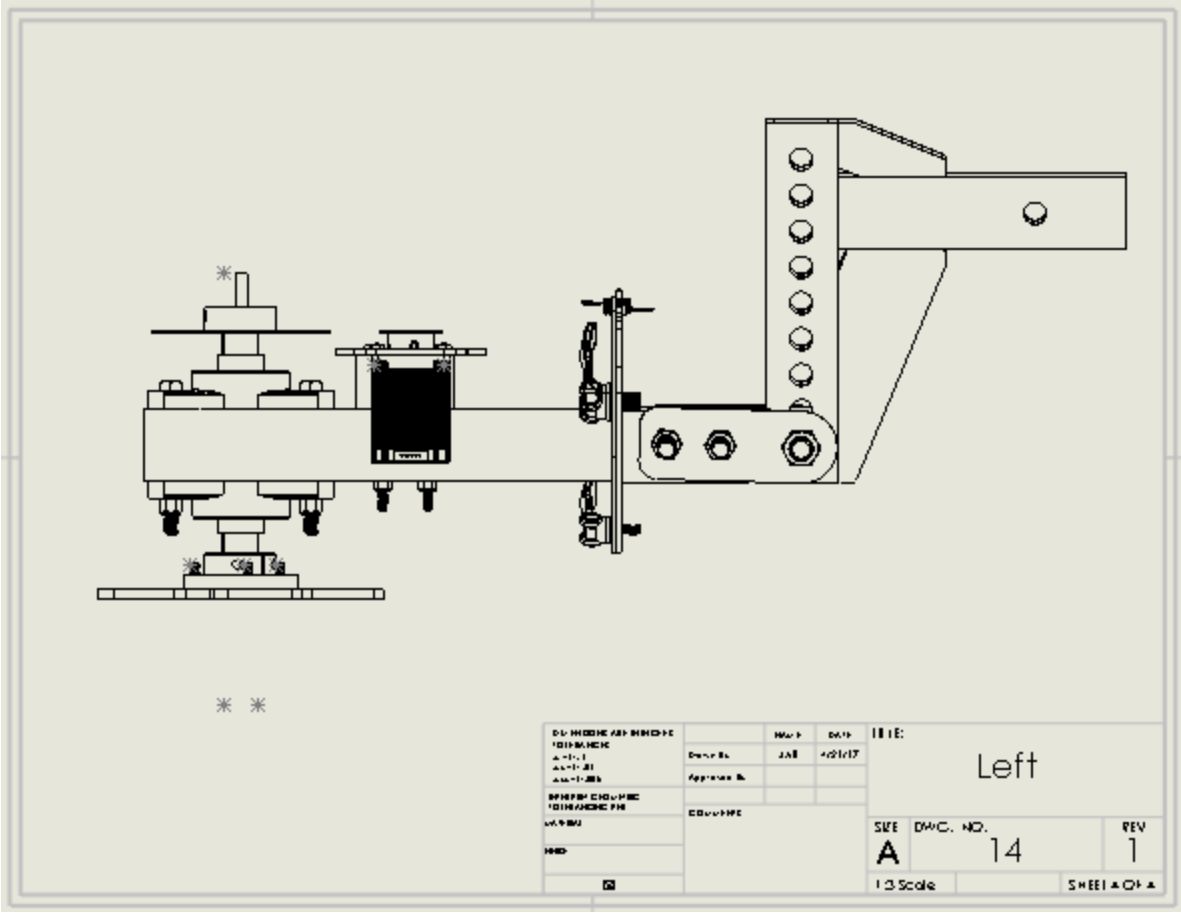
Left
SIZE
A
DWG. NO.
14
REV
1
SHEET 1 OF 1

Front Assembly: Detailed

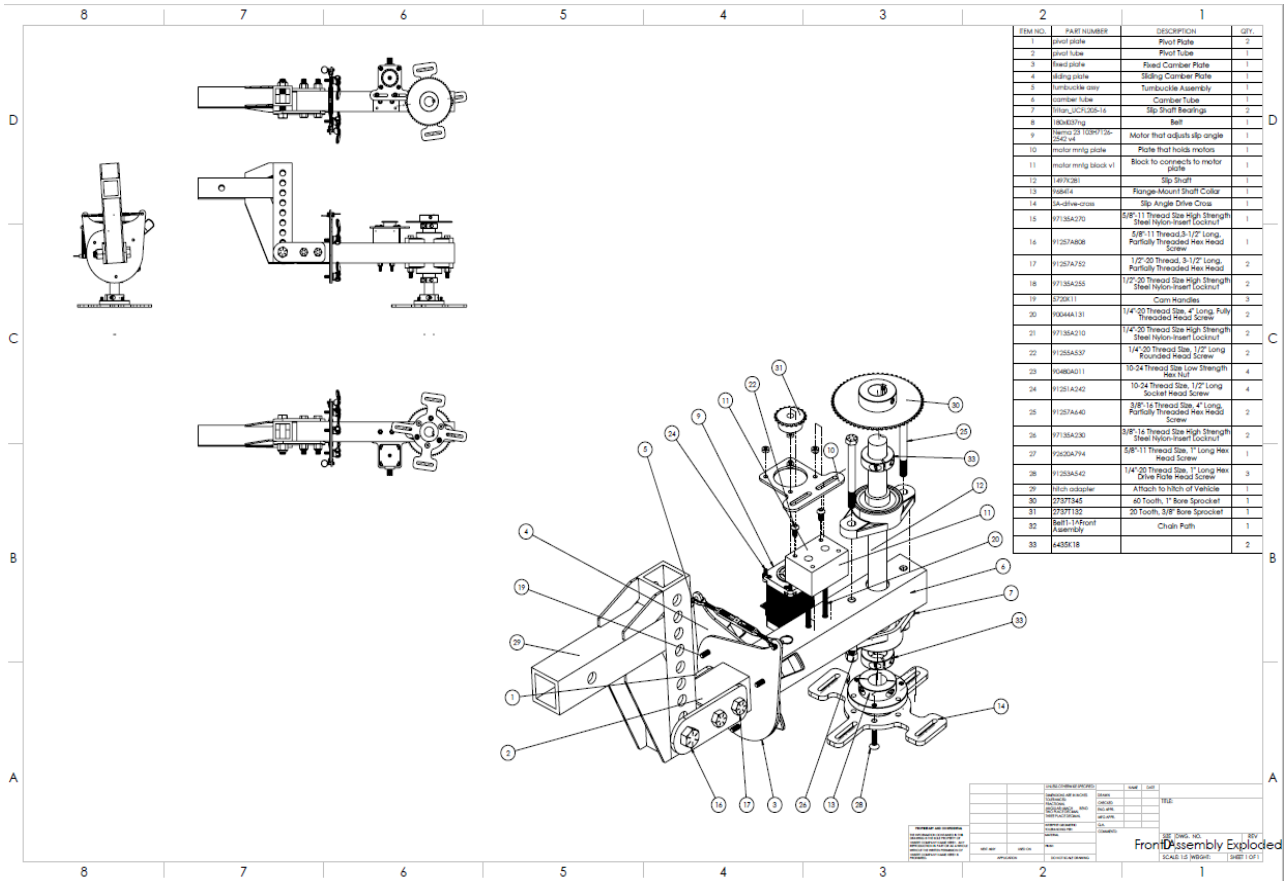

ITEM NO.	PART NUMBER	DESCRIPTION	QTY.
1	pivot plate	Pivot Plate	2
2	pivot tube	Pivot Tube	1
3	fixed plate	Fixed Camber Plate	1
4	sliding plate	Sliding Camber Plate	1
5	turnbuckle assy	Turnbuckle Assembly	1
6	camber tube	Camber Tube	1
7	Triton_UCFC208-16	Slip Shaft Bearings	2
8	180x837mg	Belt	1
9	Nema 23 103H7126-2542 v4	Motor that adjusts slip angle	1
10	motor mntg plate	Plate that holds motors	1
11	motor mntg block v1	Block to connects to motor plate	1
12	1497K281	Slip Shaft	1
13	96841-4	Flange-Mount Shaft Collar	1
14	SA-drive-cross	Slip Angle Drive Cross	1
15	97135A270	5/8"-11 Thread Size High Strength Steel Nylon-Insert Locknut	1
16	91257A808	5/8"-11 Thread,3-1/2" Long, Partially Threaded Hex Head Screw	1
17	91257A752	1/2"-20 Thread, 3-1/2" Long, Partially Threaded Hex Head	2
18	97135A255	1/2"-20 Thread Size High Strength Steel Nylon-Insert Locknut	2
19	5720K11	Cam Handles	3
20	90044A131	1/4"-20 Thread Size, 4" Long, Fully Threaded Head Screw	2
21	97135A210	1/4"-20 Thread Size High Strength Steel Nylon-Insert Locknut	2
22	91255A537	1/4"-20 Thread Size, 1/2" Long Rounded Head Screw	2
23	90480A011	10-24 Thread Size Low Strength Hex Nut	4
24	91251A242	10-24 Thread Size, 1/2" Long Socket Head Screw	4
25	91257A640	3/8"-16 Thread Size, 4" Long, Partially Threaded Hex Head Screw	2
26	97135A230	3/8"-16 Thread Size High Strength Steel Nylon-Insert Locknut	2
27	92635A794	5/8"-11 Thread Size, 1" Long Hex Head Screw	1
28	91253A542	1/4"-20 Thread Size, 1" Long Hex Drive Flate Head Screw	3
29	hitch adapter	Attach to hitch of Vehicle	1
30	2737T345	60 Tooth, 1" Bore Sprocket	1
31	2737T132	20 Tooth, 3/8" Bore Sprocket	1
32	Belt1-1A Front Assembly	Chain Path	1
33	6435K18		2

REFERENCE MOTION PROBE DRAWINGS

Main Bracket

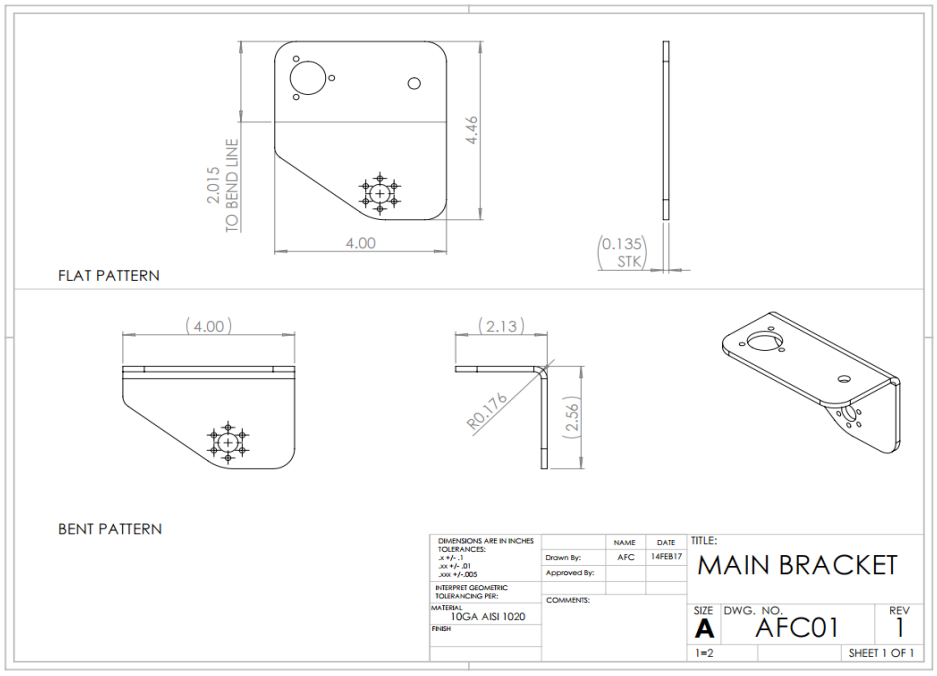

Spacer plate

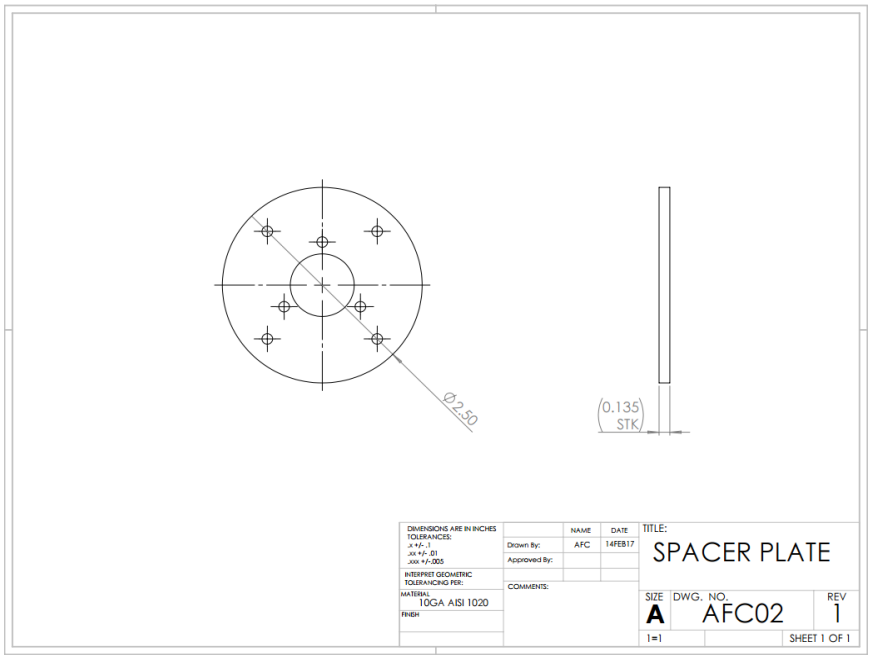

Encoder Pivot Plate

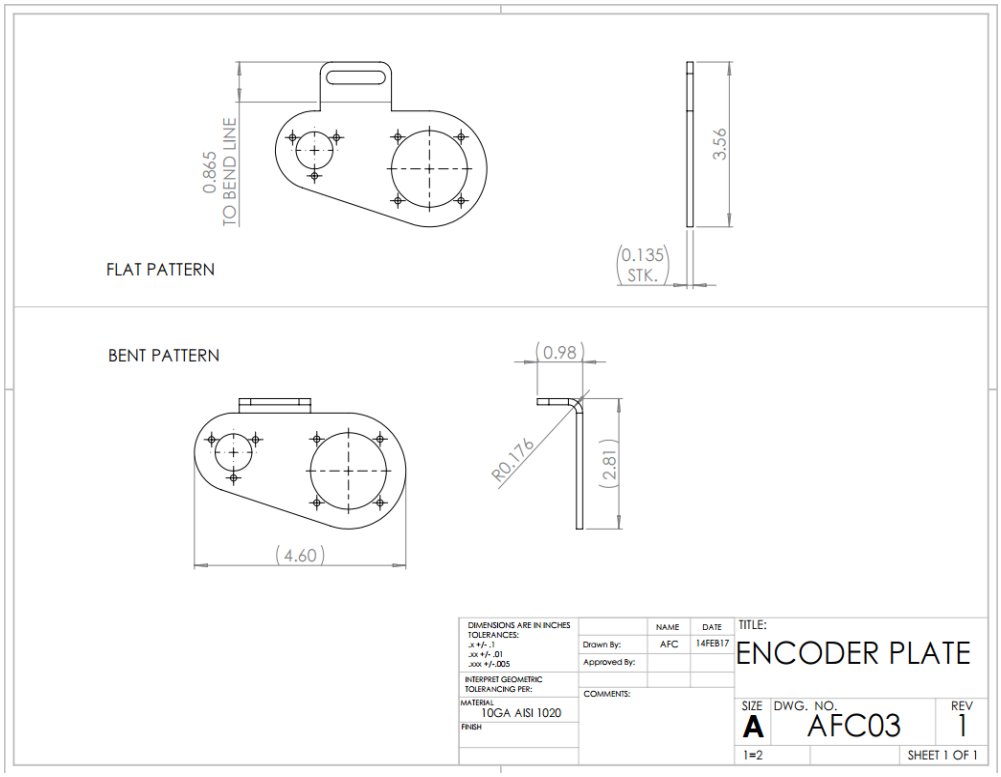

Heading Bracket

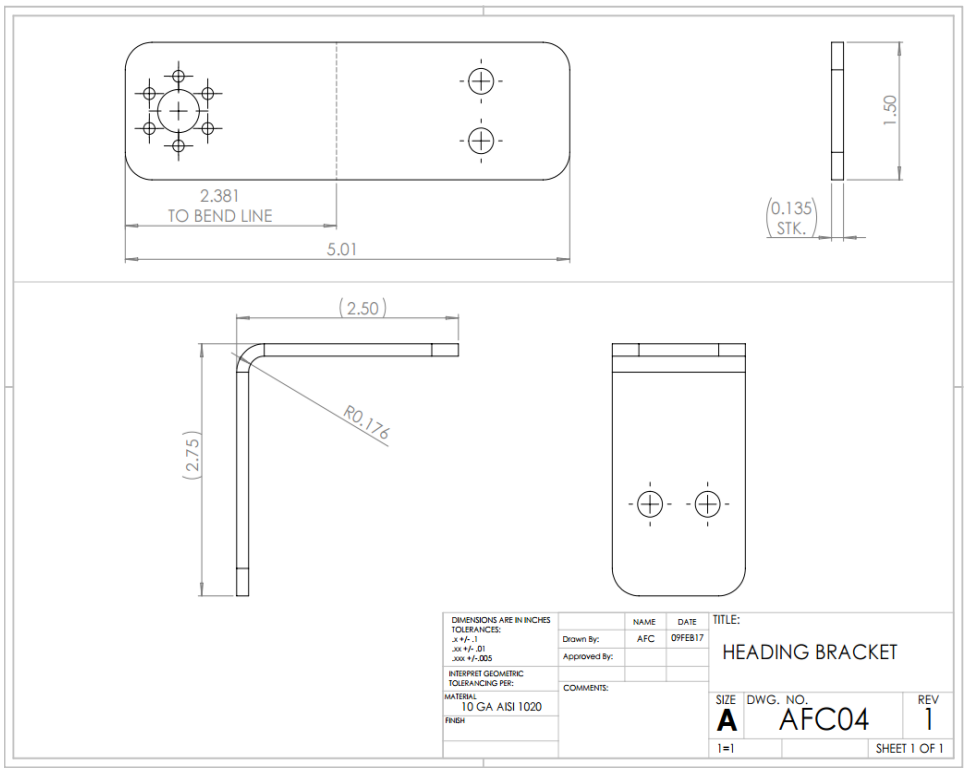

Cage Bracket

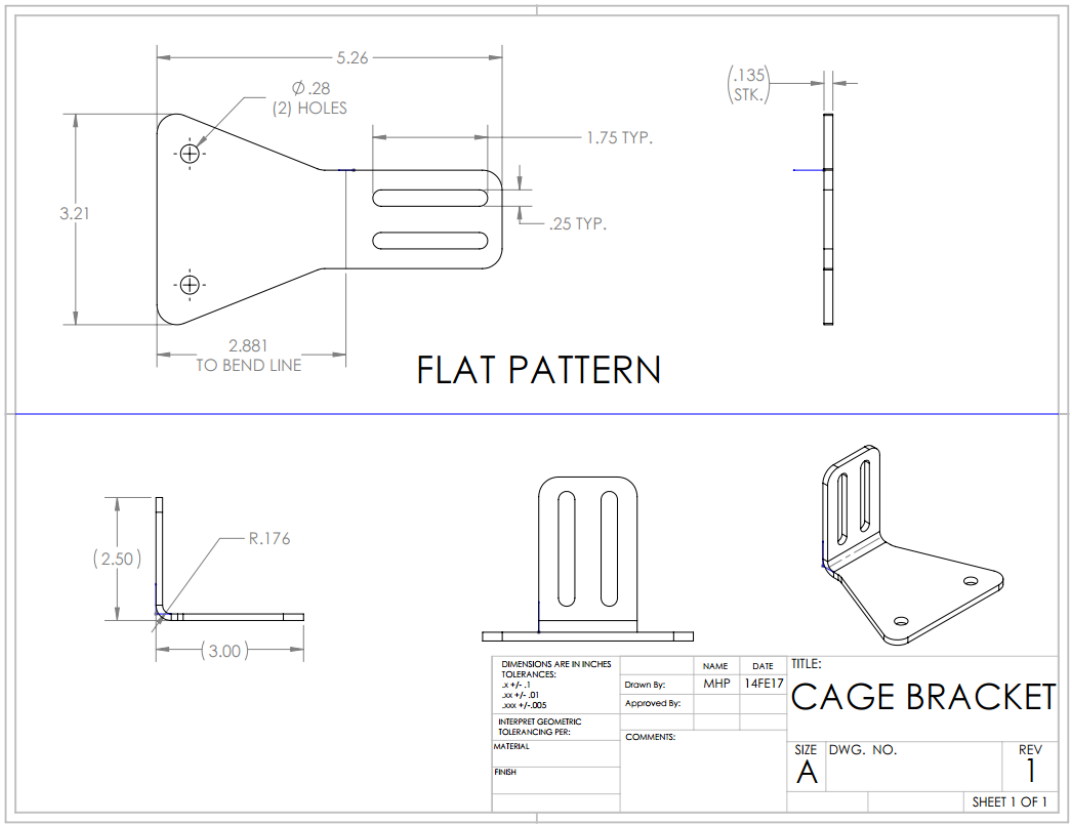

LOAD CELL CAGE DRAWINGS

LC Frame Welding Assembly

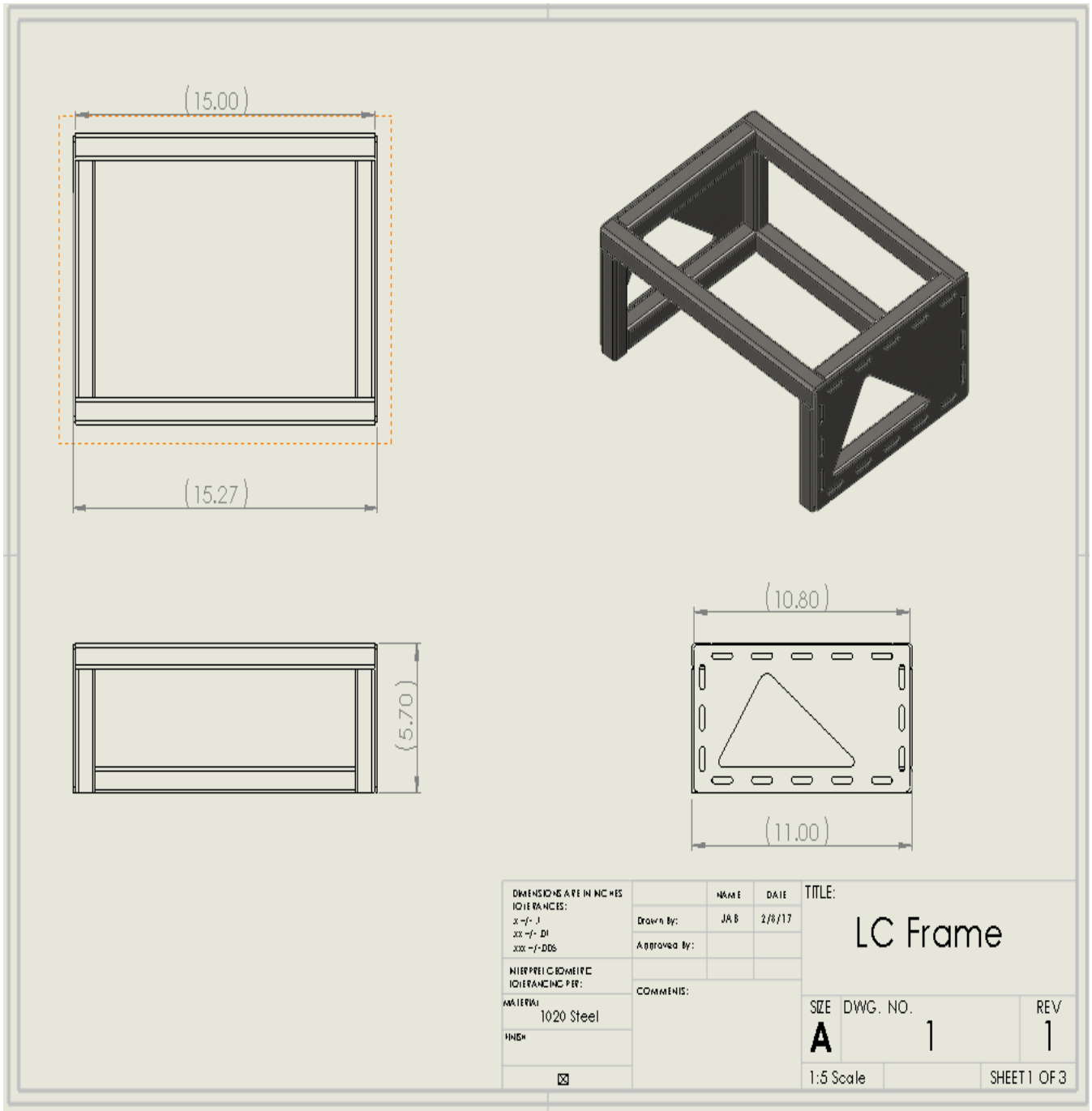

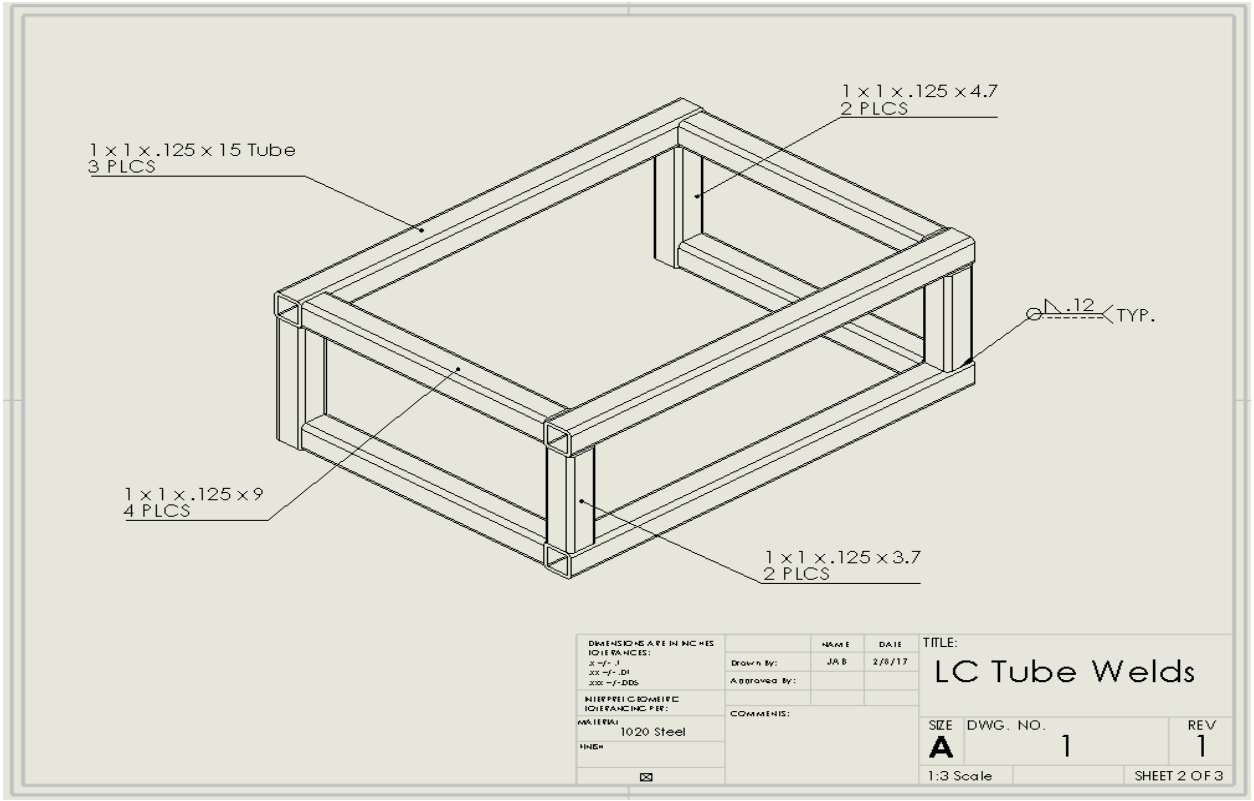
1 x 1 x .125 x 4.7
2 PLCS
1 x 1 x .125 x 15 Tube
3 PLCS
.12
TYP.
1 x 1 x .125 x 9
4 PLCS
1 x 1 x .125 x 3.7
2 PLCS
DIMENSIONS ARE IN INCHES
TOLERANCES:
NAME
DATE
Drawn by:
JAB
2/8/17
Approved By:
COMMENTS:
MATERIAL
1020 Steel
TITLE:
LC Tube Welds
SIZE
A
DWG. NO.
1
REV
1
1:3 Scale
SHEET 2 OF 3

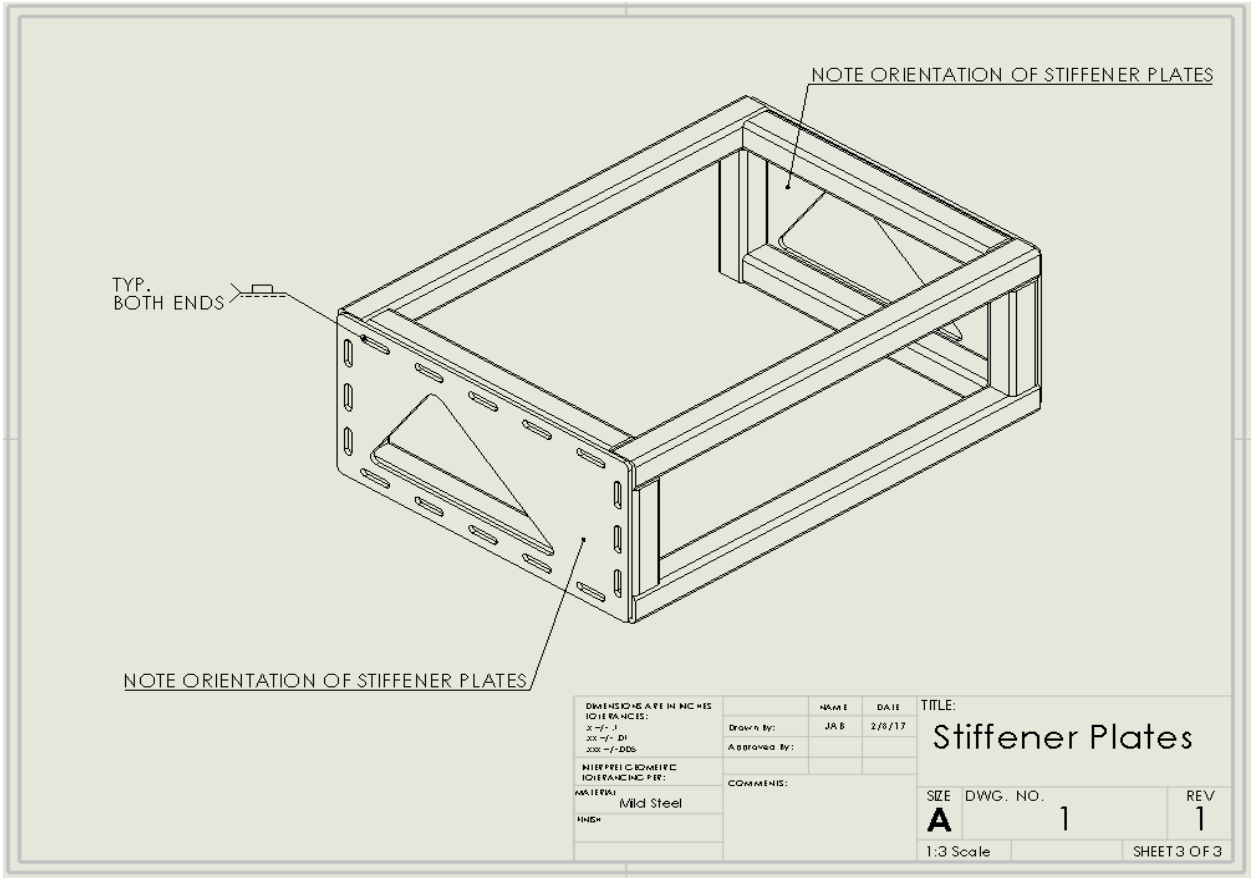
NOTE ORIENTATION OF STIFFENER PLATES
TYP.
BOTH ENDS
NOTE ORIENTATION OF STIFFENER PLATES
DIMENSIONS ARE IN INCHES
TOLERANCES:
x +/- .1
xx +/- .01
xxx +/-.005
INTERPRET GEOMETRIC TOLERANCING PER:
MATERIAL
Mild Steel
FINISH
NAME
DATE
Drawn By:
JAB
2/8/17
Approved By:
COMMENTS:
TITLE:
Stiffener Plates
SIZE
A
DWG. NO.
1
REV
1
1:3 Scale
SHEET 3 OF 3

1 x 1 x .125 x 3.7 Square Tube

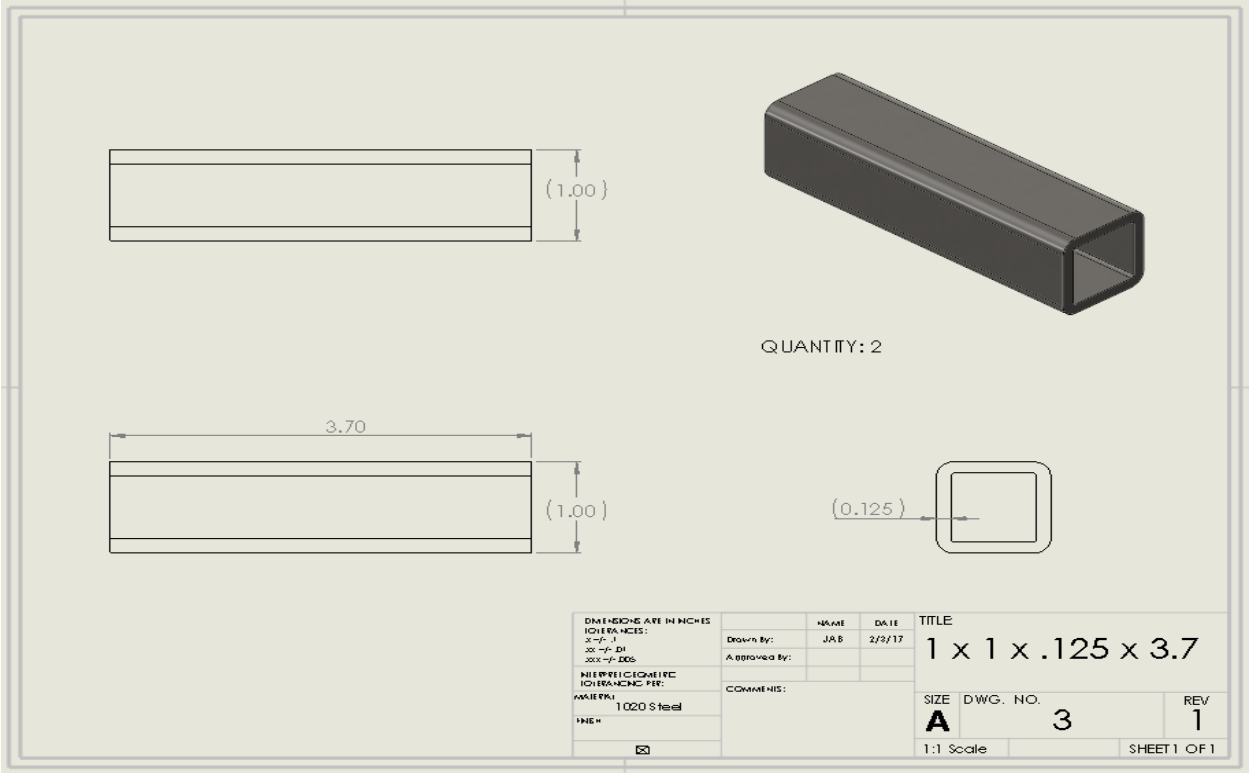

1 x 1 x .125 x 4.7 Square Tube

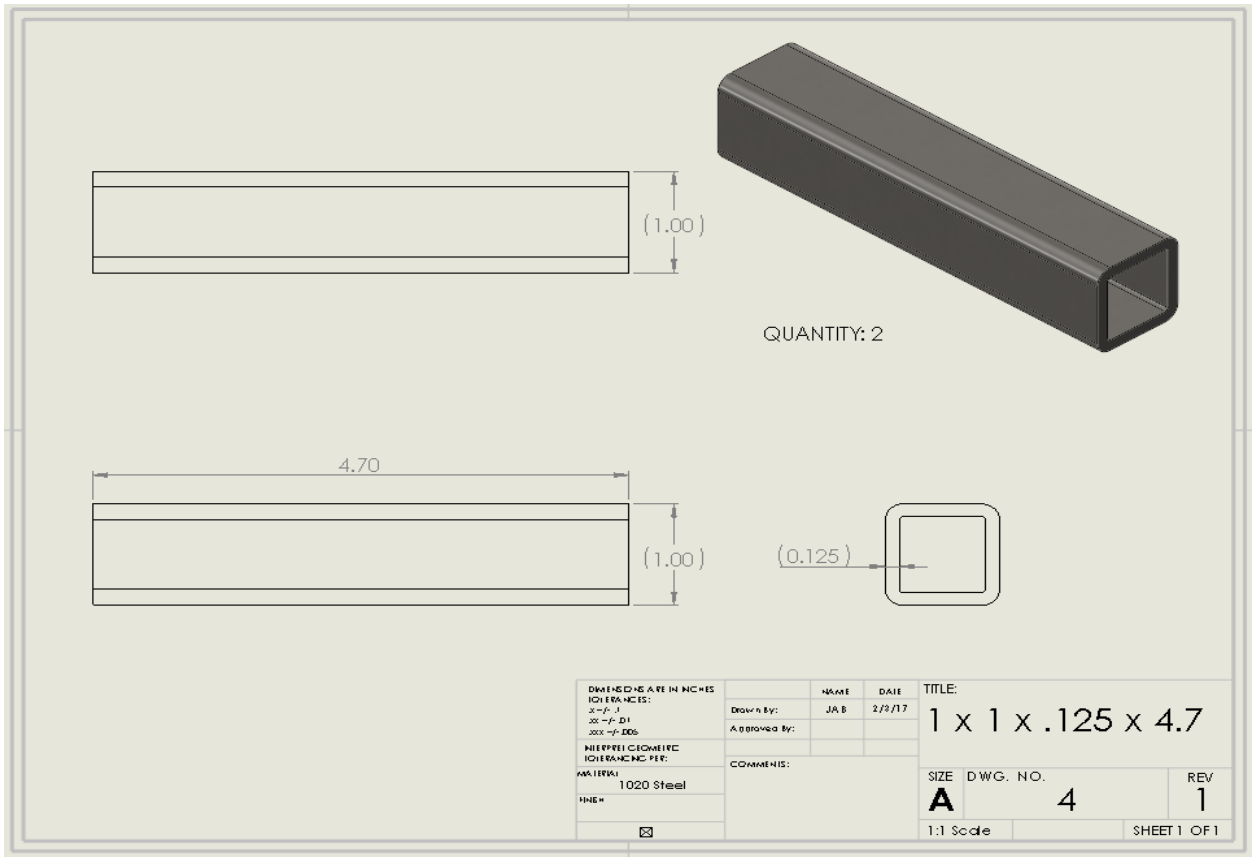

1 x 1 x .125 x 9 Square Tube

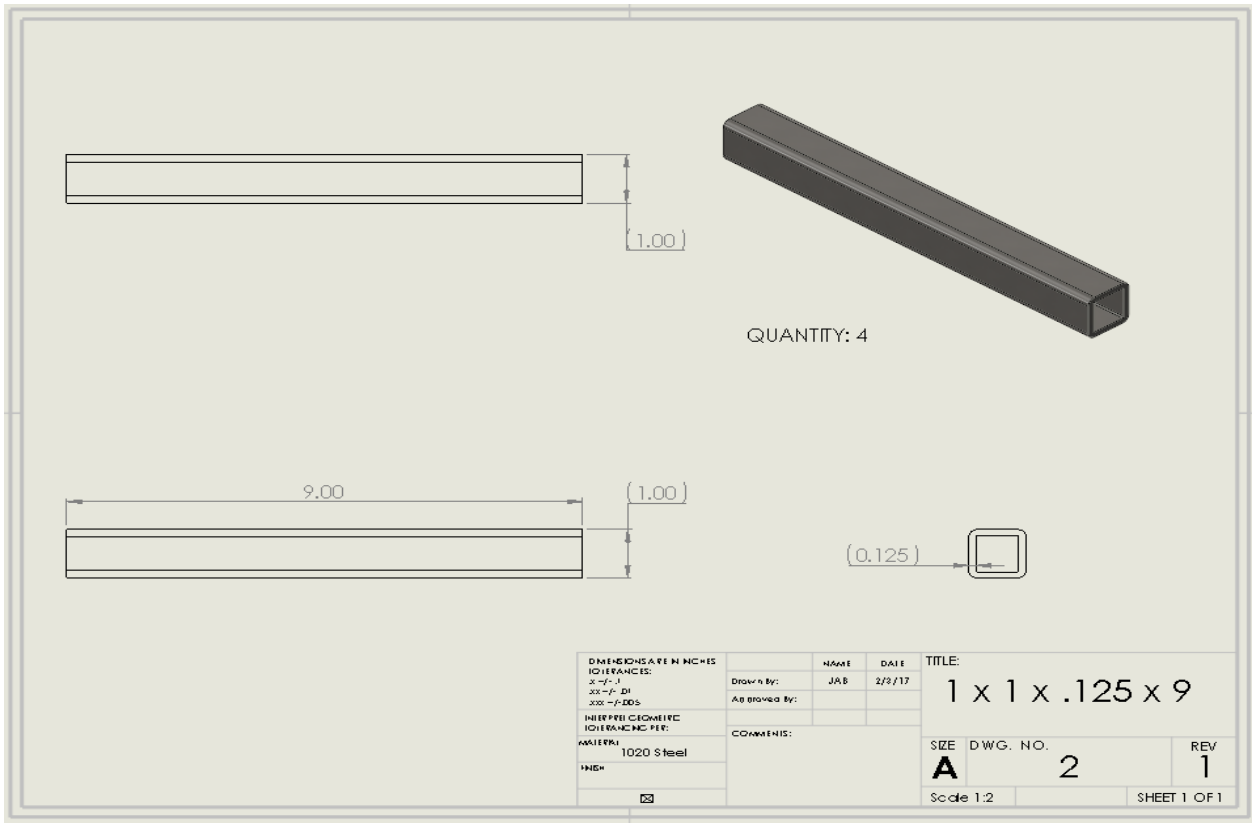

1 x 1 x .125 x 15 Square Tube

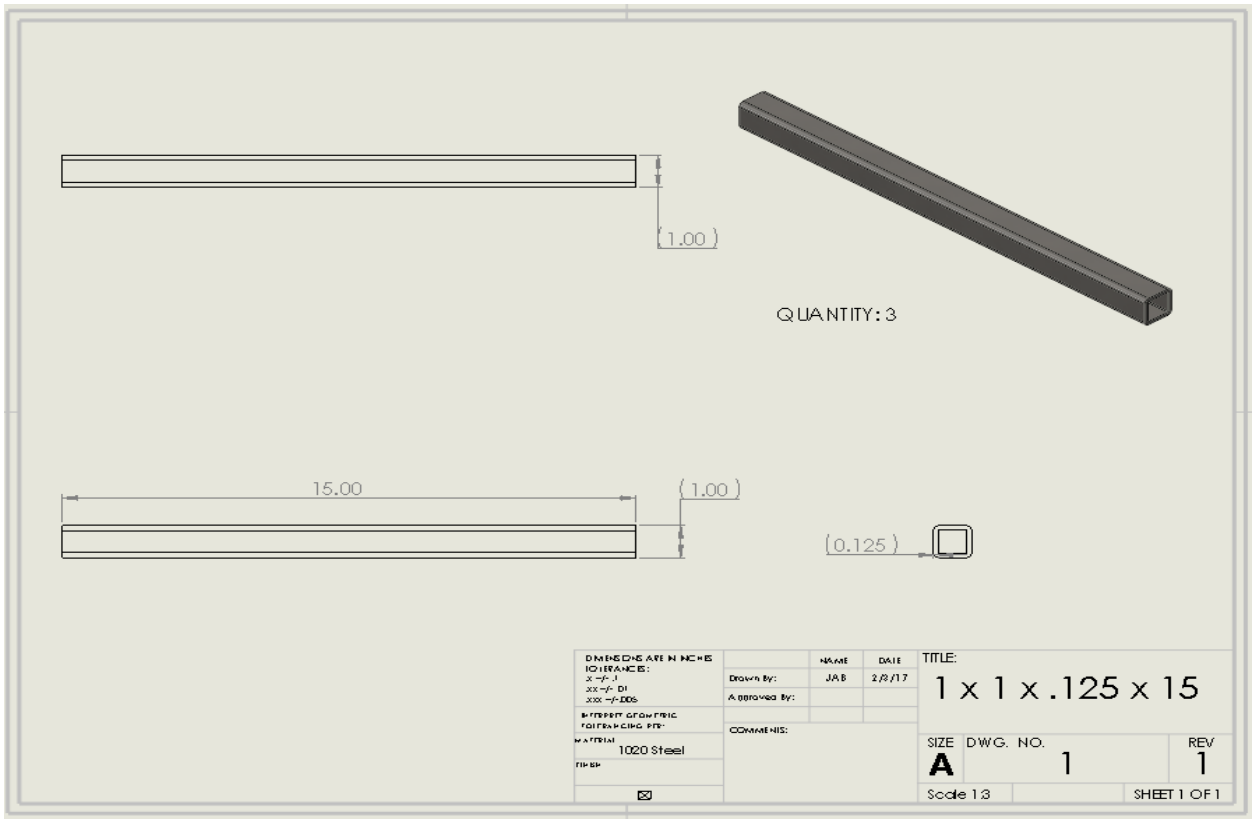

LC Frame Strap

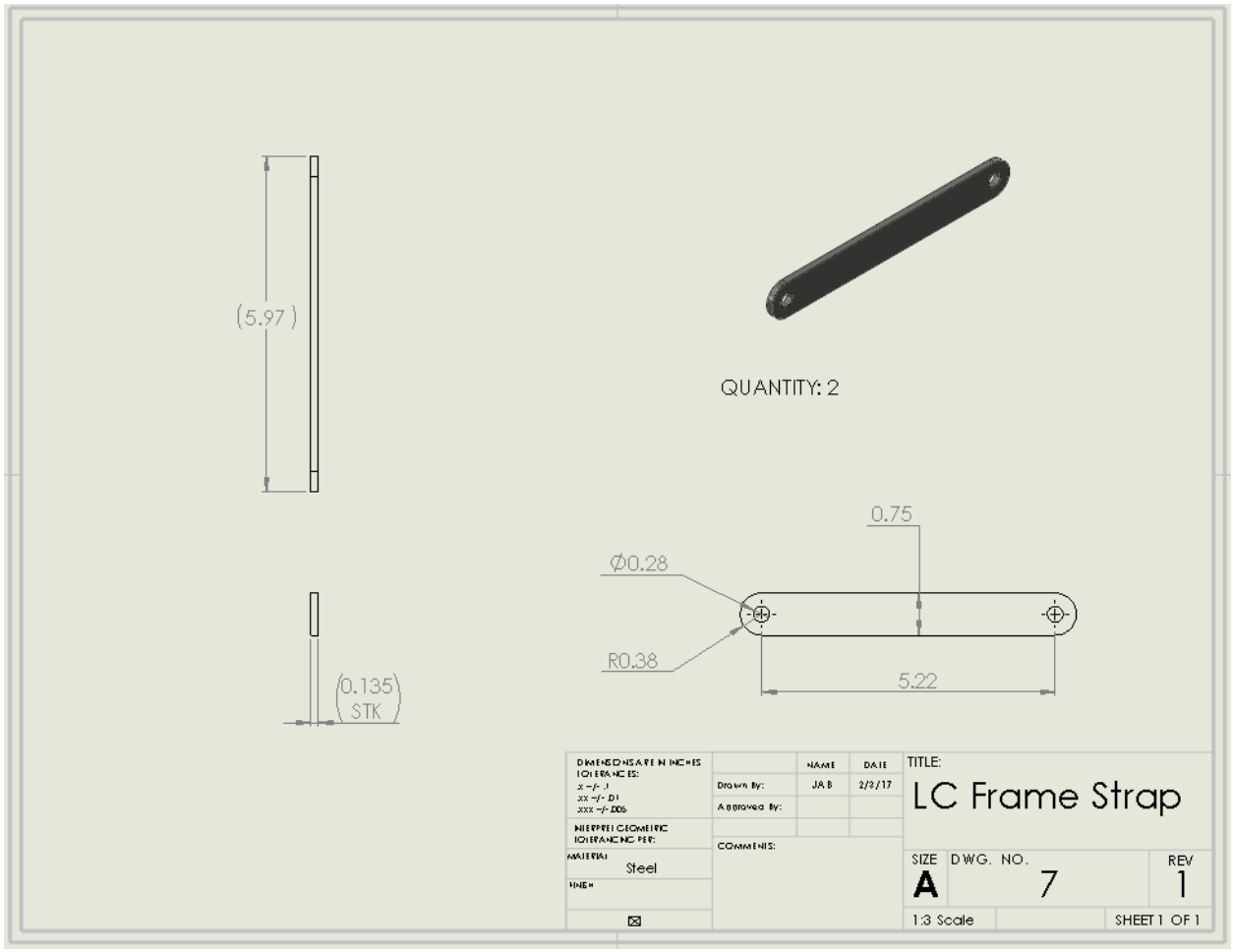

LC Frame Gusset 1

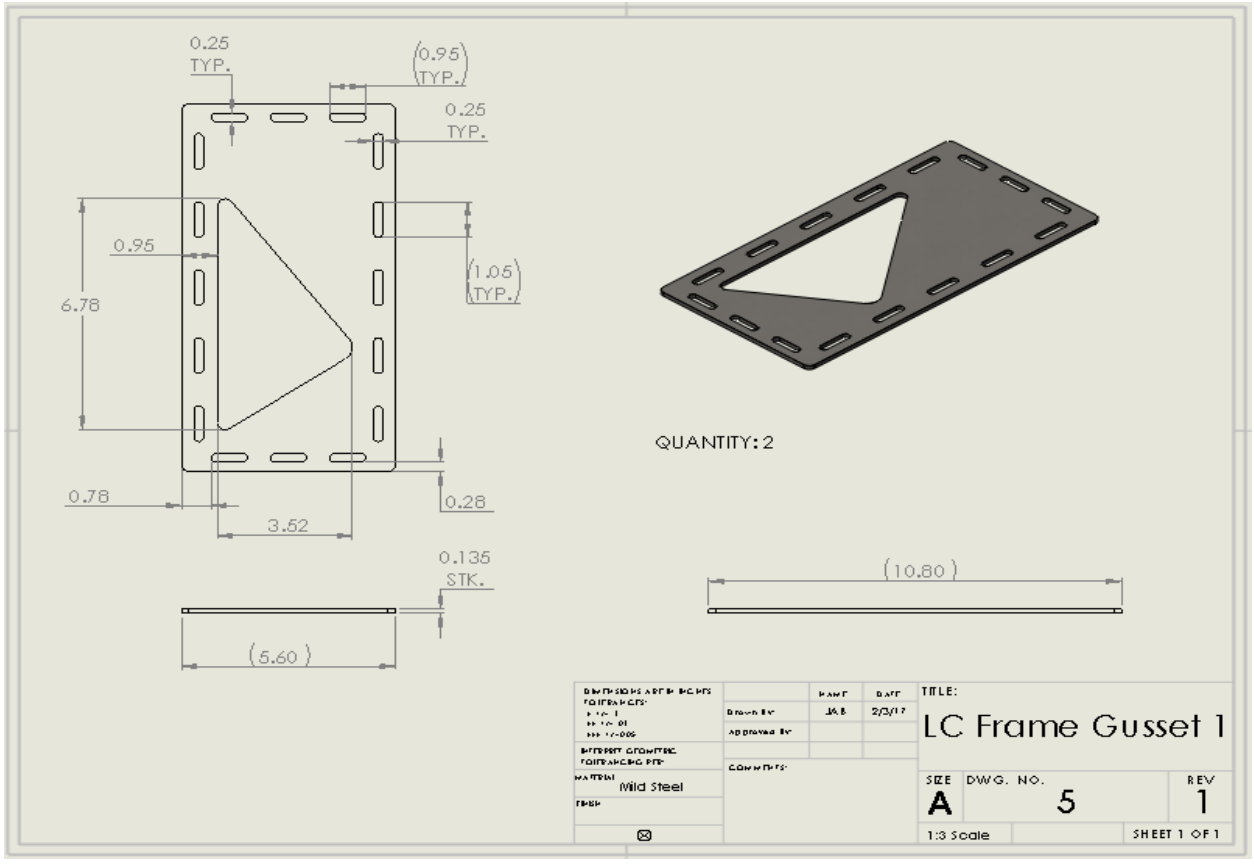

LC Frame Gusset 3

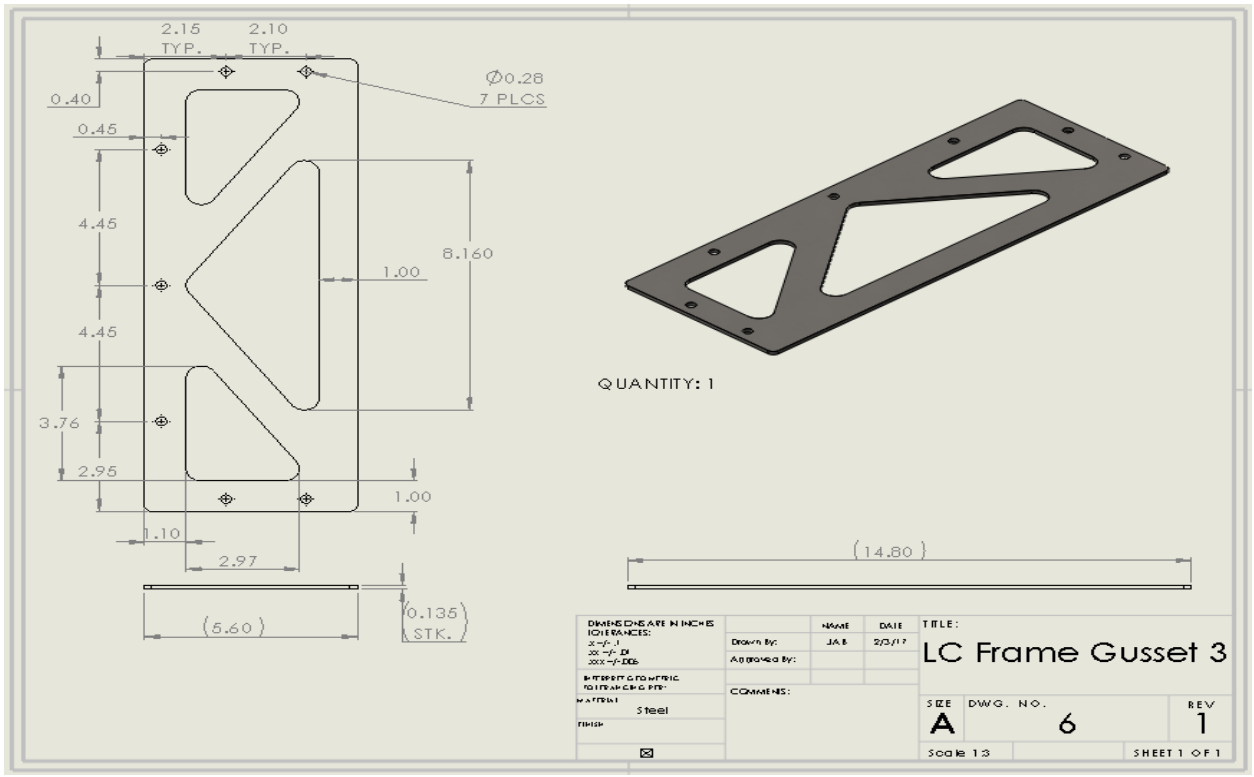

Bracket 2

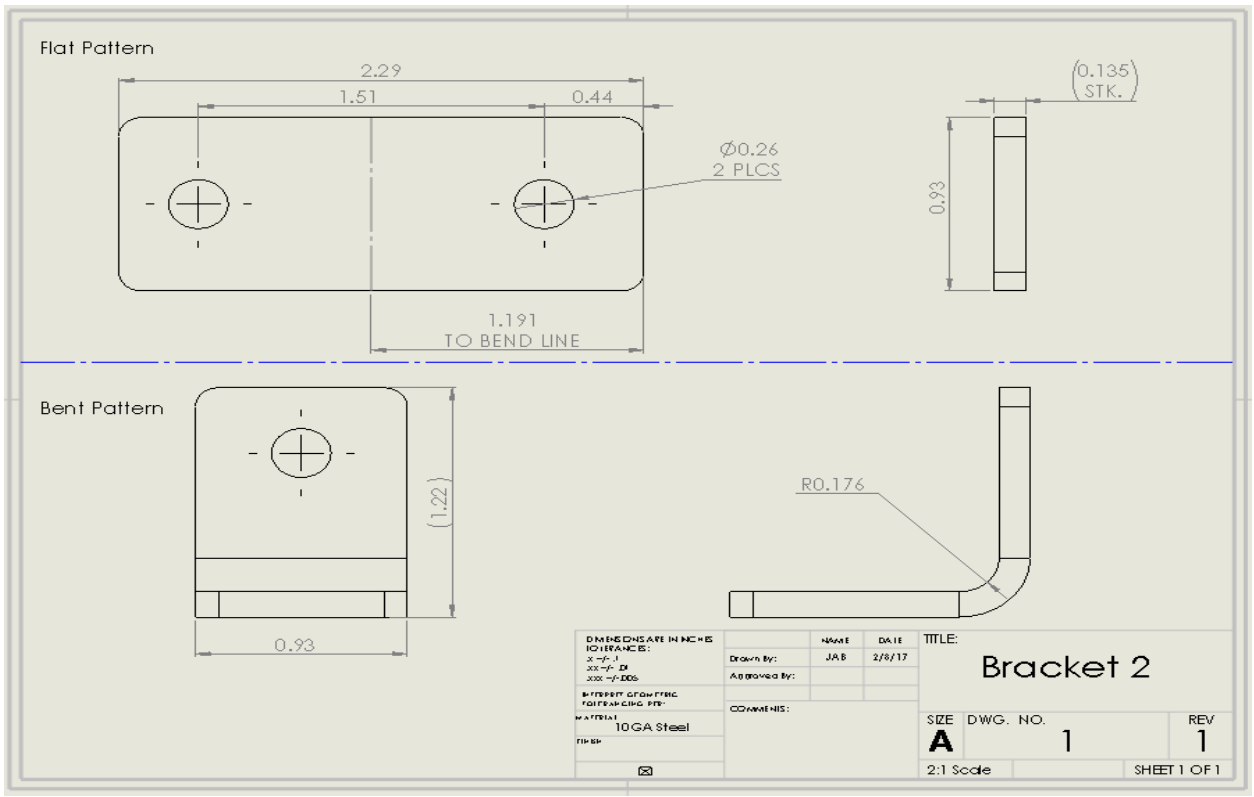

X-Axis Bracket

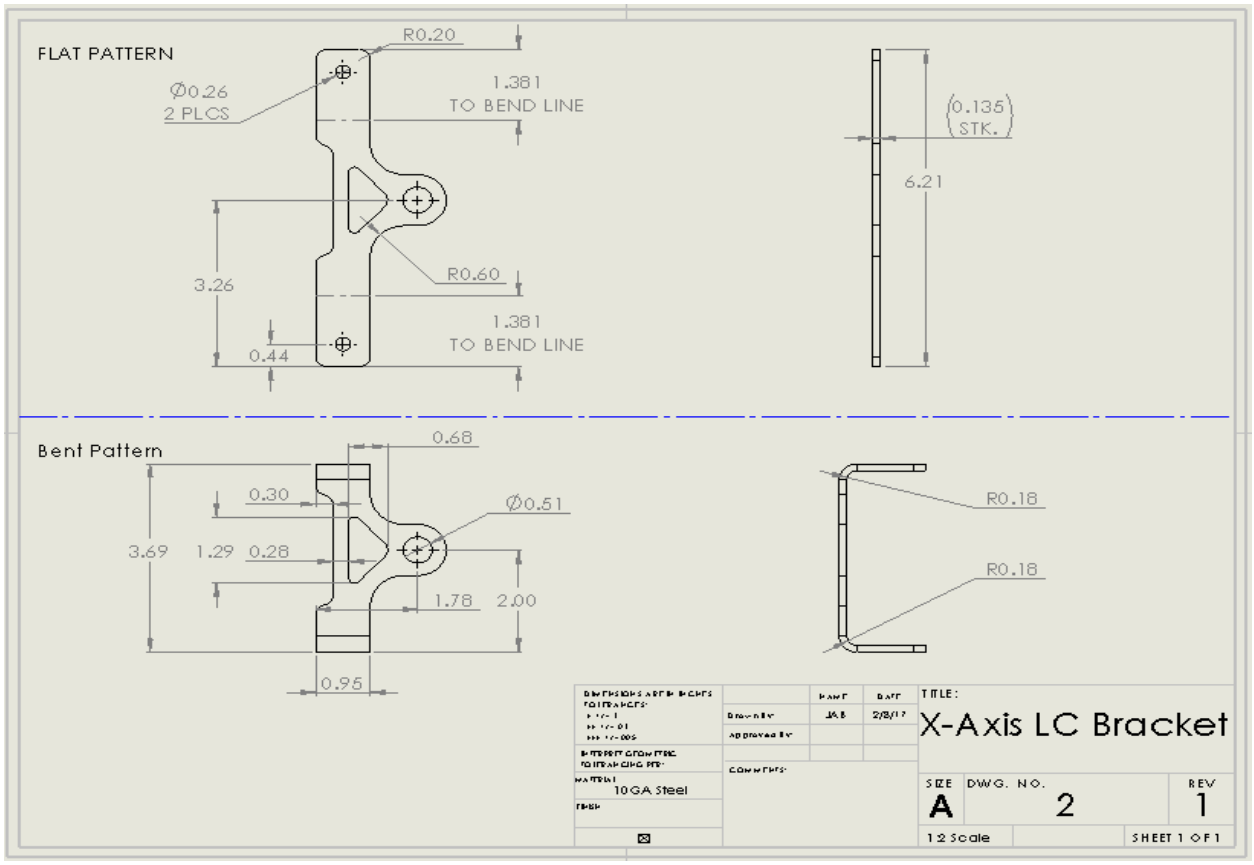

Y-Axis LC Mounting Block

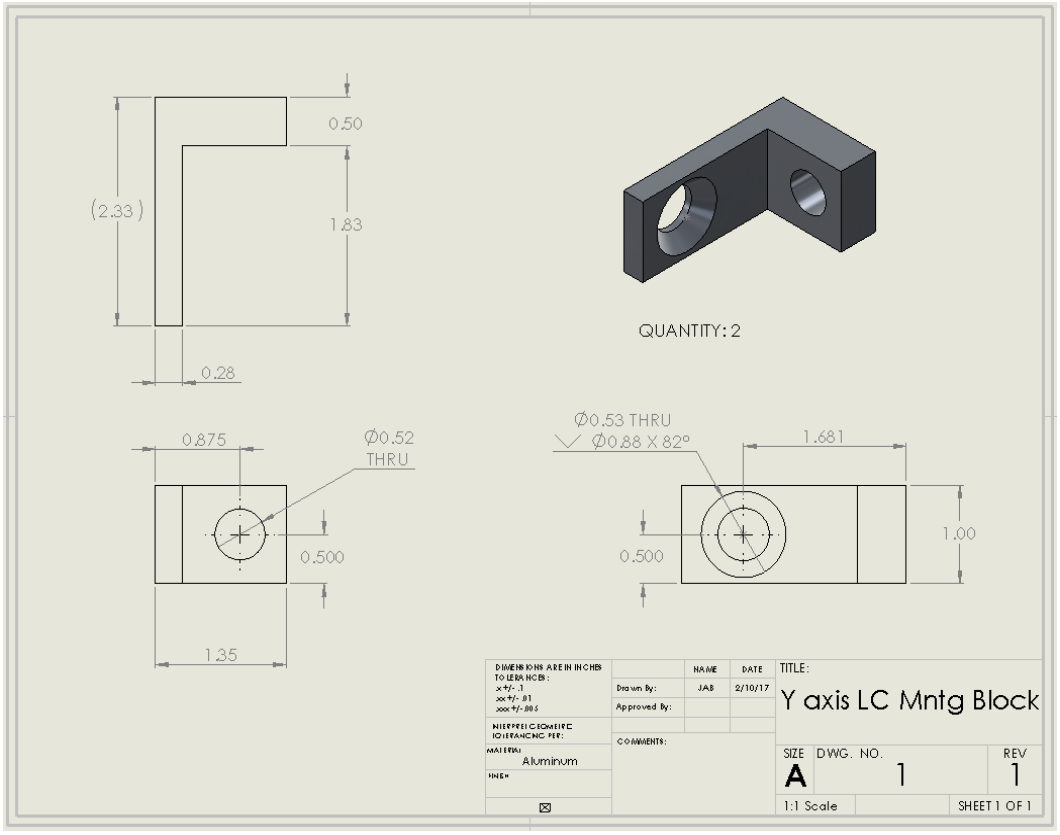

Bearing Plate

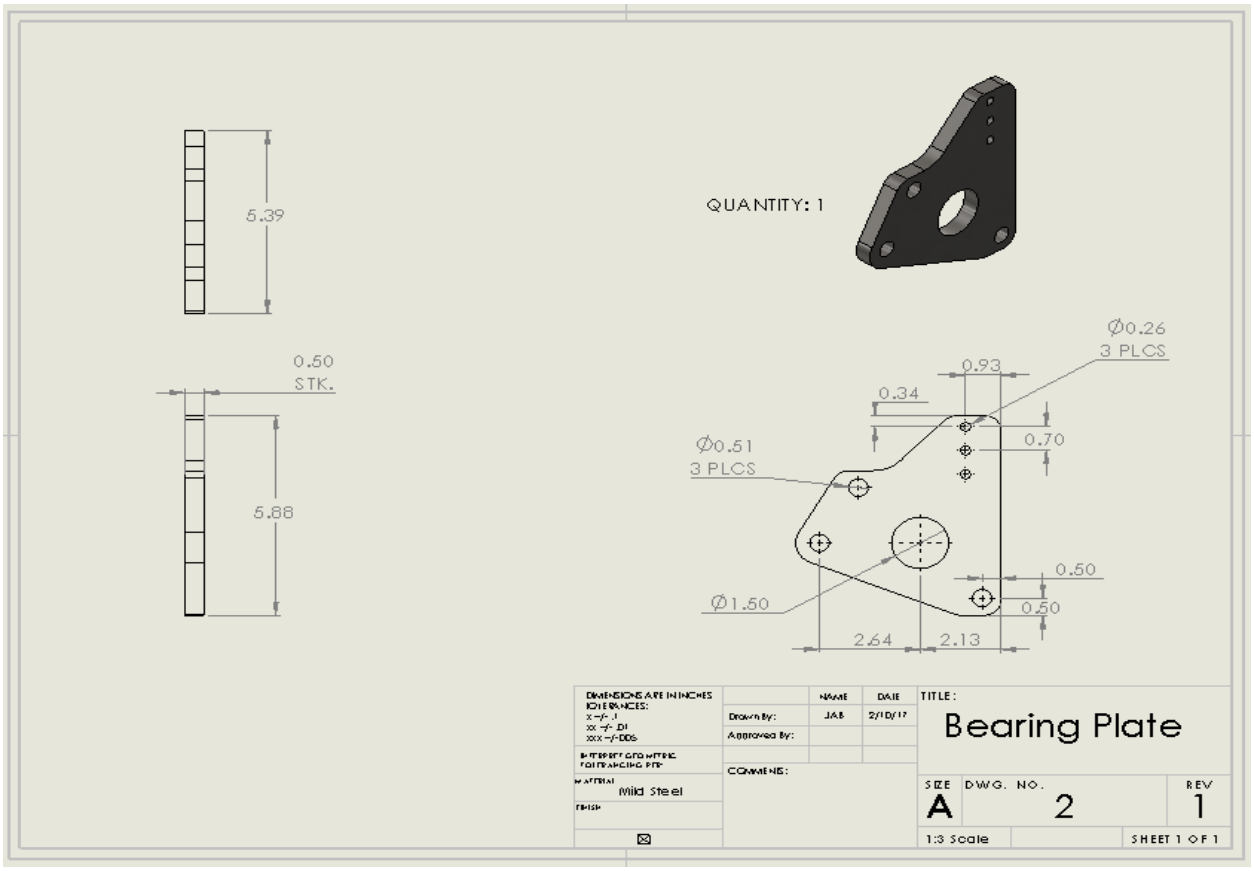

Vertical Load Support

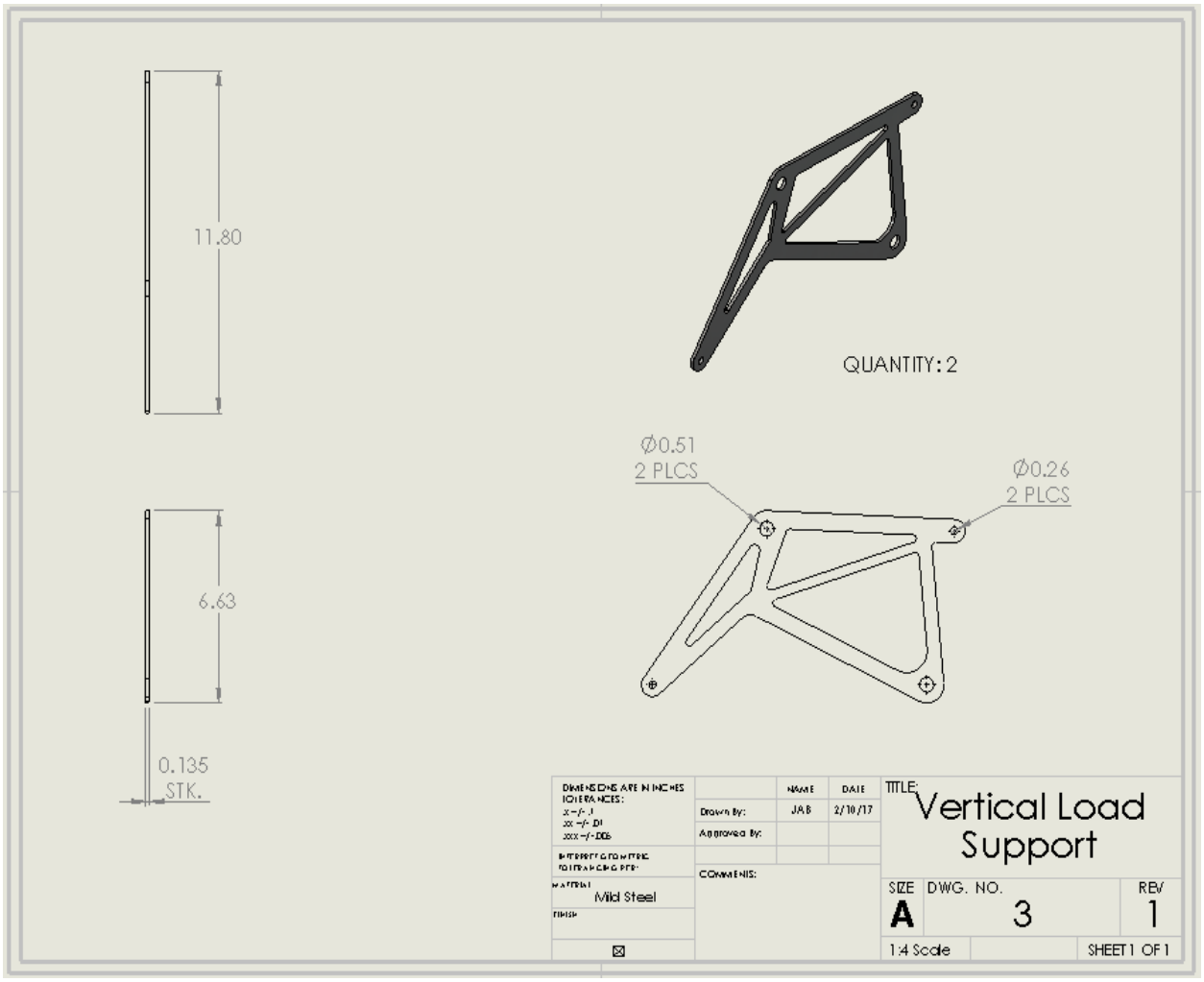

LC Sheet Bracket Gusset

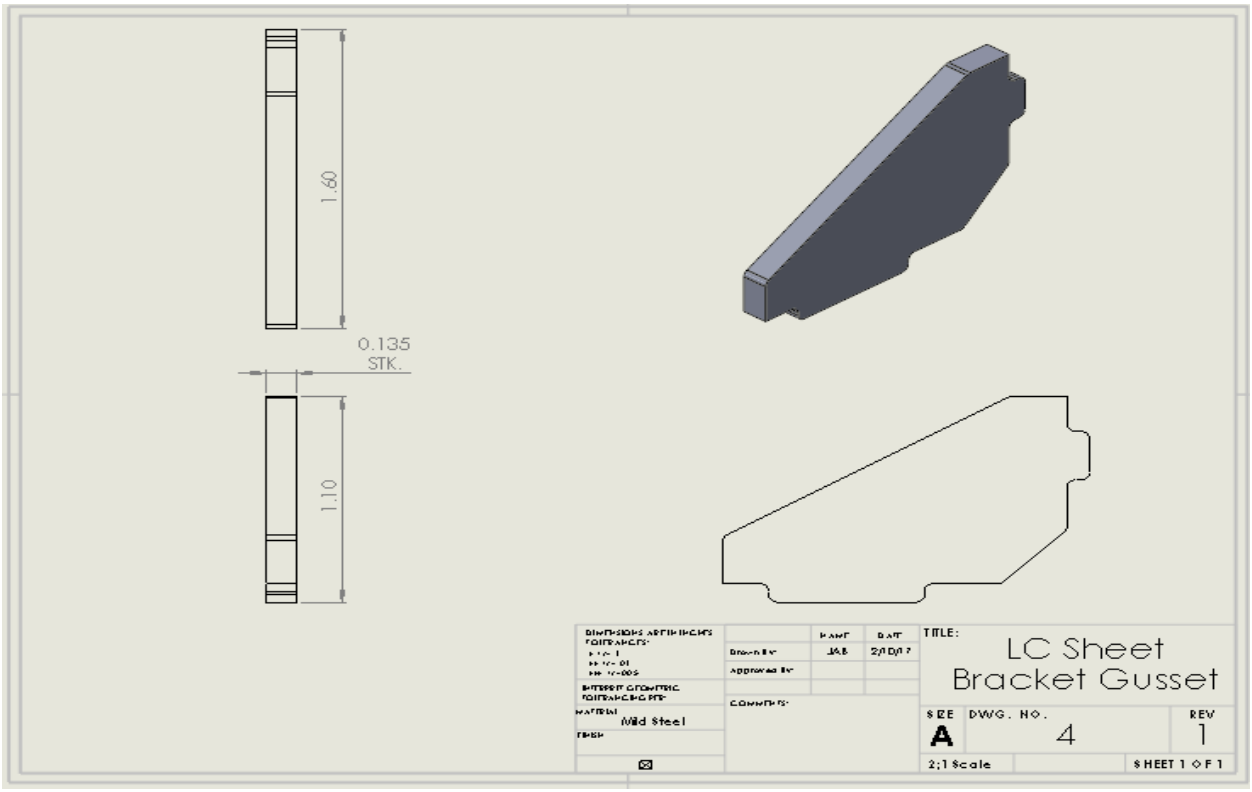

LC Sheet Bracket

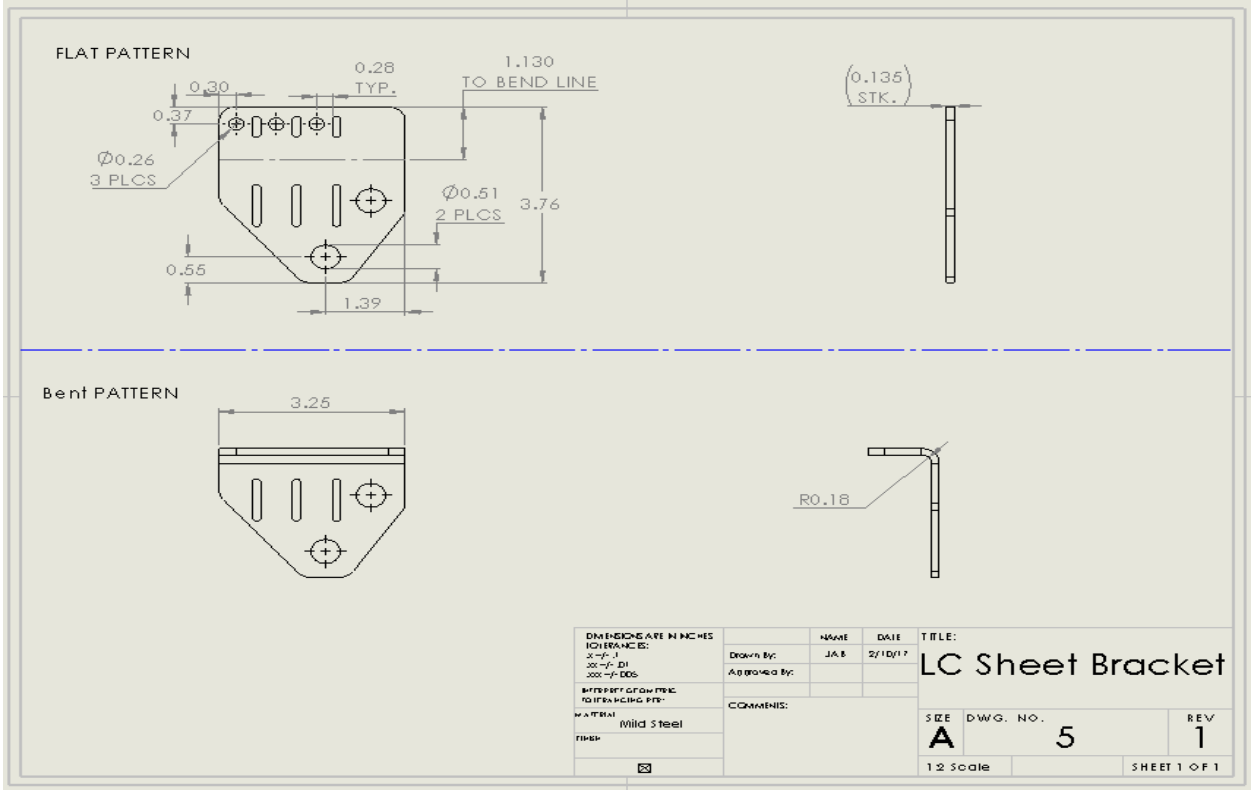

LC Sheet Bracket Weldment

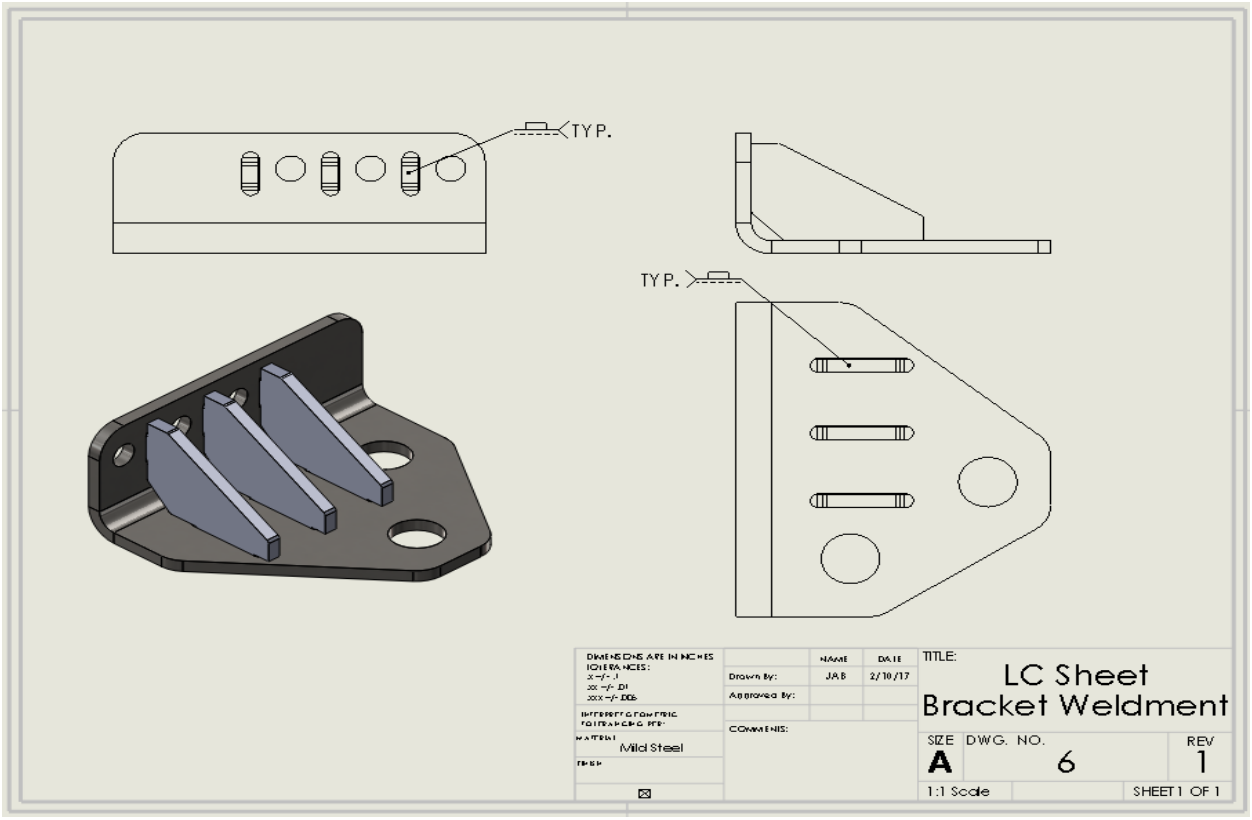

TIRE CAGE DRAWINGS

1 x 1 x .125 x 15 Square Tube

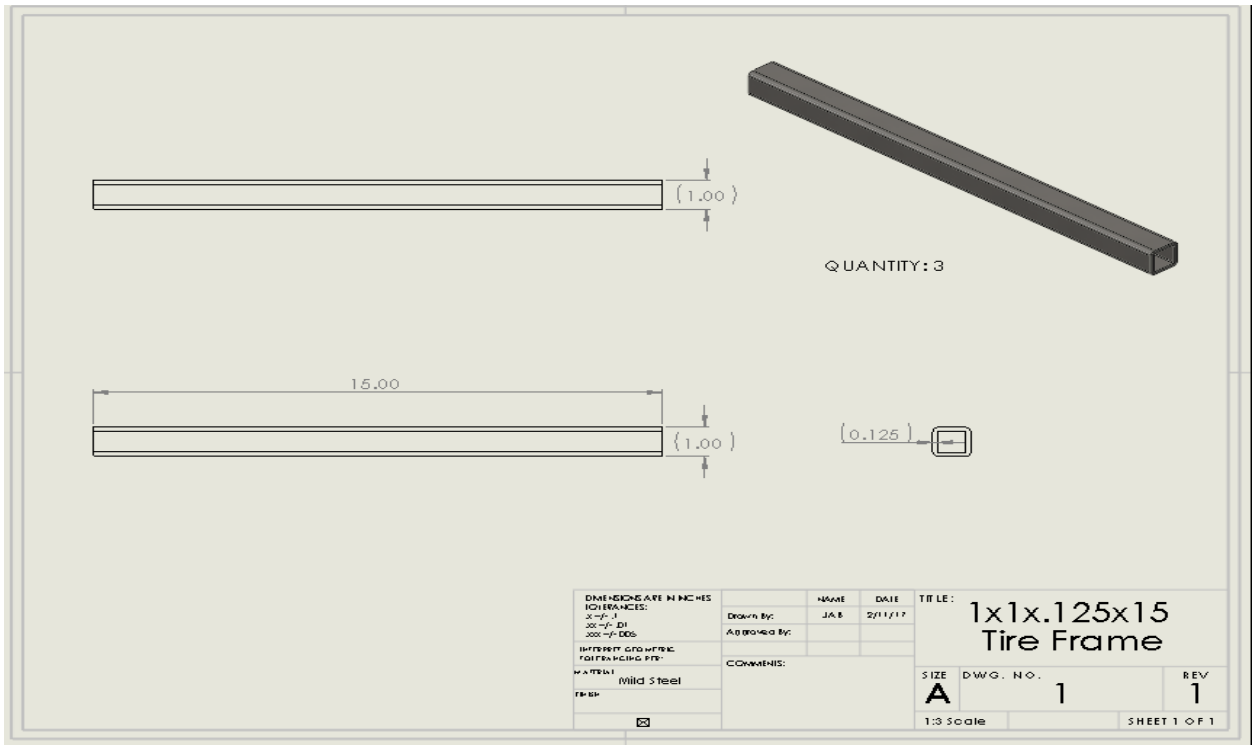

1 x 1 x .125 x 13 Square Tube

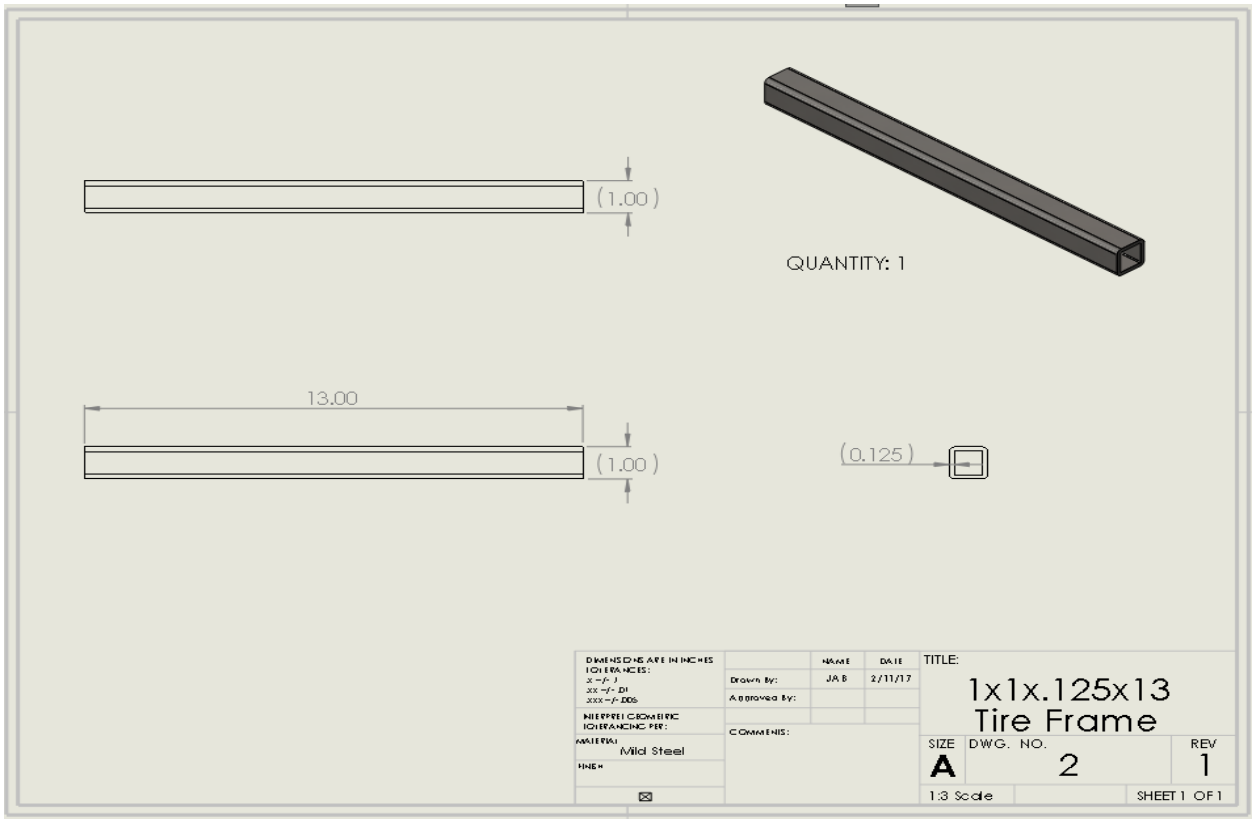

1 x 1 x .125 x 9 Square Tube

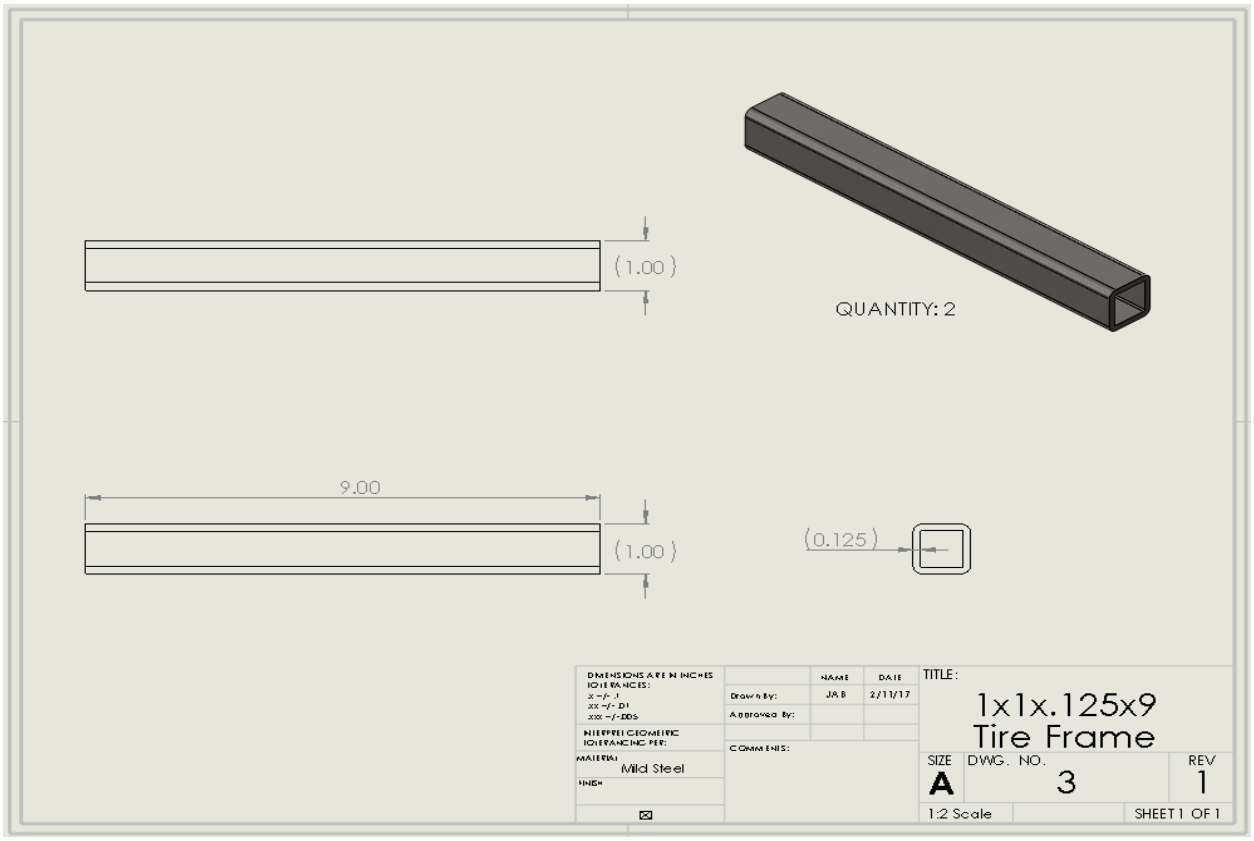

1 x 1 x .125 x 11 Square Tube

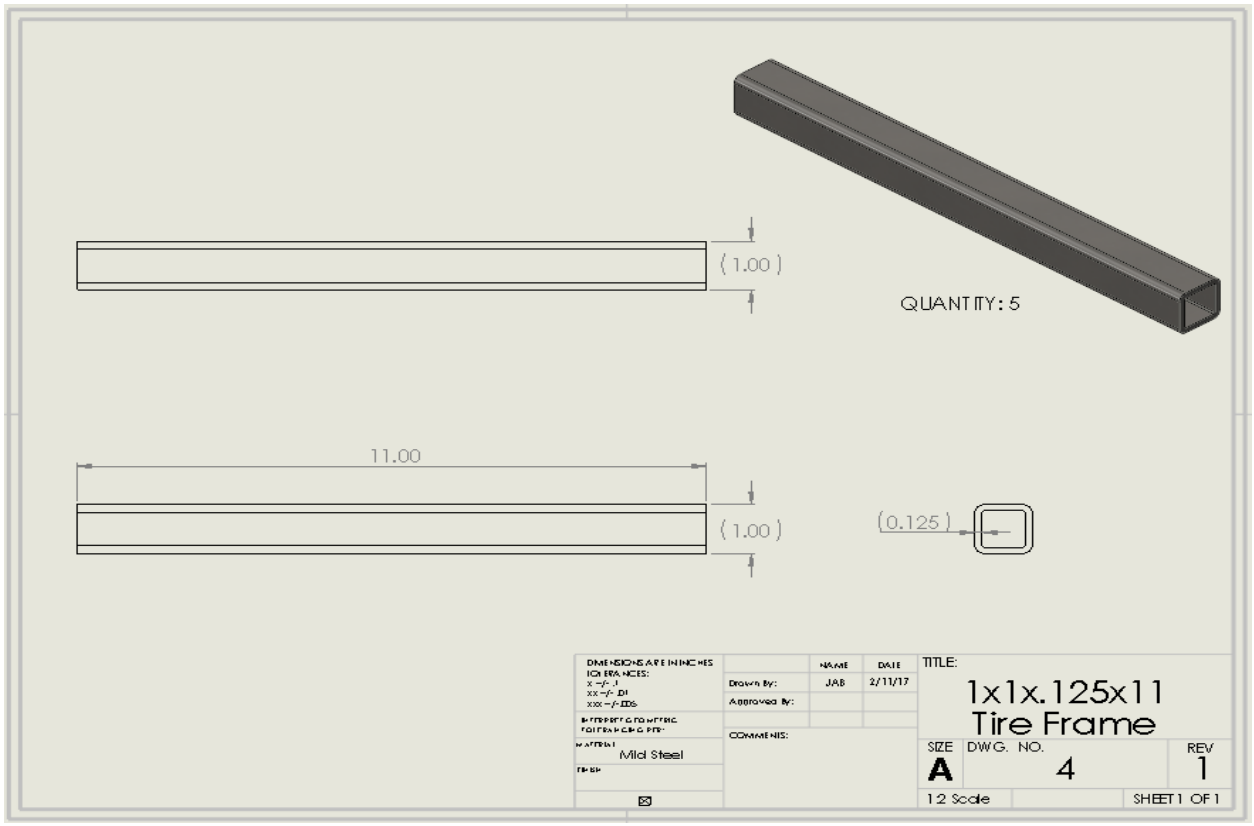

1 x 1 x .125 x 10 Square Tube

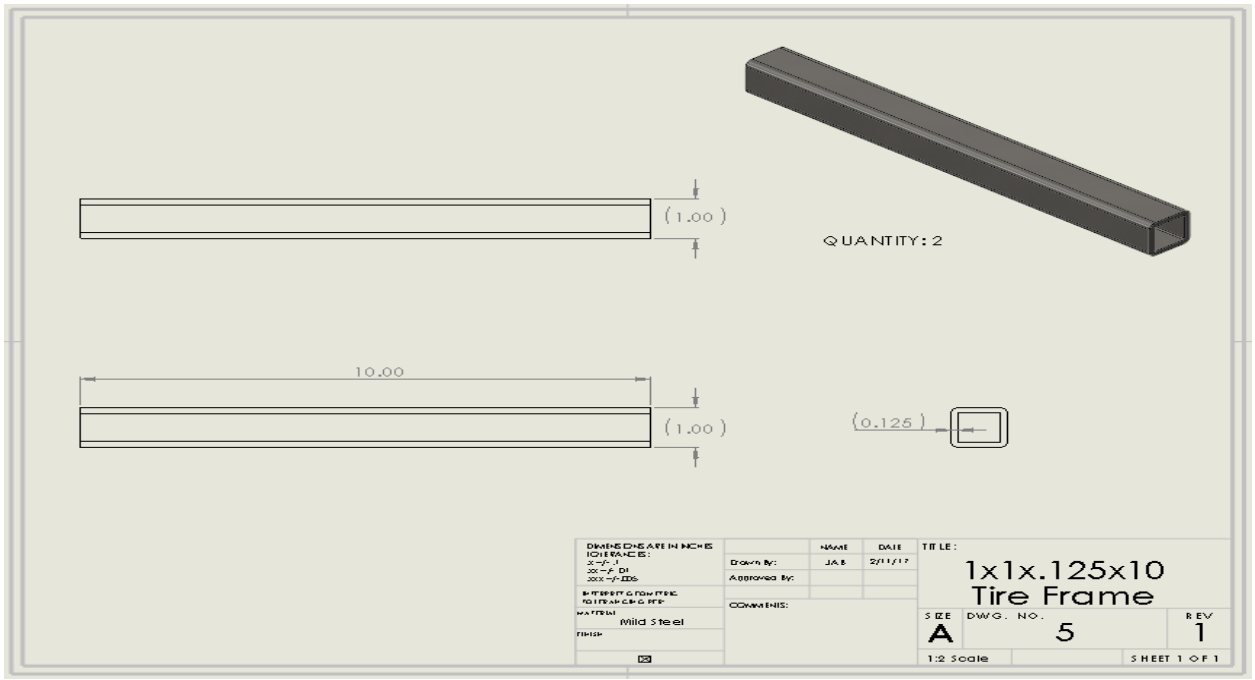

1 x 1 x .125 x 6 Square Tube

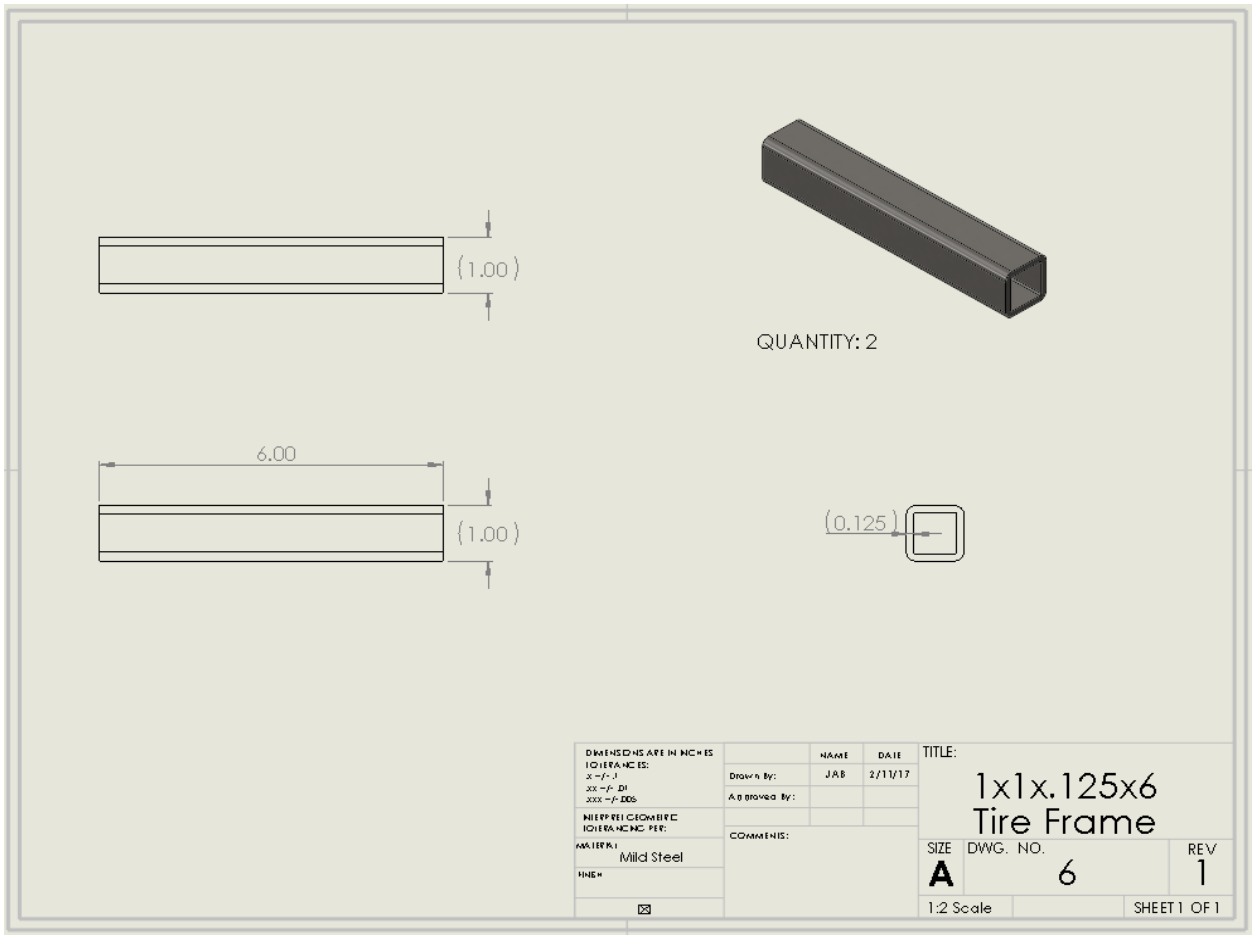

Tire Cage Stiffener

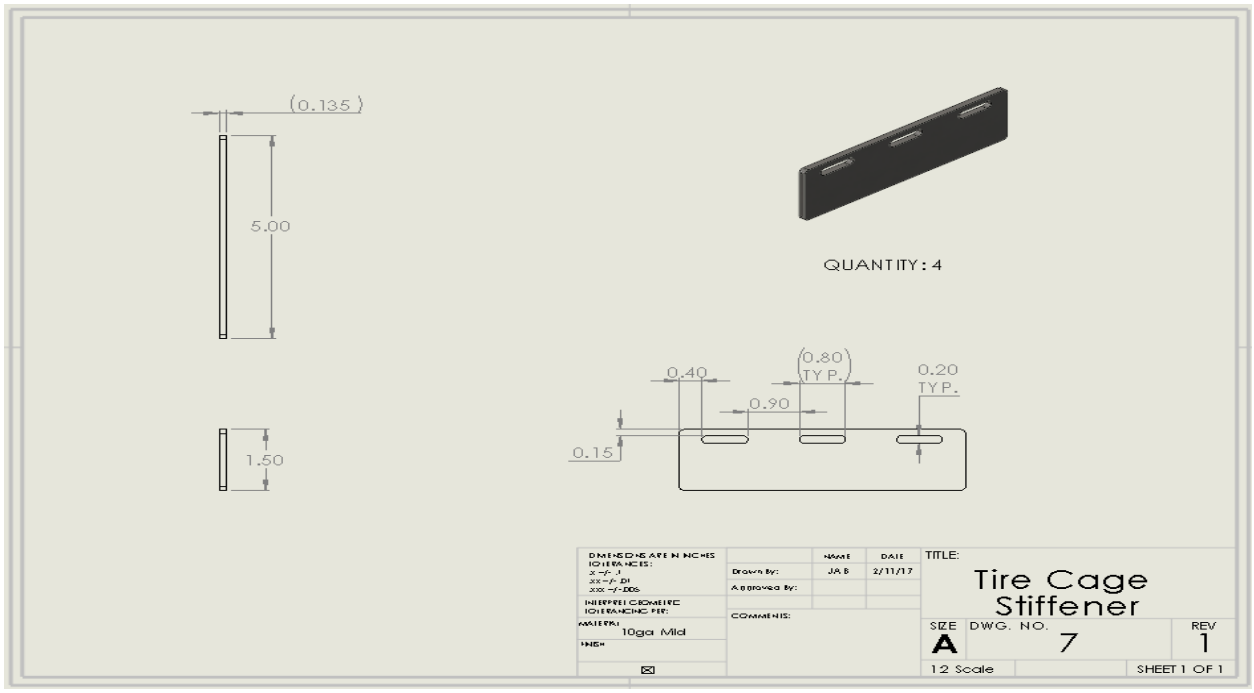

Tire Cage Stiffener1

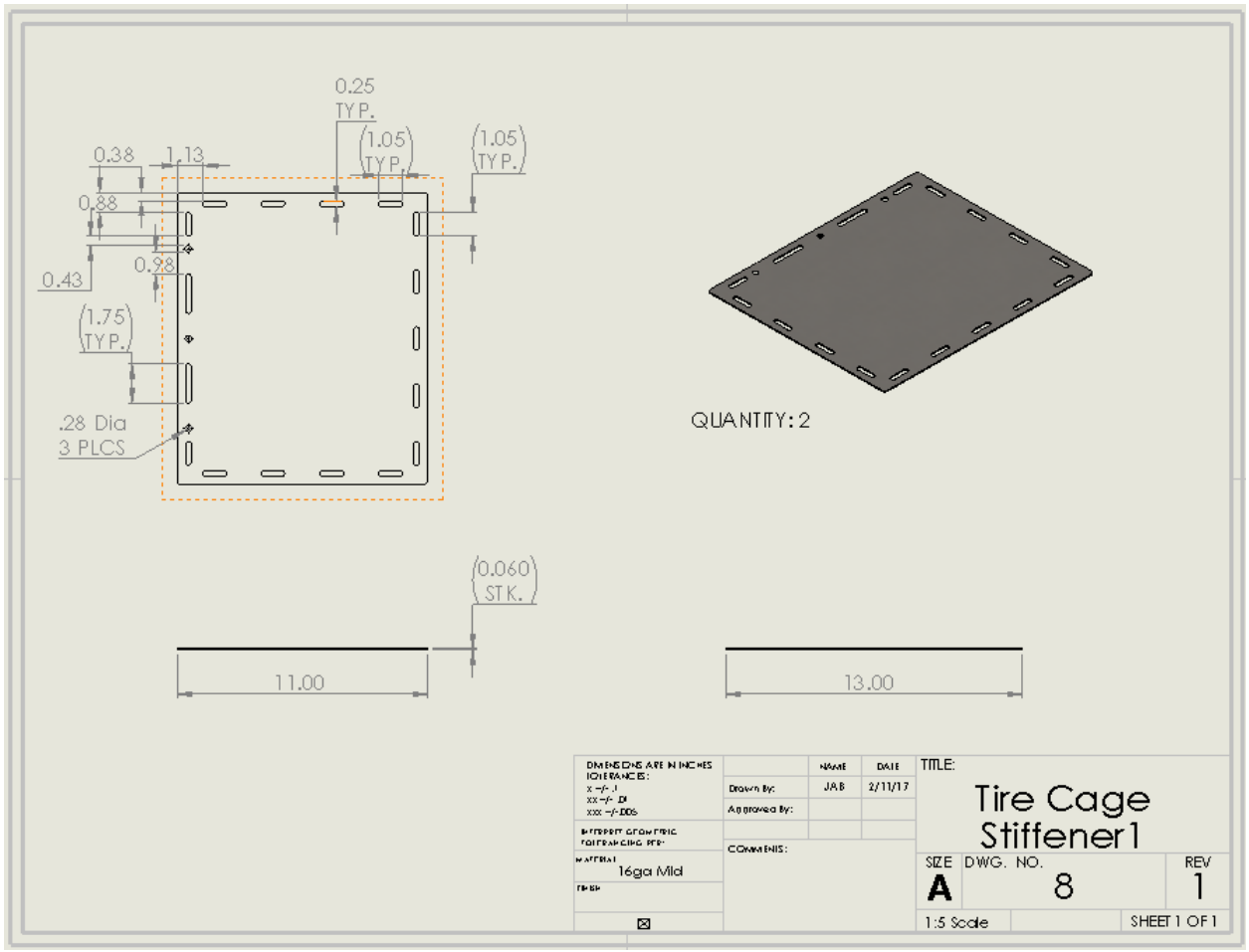

Tire Cage Stiffener2

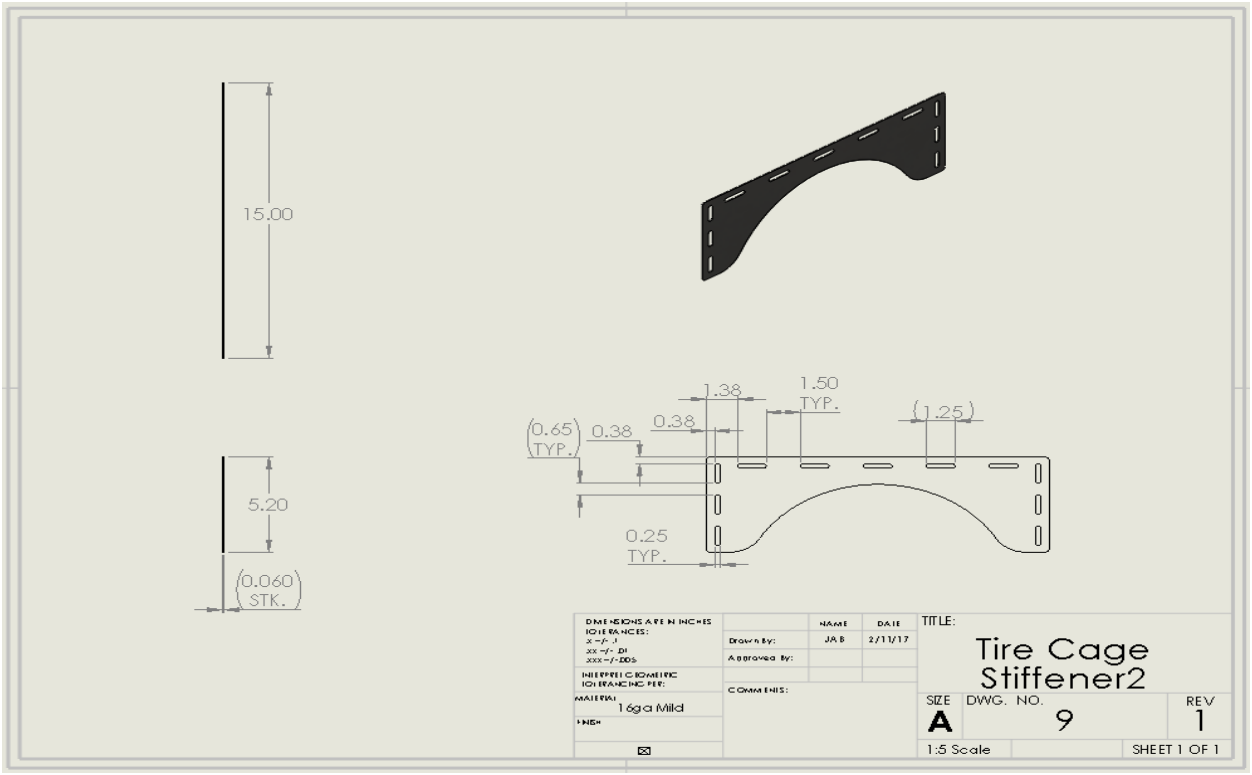

Tire Frame Assembly

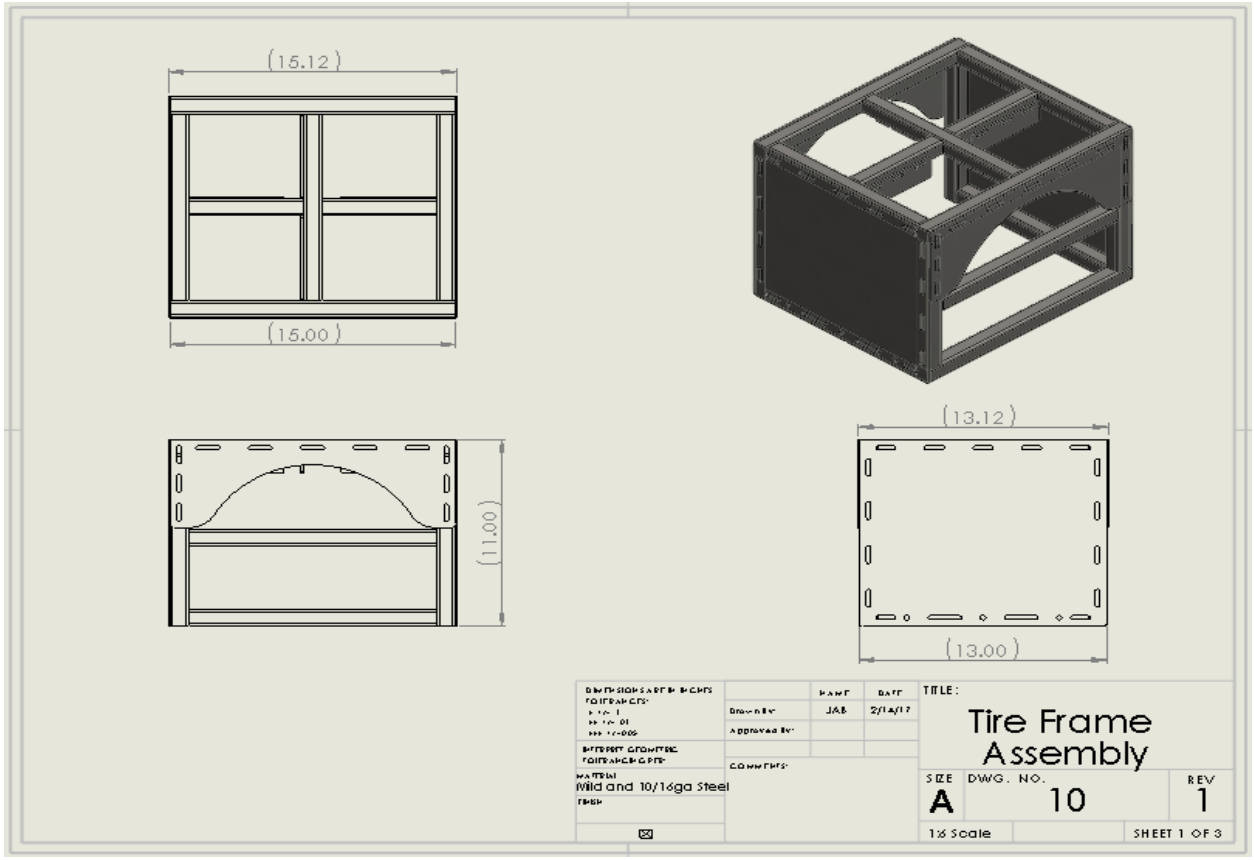

Tire Frame Tube Weldments

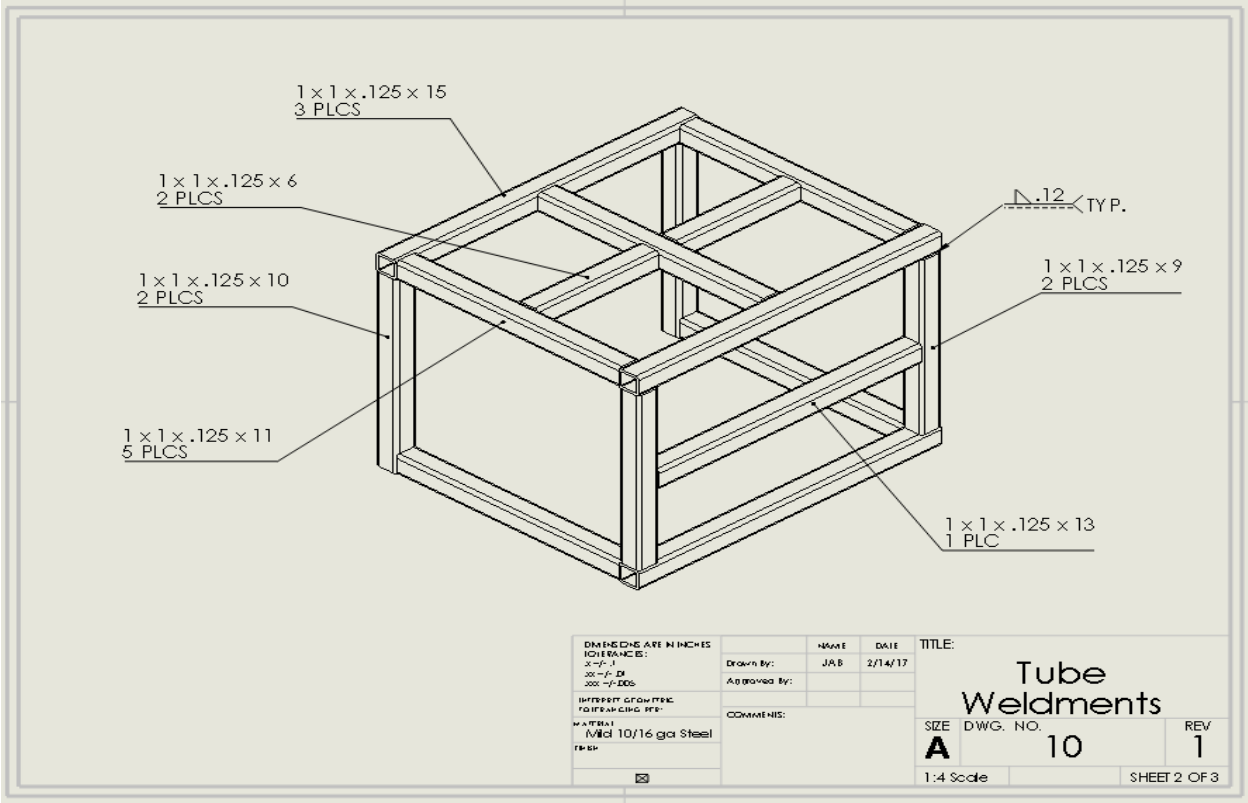

Tire Frame Stiffener Weldments

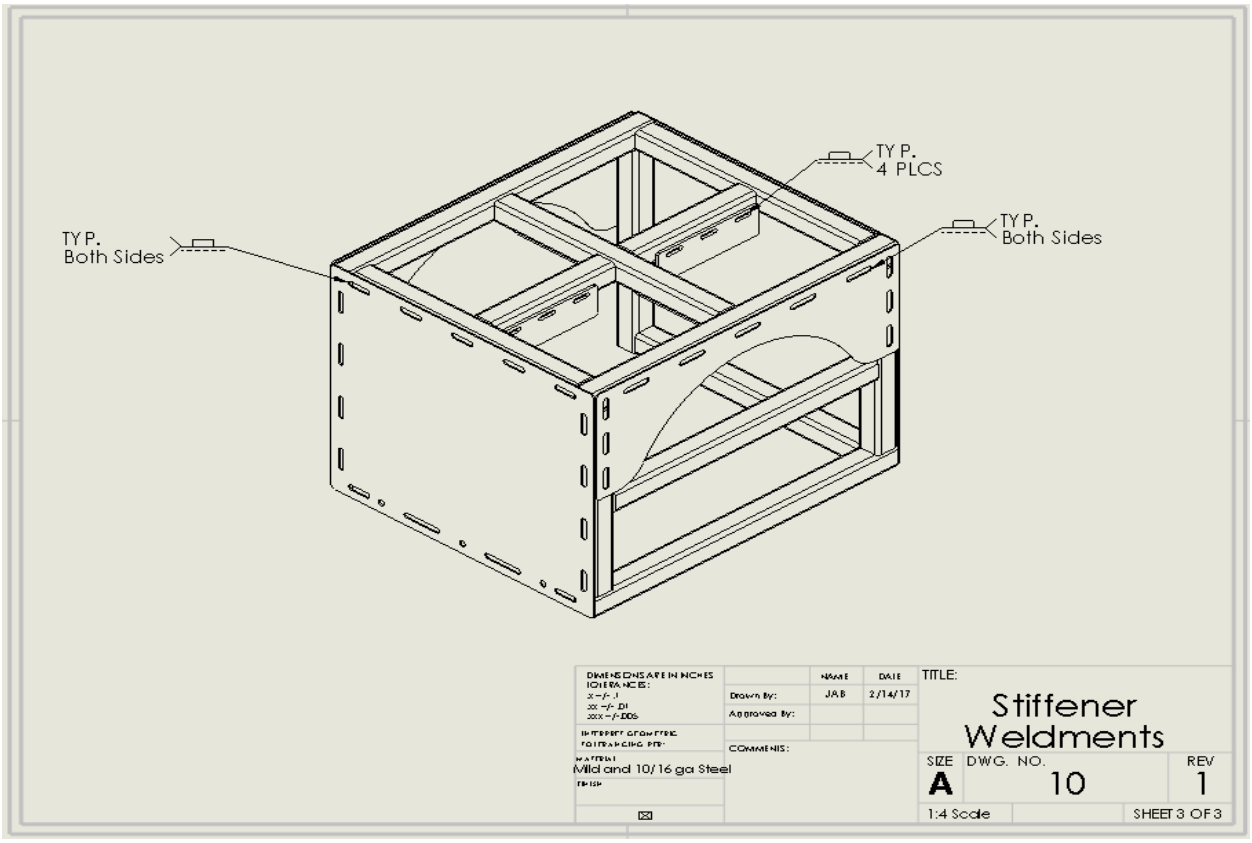

Weight Tube

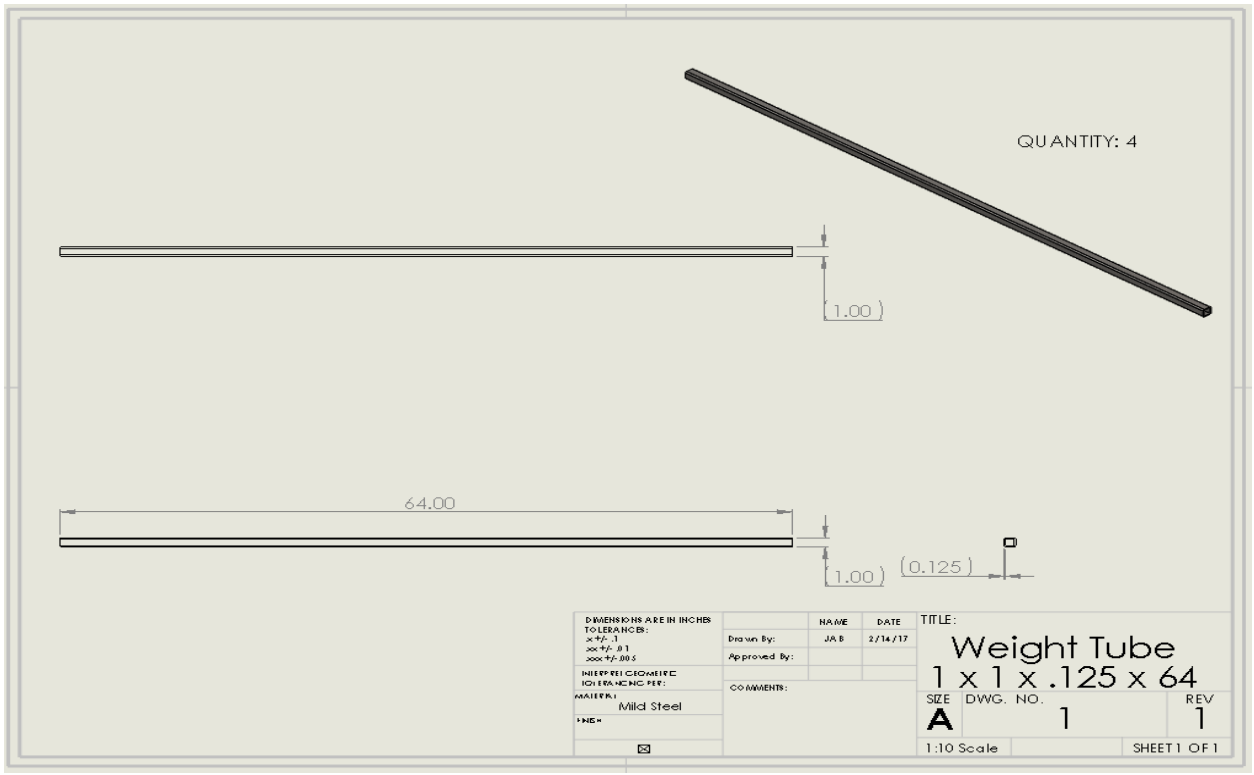

Tire Frame Closeout1

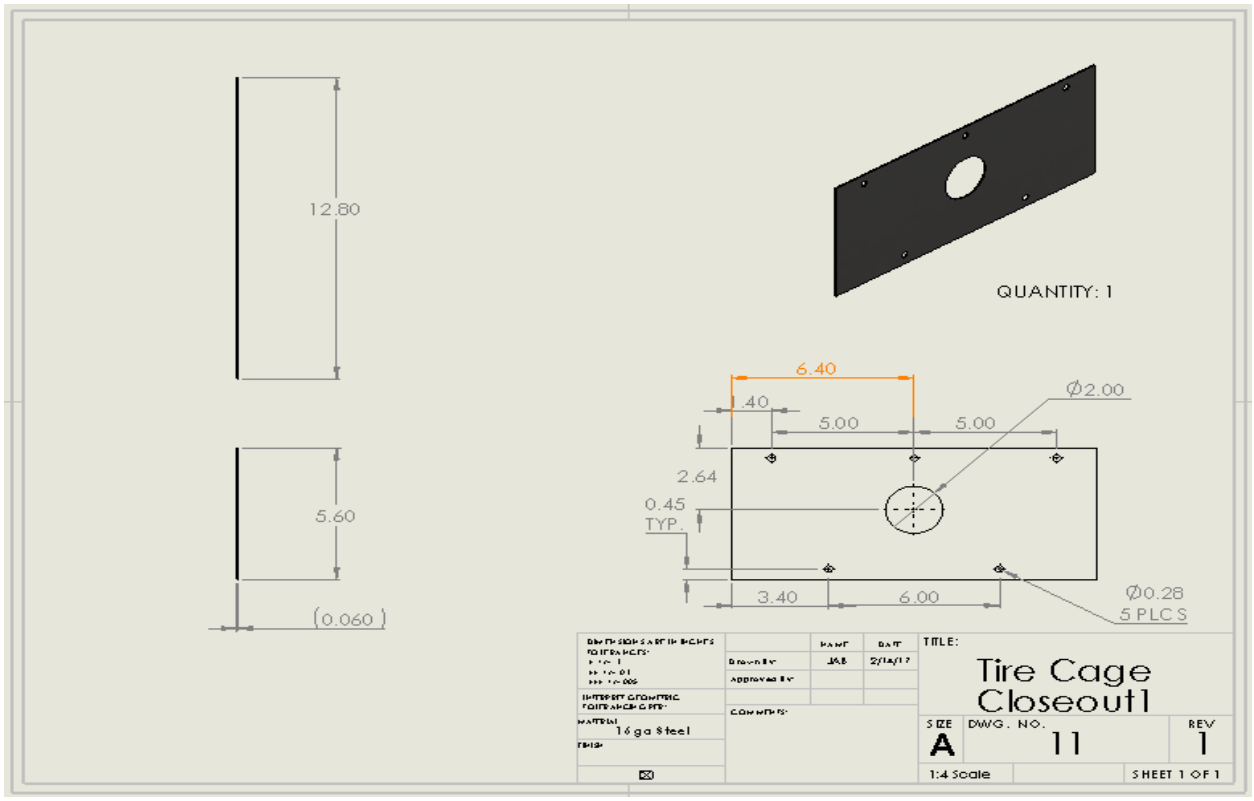

Rear Assembly: Tire and Load Cell Cages

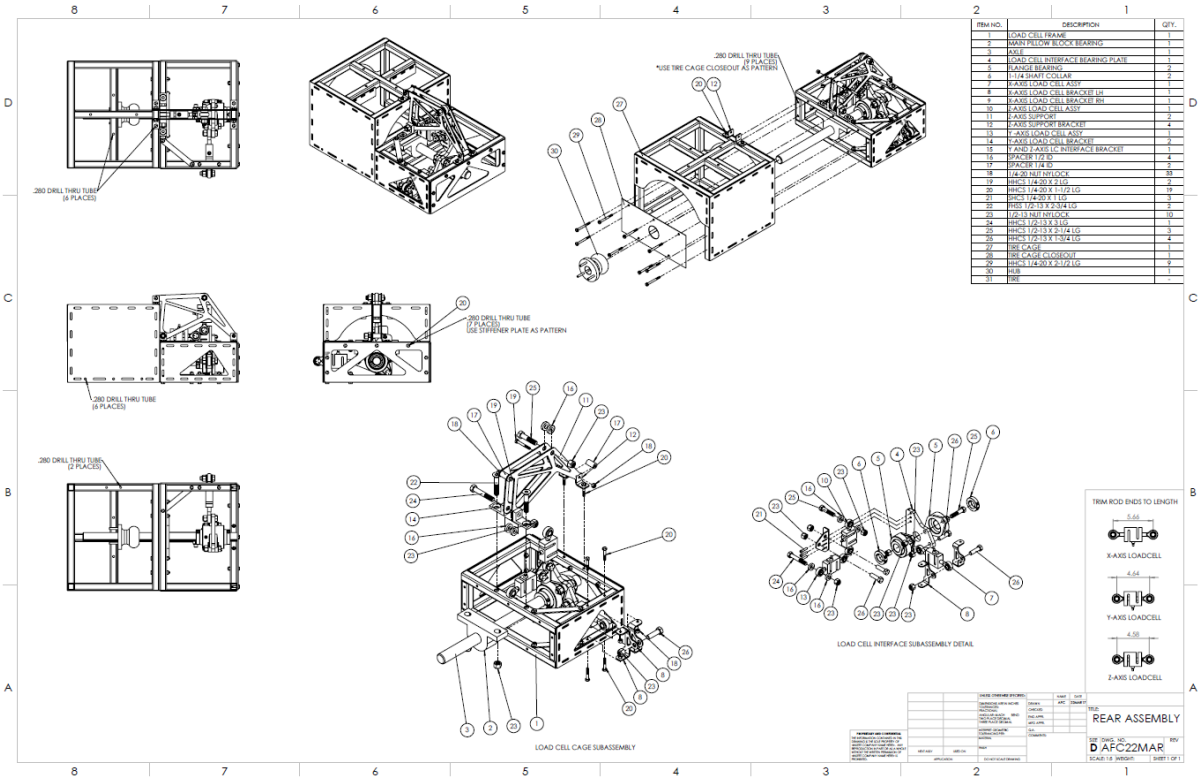

Full Assembly: Detailed

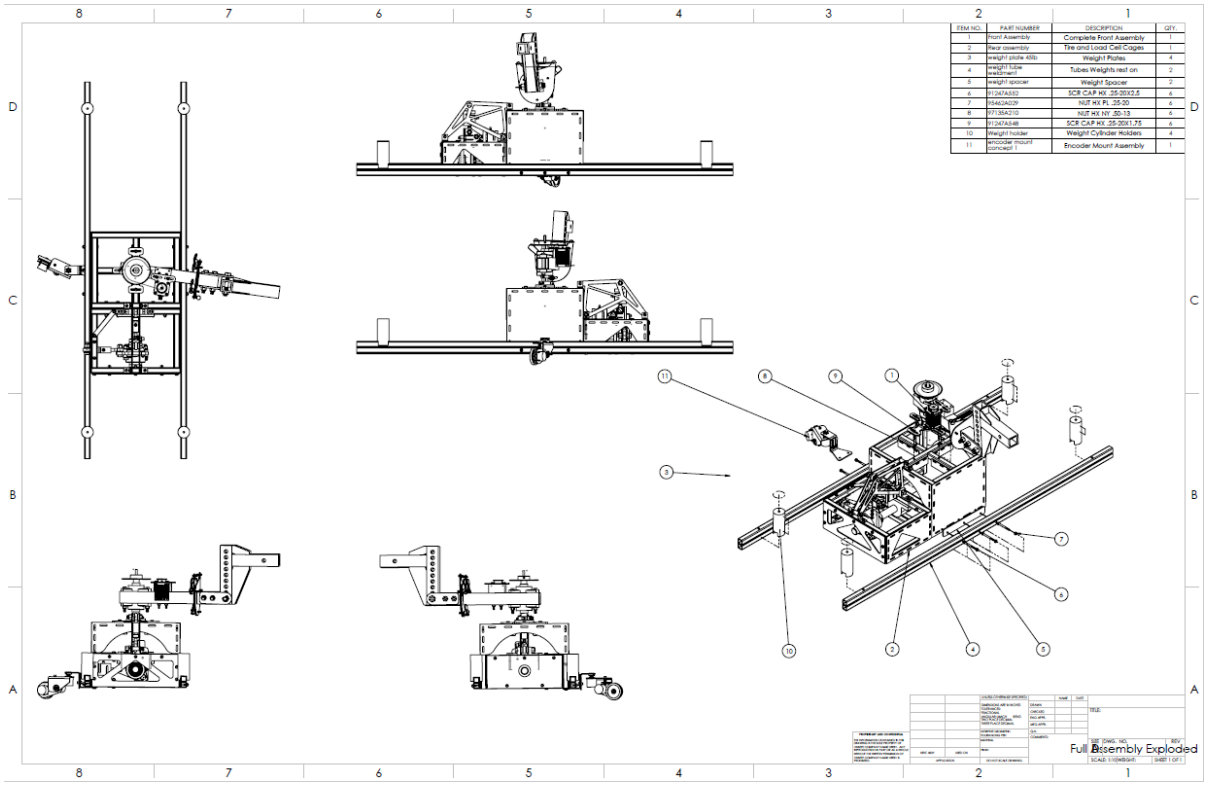

APPENDIX B

BILL OF MATERIALS

Front Assemly:

ITEM NO.	PART NUMBER	DESCRIPTION	QTY.	Have Detailed Drawi	Material	Pricing $	
1	pivot plate		2	yes	1020 Steel		
2	pivot tube		1	yes	Steel		
3	fixed plate		1	yes	Steel		
4	sliding plate		1	yes	Steel		
	turnbuckle assy	Turnbuckle	1				
	30315T611 clevis 1	clevis 1					
	30315T611 center 1	center					
5	30315T611 clevis 2	clevis 2		purchased	316 Stainless Steel	1	15.93
6	camber tube		1	yes	Steel		
7	Tritan_UCFL205-16		2	purchased		2	14.76
8	APB60XL037B-375		1	purchased		1	25
9	180xl037ng		1	purchased		3	10.5
10	APB10XL037BF-250		1	purchased		1	5.5
11	Nema 23 103H7126-	Motor	1	purchased		1	39.99
12	motor mntg plate	Plate Above Motor	1	yes	Steel		
13	motor mntg block	Motor Block	1	yes	Aluminum		0
14	1497K281	Keyed Rotary Shaft	1	yes/purchased	1045 Carbon Steel	1	27.6
15	9684T4	Flange-Mount Shaft Collar	1	purchased	Black-Oxide 1117 Ca	1	62.03
16	SA-drive-cross	SA Cross	1	yes	Steel		
17	97135A270	High Strength Steel Nylon-Insert Locknu	1	purchased	Grade 8 Steel, Zinc Y	5	4.39
18	91257A808	Hex Head Screw	1	purchased	Grade 8 Steel, Zinc Y	5	10.79
19	91257A752	Hex Head Screw	2	purchased	Grade 8 Steel, Zinc Y	5	10.41
20	97135A255	High Strength Steel Nylon-Insert Locknu	2	purchased	Grade 8 Steel, Zinc Y	10	4.39
21	5720K11	Cam Handle	3	purchased	Aluminum	3	37.29
22	90044A131	Socket Head Screw	2	purchased	Black-Oxide Alloy Ste	10	8.39
23	97135A210	High Strength Steel Nylon-Insert Locknu	8	purchased	Grade 8 Steel, Zinc Y	25	3.43
24	91255A537	Hex Drive Rounded Head Screw	2	purchased	Black-Oxide Alloy Ste	50	7.65
25	90480A011	Low Strength Hex Nut	8	purchased	Zinc-Plated Steel	100	1.84
26	91251A242	Socket Head Screw	4	purchased	Black-Oxide Alloy Ste	100	10.27
27	91257A640	Hex Head Screw	2	purchased	Grade 8 Steel, Zinc Y	10	9.22
28	97135A230	High Strength Steel Nylon-Insert Locknu	2	purchased	Grade 8 Steel, Zinc Y	20	4.02
29	92620A794	Hex Head Screw	1	purchased	Grade 8 Steel, Zinc Y	10	9.06
30	91253A542	Hex Drive Flate Head Screw	3	purchased	Black-Oxide Alloy Ste	50	8.42
31	hitch adapter	Hitch Assembly	1	yes	1020 Steel		
	2in square x 8		1	yes	Steel		
	2in square x 10 swiss		1	yes	Steel		
	3x6.5 gusset		2	yes	Steel		
	3x1.5 gusset		2	yes	Steel		

Rear Assembly:

ITEM NO.	PART NUMBER	DESCRIPTION	QTY.	Have Detailed Drawings?	Material	Pricing $	
1	Tire Frame	WELDMENT	1	YES	hopes and dreams		
	1x1x.125x15L	tube	3	YES	mild steel		
	1x1x.125x13L	tube	1	YES	mild steel		
	1x1x.125x9L	tube	2	YES	mild steel		
	1x1x.125x11L	tube	5	YES	mild steel		
	1x1x.125x10L	tube	2	YES	mild steel		
	1x1x.125x6L	tube	2	YES	mild steel		
	tire cage stiffener	LASER CUT	4	YES	10ga mild		
	tire cage stiffener1	LASER CUT	2	YES	16ga mild		
	tire cage stiffener2	LASER CUT	2	YES	16ga mild		
2	LC Frame	WELDMENT	1	YES	hopes and dreams		
	1x1x.125x15L	tube	3	YES	mild steel		
	1x1x.125x9L	tube	4	YES	mild steel		
	1x1x.125x3.7L	tube	2	YES	mild steel		
	1x1x.125x4.7L	tube	2	YES	mild steel		
	LC frame gusset 1	LASER CUT	2	YES	10ga mild		
	LC frame gusset 3	LASER CUT	1	YES	10ga mild		
	LC frame strap	LASER CUT	2	YES	10ga mild		
3	Tritan UCP206-20	pillow block brg	1		purchased	1	40
4	axle	MACHINE AT VP	1		1497K401	1	52.43
5	tire cage closeout1	LASER CUT	1	YES	16ga mild		
6	flange bearing	5968K910	2		purchased	2	104
7	bearing plate	LASER CUT	1	YES	.50 mild		
8	locking collar	6435K210	2		purchased	4	14
9	x axis LC sheet brkt_2	LASER CUT	1	YES	10ga mild		
10	x axis LC sheet brkt_2 mirror	LASER CUT	1	YES	10ga mild		
11	load cells	Optima OP-312-500	3		purchased	3	210
12	.50 rod ends	60645K161	6		purchased	6	39.5
13	bracket 2	LASER CUT	4	YES	10ga mild		
14	vertical load support v3_MHP	LASER CUT	2	YES	10ga mild		
15	Y axis LC mntg block	MACHINE AT VP	2	YES	aluminum		
16	LC sheet brkt_WELDMENT	WELDMENT	1	YES	hopes and dreams		
	LC sheet brkt_v3	LASER CUT	1	YES	10ga mild		
	LC sheet brkt gusset	LASER CUT	3	YES	10ga mild		
19	Aluminum spacer	92510a496	4		purchased	4	28
20	Aluminum spacer	92511a097	2		purchased	2	8
21	SCR CAP HX .25-20X2.5	91247a552 equivalent	10		purchased		
22	NUT HX NY .25-20	95615A120 equivalent	45		purchased		
23	SCR CAP HX .25-20X2.0	91247a550 equivalent	2		purchased		
24	SCR CAP HX .25-20X1.5	91247a546 equivalent	19		purchased		
25	SCR CAP SK .25-20x1.0	91251a542 equivalent	3		purchased		
26	SCR FL .50-13x2.75	91253a723 equivalent	2		purchased		
27	NUT HX NY .50-13	95615a210 equivalent	10		purchased		
28	SCR CAP HX .50-13X3.0	91247a724 equivalent	1		purchased		
29	SCR CAP HX .50-13X2.25	91247a721 equivalent	3		purchased		
30	SCR CAP HX .50-13X1.75	92865a718 equivalent	4		purchased		